

MESON DECAYS WITH ISOSPIN BREAKING
AT TWO LOOPS

KARIM GHORBANI



DEPARTMENT OF THEORETICAL PHYSICS

LUND UNIVERSITY 2007

MESON DECAYS WITH ISOSPIN BREAKING AT TWO LOOPS

KARIM GHORBANI

DEPARTMENT OF THEORETICAL PHYSICS

LUND UNIVERSITY, SWEDEN

THESIS FOR THE DEGREE OF DOCTOR OF PHILOSOPHY
IN PHYSICS

THESIS ADVISOR: JOHAN BIJNENS

FACULTY OPPONENT: GILBERTO COLANGELO

TO BE PRESENTED, WITH THE PERMISSION OF THE FACULTY OF NATURAL SCIENCE OF LUND
UNIVERSITY, FOR PUBLIC CRITICISM IN LECTURE HALL F OF THE DEPARTMENT OF
THEORETICAL PHYSICS ON FRIDAY, NOVEMBER 23TH, 2007, AT 10.15 A.M.

Organization LUND UNIVERSITY Department of Theoretical Physics Sölvegatan 14A SE-223 62 LUND Sweden		Document name DOCTORAL DISSERTATION	
Author Karim Ghorbani		Date of issue October 2007	Subject designator
		Project name	
Sponsoring organization			
Document title Meson Decays with Isospin Breaking at Two Loops			
Abstract In all calculations done in this thesis, the evaluation of higher order quantum corrections has been central. In the first paper included in this thesis we have investigated the effects of finite volume meson propagators for quark-antiquark vacuum expectation value at two-loop level. In the second paper we have improved the earlier calculations for the eta decay to three pions by implementing two-loop quantum corrections. The low energy constants of order p^6 are estimated by means of a resonance chiral Lagrangian. In addition, the experimental charged decay rate leads to the determination for the isospin breaking quantities. Finally, we have studied the isospin breaking effects on the vector and scalar form-factors of semi-leptonic kaon decays, both rare and weak semi-leptonic decays. Semi-leptonic kaon decays provide a rich laboratory to find the CKM matrix element V_{us} and the rare decays provide a good environment to search for the possible new physics beyond the Standard Model in the flavor sector.			
Key words Chiral Lagrangian, Quantum correction, Standard Model, Hadron physics			
Classification system and/or index terms			
Supplementary bibliographical information		Language English	
ISSN and key title		ISBN 978-91-628-7298-4	
Recipient's notes		Number of pages 137	Price
		Security class	

DOKUMENTTABLAD
en SIS 61 41 21

Distributor
Karim Ghorbani
Department of Theoretical Physics, Sölvegatan 14A, SE-223 62 Lund, Sweden

I, the undersigned, being the copyright owner of the abstract of the above-mentioned dissertation, hereby grant to all reference sources the permission to publish and disseminate the abstract of the above-mentioned dissertation.

Signature _____

Date 2007-10-14

To My Parents

This thesis is based on the following publications:

- I Johan Bijnens and Karim Ghorbani
Finite Volume Dependence of the Quark-Antiquark Vacuum Expectation Value.
Phys. Lett. B **636**, 51 (2006),
 LU TP 06-11.
- II Johan Bijnens and Karim Ghorbani
 $\eta \rightarrow 3\pi$ at Two Loops In Chiral Perturbation Theory.
Submitted to JHEP , (2007),
 LU TP 07-26.
- III Johan Bijnens and Karim Ghorbani
Isospin breaking in $K\pi$ vector form-factors for the weak and rare decays K_{l3} and $K \rightarrow \pi l^+ l^-$.
Submitted to JHEP , (2007),
 LU TP 07-29.

The following two proceedings are not included to the thesis:

- I Johan Bijnens and Karim Ghorbani
Quark anti-quark expectation value in finite volume
In the Proceedings of IPM School and Conference on Lepton and Hadron Physics (IPM-LHP06), Tehran, Iran, 15-20 May 2006, pp 0009.
- I Johan Bijnens, Niclas Danielsson, Karim Ghorbani and Timo Lahdeh
Two loop partially quenched and finite volume chiral perturbation theory results.
Published in PoS LAT2005:058,2006.

Contents

Prologue	1
1 Introduction	3
1.1 Quantum Field Theory	3
1.2 Why do we do loop calculations?	5
1.3 Goldstone's Theorem	7
1.4 QCD Lagrangian and its Symmetries	9
1.5 Effective Field Theory	11
1.5.1 Sigma-model and Non-linear Effective Action	11
1.5.2 Lowest Order Effective Lagrangian with Global Flavor Symmetry	14
1.5.3 Chiral Effective Lagrangian with Local Flavor Symmetry	19
1.6 Higher Order Chiral Lagrangians	21
1.7 Power counting scheme	22
1.8 Regularization and Renormalization	24
1.9 Quark-Antiquark Vacuum Expectation Value at One-loop Order	25
1.10 Kaon Semi-leptonic Decays and V_{us}	28
1.11 The Papers	30
Paper I	30
Paper II	31
Paper III	32
Acknowledgments	35
2 Finite Volume Dependence of the Quark-antiquark Vacuum Expectation Value	37
2.1 Introduction	40
2.2 A Lüscher Formula for the Vacuum Condensate	41
2.3 The finite volume vacuum condensate at two-loops	43
2.4 Comparison and conclusions	46

3	$\eta \rightarrow 3\pi$ at Two Loops In Chiral Perturbation Theory	51
3.1	Introduction	54
3.2	Chiral Perturbation Theory	56
3.3	Eta decay amplitude: formalism	59
3.3.1	Matrix-elements in the presence of mixing	59
3.3.2	Kinematics and isospin	63
3.3.3	A simplified form for the amplitude to order p^6	64
3.3.4	Feynman Graphs	64
3.3.5	Regularization, renormalization and integrals	65
3.4	Analytical results	66
3.4.1	Order p^2	66
3.4.2	Order p^4	66
3.4.3	Order p^6	67
3.5	Resonance estimates of the p^6 LECs and the inclusion of the η'	68
3.6	Numerical results	72
3.6.1	A first look	72
3.6.2	Comparison with the dispersive result	75
3.6.3	Dalitz Plot Parameters	77
3.6.4	The ratio r and decay rates	82
3.6.5	Discussion and the values of R and Q	83
3.7	Conclusions	85
3.A	A discussion on Dalitz plot parameters and the sign of α	86
3.B	The order p^4 expression	87
3.C	The order p^6 LECs dependent part	89
4	Isospin breaking in $K\pi$ vector form-factors for the weak and rare decays K_{l3}, $K \rightarrow \pi\nu\bar{\nu}$ and $K \rightarrow \pi l^+ \bar{l}^+$	95
4.1	Introduction	98
4.2	Form-factors and isospin relations	99
4.3	Chiral Perturbation Theory	100
4.4	Matrix-elements in the presence of mixing	102
4.5	Analytical results and ratios of form-factors	104
4.6	Resonance estimate of the contribution from the C_i^r	107
4.7	Numerical results	108
4.7.1	Input parameters	108
4.7.2	$f_+^{K^i\pi^j}(0)$	109
4.7.3	$f_+^{K^i\pi^j}(t)$	111
4.7.4	$f_0^{K^i\pi^j}(t)$	113
4.7.5	Callan-Treiman point	117
4.8	Conclusions	118
4.A	The order p^4 expression	119
4.B	The order p^6 LECs dependent part	125

Prologue

*The secrets eternal neither you know nor I
And answers to the riddle neither you know nor I
Behind the veil there is much talk about us, why
When the veil falls, neither you remain nor I*

Omar Khayyam (1048-1131)

Quantum Chromo Dynamics (QCD) is the theory behind the strong interactions or the strong force. These interactions occur among quarks and gluons. Quarks and gluons play the same role as electrons and photons in electromagnetism respectively. Nevertheless, the strong interactions exhibit a richer and exquisite tapestry of involvement and nonlinearity. This stems from the fact that the Non-Abelian gauge symmetry of QCD allows self interaction of gluons whereas there is no such interaction in electromagnetism which is governed by an Abelian gauge symmetry. Two or even three phenomena in QCD are rather stunning. Asymptotic freedom and confinement are the first two and we may also contemplate taking the spontaneous symmetry breaking as prominent a phenomenon as the first two. These extremely interesting phenomena stand out of the other properties of QCD, those which may be regarded as the byproduct of the most fundamental ones. Asymptotic freedom was discovered almost thirty years ago by David Gross, Frank Wilczek and David Politzer who received the Nobel prize in physics in 2004 for this discovery. Asymptotically free theories are weakly interacting theories at very high energy. In principle, this type of theories are easier to deal with at high energies. In the other extreme, by which I mean at very low energies, the strong interactions become really strong and this may be the reason behind the yet-to-be-understood confinement phenomenon. Confinement prevents quarks and gluons from being observed as free entities. At very high energy, jet production alludes to the existence of free quarks and gluons. The focus in this thesis is going to be on the low energy hadronic physics. Lattice QCD is the *brute force* method of numer-

ical computations of the unknowns of QCD in this energy domain where the standard perturbative technology stops working. Lattice results, however, need at the end to be extrapolated to the continuum. This may be accomplished by means of effective field theories. Effective field theories are of course useful also on their own. Among them, is Chiral Perturbation Theory (ChPT) which is known to be a good low energy theory of QCD. But is the fact that an effective field theory can be a plausible representative of the original theory up to a given mass scale trivial? I leave out the answer and only quote the following conjectured theorem by Weinberg: *If one writes down the most general possible Lagrangian, including all terms consistent with assumed symmetry principle, and then calculates matrix elements with this Lagrangian to any given order of perturbation theory, the result will simply be the most general possible S-matrix consistent with analyticity, perturbative unitarity, cluster decomposition and assumed symmetry principle.* ChPT, like other effective field theories, has more unknown constants than the underlying theory. In fact to all orders the number is finite. All these can not be determined from experimental data which are available to us. Invoking other theoretical approaches, like resonance chiral perturbation theory, for approximate estimates of the unknown low-energy constants has been practiced systematically. However, estimates with more precision are required for ChPT to be adequate for precision physics research. To circumvent the problem of having many unknown parameters in the effective Lagrangian the method of dispersion analysis is considered. The application of the dispersion relation analysis has a long history in particle physics. It works based on the fundamental axioms of quantum mechanics such as analyticity and unitarity of the S-matrix. It turns out that scattering amplitudes can be calculated by only knowing the imaginary part of the amplitude. To make the integration over the imaginary part converge it is necessary to do subtractions. The emerging subtraction constants can be fixed by matching the dispersive result to the result obtained from ChPT. One example of such a calculation is that of the eta decay to three pions. We have confronted this known result by doing higher order calculation in ChPT for this process. We also performed a similar higher order calculation for certain Kaon decays. I give an introduction to the area and to the papers followed then by the papers.

Introduction

1.1 Quantum Field Theory

In the realm where relativistic effects become important, the one-particle formalism of quantum mechanics falls apart. The famous relation $m = E/c^2$ indicates that energy can be converted to matter and matter can be converted to energy. This then requires a multi-particle formalism at high energy where particle creation and annihilation is possible. On the other hand, the Heisenberg uncertainty principle allows the violation of energy conservation according to the relation $\Delta E \cdot \Delta t \approx \hbar$. This implies the importance of the virtual particle contributions when we perform higher order corrections in perturbation theories.

We already know that field theory provides the solution. We may begin with the classical field theory of a single real scalar field $\phi(x)$. The field $\phi(x)$ is a continuous function defined in all points in space-time and will play the role of dynamical variable. In a local field theory the action can be written as the integration of the Lagrangian density, denoted by \mathcal{L} , over four-dimensional space-time

$$\mathcal{S} = \int \mathcal{L}(\phi, \partial_\mu \phi) d^4x. \quad (1.1)$$

Applying the least action principle we find the Euler-Lagrange equation of motion

$$\partial_\mu \left(\frac{\partial \mathcal{L}}{\partial(\partial_\mu \phi)} \right) - \frac{\partial \mathcal{L}}{\partial \phi} = 0. \quad (1.2)$$

As a simple example we take the Klein-Gordon Lagrangian which is a relativistic field theory for a scalar particle

$$\mathcal{L} = \frac{1}{2}(\partial_\mu \phi)^2 - \frac{1}{2}m^2 \phi^2. \quad (1.3)$$

we obtain for the equation of motion (EOM)

$$(\partial^\mu \partial_\mu + m^2) \phi(x) = 0. \quad (1.4)$$

The conjugate momentum p for a discrete system is defined in classical mechanics as $p = \frac{\partial L}{\partial \dot{q}}$, for each dynamical degree of freedom q . This may be generalized to a relativistic continuous system where we define the momentum density conjugate as

$$\Pi(x) = \frac{\partial \mathcal{L}}{\partial \dot{\phi}(x)}. \quad (1.5)$$

To promote the classical fields to quantum fields we exploit the standard canonical commutation relations to quantize the classical fields. To this end, we promote both $\phi(x)$ and $\Pi(x)$ to operators that satisfy the equal time commutation relations

$$\begin{aligned} [\phi(\mathbf{x}), \Pi(\mathbf{y})] &= i\delta^3(\mathbf{x} - \mathbf{y}), \\ [\phi(\mathbf{x}), \phi(\mathbf{y})] &= [\Pi(\mathbf{x}), \Pi(\mathbf{y})] = 0. \end{aligned} \quad (1.6)$$

The field quantization procedure can be carried out by treating the fields as harmonic oscillators. As an analogy, we take the harmonic oscillator with frequency $\omega_p = \sqrt{\mathbf{p}^2 + m^2}$ and EOM as in Eq. (1.4) and we will expand $\phi(\mathbf{x})$ and $\Pi(\mathbf{x})$ in terms of operators in such a way to fulfill the commutation relations given above.

$$\begin{aligned} \phi(\mathbf{x}) &= \int \frac{d^3p}{(2\pi)^3} \frac{1}{\sqrt{2\omega_p}} (a_p \exp(i\mathbf{p}\cdot\mathbf{x}) + a_p^\dagger \exp(-i\mathbf{p}\cdot\mathbf{x})), \\ \Pi(\mathbf{x}) &= \int \frac{d^3p}{(2\pi)^3} -i\sqrt{\frac{\omega_p}{2}} (a_p \exp(i\mathbf{p}\cdot\mathbf{x}) - a_p^\dagger \exp(-i\mathbf{p}\cdot\mathbf{x})). \end{aligned} \quad (1.7)$$

This in turn requires the commutation relation

$$[a_{\mathbf{p}}, a_{\mathbf{p}'}^\dagger] = (2\pi)^3 \delta^3(\mathbf{p} - \mathbf{p}'). \quad (1.8)$$

where a_p^\dagger and a_p are familiar ladder operators. In fact, the operator a^\dagger (a) creates (annihilates) an excitation or particle (antiparticle) with momentum \mathbf{p} and energy $\omega_p = \sqrt{\mathbf{p}^2 + m^2}$. We can then define the one particle state by operating a^\dagger on the ground state or vacuum as $|p\rangle = \sqrt{2E_p} a_p^\dagger |0\rangle$ where $E_p = \omega_p$. We are now ready to reach an interpretation for the state $\phi(\mathbf{x})|0\rangle$. First we find that

$$\phi(\mathbf{x})|0\rangle = \int \frac{d^3p}{(2\pi)^3} \frac{1}{2E_p} \exp(-i\mathbf{p}\cdot\mathbf{x}) |\mathbf{p}\rangle. \quad (1.9)$$

We therefore conclude that operator valued function $\phi(\mathbf{x})$, acting on the vacuum gives rise to a linear superposition of one-particle states with well-defined momenta, at position \mathbf{x} .

One important question is what does the propagator look like in relativistic quantum field theory? In quantum field theory we compute observables which are defined as various type of correlation functions. The most basic type of these functions is the two-point correlation function. Two-point correlation function of a non-interacting theory gives the propagation of the free particle corresponding to the field content of the theory. Let us assume that a particle is created at point (x_0, \mathbf{x}) in space-time and then propagates until it gets annihilated at point (y_0, \mathbf{y}) . It is evident that two fields are needed here to act on the vacuum. One field to create a particle and the second field to annihilate the excited state back to vacuum again. We define the propagator amplitude for a scalar free particle which propagates between point y and point x , as follows

$$\begin{aligned} D_F(x-y) &= \langle 0|T\phi(x)\phi(y)|0\rangle \\ &\equiv \theta(x^0 - y^0) \langle 0|\phi(x)\phi(y)|0\rangle + \theta(y^0 - x^0) \langle 0|\phi(y)\phi(x)|0\rangle. \end{aligned} \quad (1.10)$$

Where θ is the Heaviside function. T stands for time-ordering and this is for putting the creation and annihilation time in order, depending on which direction the propagation occurs. It turns out that $D_F(x-y)$ is the Green function of the Klein-Gordon operator which is defined in Eq. (1.4). We then find

$$D_F(x-y) = \int \frac{d^4p}{(2\pi)^4} \frac{i}{p^2 - m^2 + i\epsilon} \exp(-ip \cdot (x-y)). \quad (1.11)$$

The propagator above is given in the Feynman prescription. This prescription is pretty useful for the following reason. The momentum integral has two poles at $p^0 = \pm(E_p - i\epsilon)$. If we perform the integral over p^0 by closing the contour below, the amplitude corresponds to a particle that propagates from y to x . If we close the contour above, the amplitude corresponds to a particle that propagates from x to y . We end this section at this point and for extensive discussion refer the reader to the books[1, 2].

1.2 Why do we do loop calculations?

To answer this question let us see what constraint unitarity imposes on the non-trivial part of the S matrix. We define $S = 1 + iT$. The unitarity of the S-matrix implies the following relation for the non-trivial part of the S-matrix, namely T-matrix,

$$S^\dagger S = 1 \quad \Rightarrow \quad T^\dagger T = -i(T - T^\dagger). \quad (1.12)$$

We may consider a generic scattering process in which the initial state $|i, in\rangle$ makes transition into the final state $|f, out\rangle$. The matrix element for this pro-

cess is

$$\langle f|T|i\rangle = (2\pi)^4\delta^4(p_f - p_i)\mathcal{T}_{fi}. \quad (1.13)$$

Here we have brought out the part which corresponds to the momentum-energy conservation in the process. Let us now calculate the matrix element of the operator given in Eq. (1.12) and at the same time insert all the possible intermediate states between initial and final states, we then obtain

$$\langle f|T|i\rangle - \langle f|T^\dagger|i\rangle = i \sum_n \langle f|T^\dagger|n\rangle \langle n|T|i\rangle. \quad (1.14)$$

We write the relation above in terms of matrix elements \mathcal{T}_{if} defined in Eq. (1.13) and obtain

$$\mathcal{T}_{fi} - \mathcal{T}_{if}^* = i \sum_n (2\pi)^4\delta^4(p_n - p_i) \mathcal{T}_{nf}^* \mathcal{T}_{ni}. \quad (1.15)$$

For a special case of forward scattering where $|f\rangle = |i\rangle$ we obtain a simpler identity

$$2Im\mathcal{T}_{ii}^* = \sum_n (2\pi)^4\delta^4(p_n - p_i) |\mathcal{T}_{ni}|^2. \quad (1.16)$$

This identity has a very interesting consequence. Hereafter we suppress the subscripts in \mathcal{T}_{fi} . A non-zero value for the imaginary part of the scattering amplitude requires a branch cut singularity. Let us show how it is possible. For the center of mass energy s below the leading threshold energy s_{th} , the scattering amplitude is a real function of variable s , because here there is not enough energy accessible for the intermediate particles to go on-shell. According to the Schwarz reflection principle if, $\mathcal{T}(s)$ is analytic in a connected region which includes part of the real axis and $\mathcal{T}(s)$ is real-valued on this part of the real axis, then

$$\mathcal{T}(s^*) = \mathcal{T}^*(s). \quad (1.17)$$

This function can analytically be continued to complex values of s . For a complex value s very close to the the threshold and $s > s_{th}$, Eq. (1.17) gives the following identity

$$Re\mathcal{T}(s - i\epsilon) + iIm\mathcal{T}(s - i\epsilon) = Re\mathcal{T}(s + i\epsilon) - iIm\mathcal{T}(s + i\epsilon). \quad (1.18)$$

This identity implies

$$\begin{aligned} Re\mathcal{T}(s - i\epsilon) &= Re\mathcal{T}(s + i\epsilon) \\ Im\mathcal{T}(s - i\epsilon) &= -Im\mathcal{T}(s + i\epsilon). \end{aligned} \quad (1.19)$$

The preceding relations reflect the fact that branch cut singularity always appears when the scattering amplitude develops an imaginary part. Now we show that this type of singularities also appear in an effective field theory like chiral perturbation theory only beyond tree level. We will show in the later sections that at tree level the scattering amplitude is a real function. Therefore it is only at one-loop level and beyond, that the scattering amplitude can be a complex-valued function. We proved above that having the branch cut singularity is equivalent to having the complex-valued scattering amplitude for some $s > s_{th}$. So the task is to demonstrate how Feynman diagram may have discontinuity across the real axis for $s > s_{th}$. The method of computing the discontinuity of the Feynman diagrams is given by a set of rules which referred to as *cutting rules*. For a simple case of one-loop Feynman diagram with two propagators, one computes a Feynman momentum integral by replacing each of the propagators by a delta function and it can be seen that a discontinuity will arise in a region of momentum integration where two delta functions are simultaneously satisfied. This indeed occurs when two propagators go simultaneously on-shell. Therefore, it is only when loop diagrams are included unitarity can be satisfied for the S-matrix in perturbative calculations.

1.3 Goldstone's Theorem

We begin this section by giving a general proof of the Goldstone's theorem for the case of scalar quantum field theory. We consider the Lagrangian \mathcal{L} containing a set of elementary scalar fields Φ_i with $i = 1, \dots, N$ and assume that the theory is invariant under the symmetry group G.

$$\mathcal{L} = \frac{1}{2} \partial_\mu \Phi_i \partial^\mu \Phi_i - V(\Phi_i \cdot \Phi_i). \quad (1.20)$$

We will show in the following lines that the spontaneous breakdown of the global symmetry G of the action, generated by charges Q^a , implies the existence of poles at $p^2 = 0$ in the Green functions, and consequently will give rise to the appearance of massless bosons in the physical spectrum. For spontaneous symmetry breaking to occur, a non-vanishing vacuum expectation value for some of the fields Φ_i is sufficient

$$\langle 0 | \Phi_i | 0 \rangle = v_i \neq 0. \quad (1.21)$$

The transformation property of the fields Φ_i under the symmetry group G is considered as

$$\Phi_i \rightarrow \Phi'_i = \Phi_i - i\delta\alpha^a T_{ij}^a \Phi_j, \quad (1.22)$$

Where, T^a are the matrix representations of the generators Q^a in the N -dimensional space of Φ_i . On the other hand, there exist another way to look

on the transformation of the scalar fields as

$$\Phi_i \rightarrow \Phi'_i = \exp(i\alpha^a Q^a) \Phi_i \exp(-i\alpha^a Q^a) \approx \Phi_i + i\alpha^a [Q^a, \Phi_i]. \quad (1.23)$$

Comparing Eq. (1.22) and Eq. (1.23), leads us to obtain a useful commutation relation between the generators Q^a and fields Φ_i

$$[Q^a, \Phi_i(\mathbf{x}, t)] = -T_{ij}^a \Phi_j(\mathbf{x}, t). \quad (1.24)$$

Now we start out the derivation by considering the two-point Green function

$$G_{\mu i}^a(x-y) = \langle 0 | T J_\mu^a(x) \Phi_i(y) | 0 \rangle, \quad (1.25)$$

in which the current J_μ^a corresponds to the generator Q^a of the symmetry group G. The reason we chose this particular Green function will become clear in later steps. The Green function satisfies a Ward identity by differentiating Eq. (1.25) with respect to x . We assume the current conservation $\partial^\mu J_\mu(x) = 0$,

$$\begin{aligned} \partial^\mu G_{\mu i}^a(x-y) &= \partial^\mu \theta(x_0 - y_0) \langle 0 | J_\mu^a(x) \Phi_i(y) | 0 \rangle \\ &\quad + \partial^\mu \theta(y_0 - x_0) \langle 0 | \Phi_i(y) J_\mu^a(x) | 0 \rangle \\ &= \delta(x_0 - y_0) \langle 0 | [J_0^a(x) \Phi_i(y)] | 0 \rangle. \end{aligned} \quad (1.26)$$

We may slightly alter our commutation relation given in Eq. (1.24) to be used in the above Ward identity. We therefore get the relation below if we identify J_0^a with generators Q^a of the group G

$$[J_0^a(\mathbf{x}, t), \Phi_i(\mathbf{y}, t)] = -T_{ij}^a \Phi_j(\mathbf{x}, t) \delta^3(\mathbf{x} - \mathbf{y}). \quad (1.27)$$

One then obtains the following Ward identity by taking into account the translational invariance of the vacuum and fields

$$\partial^\mu G_{\mu i}^a(x-y) = -\delta^4(x-y) T_{ij}^a \langle 0 | \Phi_j(0) | 0 \rangle. \quad (1.28)$$

Let us define $\tilde{G}_{\mu i}^a(p)$ as the Fourier transformation of $G_{\mu i}^a(x-y)$. It is now pretty straightforward to achieve the interesting relation

$$ip^\mu \tilde{G}_{\mu i}^a(p) = T_{ij}^a \langle 0 | \Phi_j(0) | 0 \rangle. \quad (1.29)$$

We can now readily conclude that in case $\langle 0 | \Phi_j(0) | 0 \rangle$ does not vanish for some of the fields, the preceding equation implies that the Green function must develop a singularity at $p^2 = 0$. From Lorentz invariance it requires $\tilde{G}_{\mu i}^a(p)$ to be proportional to p^μ and therefore it can be expressed as

$$\tilde{G}_{\mu i}^a(p) = -i \langle 0 | \Phi_j(0) | 0 \rangle T_{ij}^a \frac{p^\mu}{p^2}. \quad (1.30)$$

The second part of the proof is to demonstrate that the pole in the Green function is consistent with the existence of a massless boson in the physical spectrum. To this end, we define in the following a matrix element involving the particle state $|\pi^i(p)\rangle$ associated with the field Φ_i which has mass m_i

$$\langle 0|J_\mu^a(x)|\pi^i(p)\rangle = if_i^a p_\mu \exp(-ip.x). \quad (1.31)$$

By the use of the LSZ reduction formula we are able to relate the matrix element to the Green function in a way given below

$$\langle 0|J_\mu^a(x)|\pi^i(p)\rangle = -i \exp(-ip.x) \lim_{p^2 \rightarrow m_i^2} \tilde{G}_{\mu i}^a(p)(p^2 - m_i^2). \quad (1.32)$$

By comparing Eq. (1.31) and Eq. (1.32) we arrive at the identity

$$f_i^a p_\mu = - \lim_{p^2 \rightarrow m_i^2} \tilde{G}_{\mu i}^a(p)(p^2 - m_i^2). \quad (1.33)$$

Now if $\tilde{G}_{\mu i}^a(p)$ is one of the Green functions which has a pole at $p^2 = 0$, to get a finite value for the LHS of the Eq. (1.33), it needs to have $m_i = 0$ and therefore $f_i^a \neq 0$ and we can now find a relation which links the constant f_i^a to the vacuum expectation value. Let us replace $\tilde{G}_{\mu i}^a(p)$ by its value given in Eq. (1.30) and take the limit $p^2 \rightarrow 0$, we then find

$$f_i^a = i \langle 0|\Phi_j(0)|0\rangle T_{ij}^a. \quad (1.34)$$

In other words, corresponding to each broken generator which does not leave the vacuum invariant i.e. $\langle 0|\Phi_j(0)|0\rangle T_{ij}^a \neq 0$ there exist a massless boson.

1.4 QCD Lagrangian and its Symmetries

Quantum Chromo dynamics or QCD is a non-Abelian gauge theory with gauge group $SU(3)_c$ coupled to quarks in the fundamental representation. The QCD Lagrangian reads

$$\begin{aligned} \mathcal{L}_{QCD} = & -\frac{1}{4} G_a^{\mu\nu} G_{\mu\nu}^a + \sum_{q=u,d,\dots} \bar{q}_R i\gamma^\mu D_\mu q_R + \bar{q}_L i\gamma^\mu D_\mu q_L \\ & -(\bar{q}_R M_q q_L + \bar{q}_L M_q q_R) + \dots, \end{aligned} \quad (1.35)$$

Where q_R and q_L are the right-handed and left-handed components of the quark fields respectively. The ellipsis stands for the sum of the ghost term, the gauge-fixing terms and the θ -term. The gauge field strength tensor is given as

$$G_a^{\mu\nu} = \partial_\mu G_\nu^a - \partial_\nu G_\mu^a + gf_{abc} G_\mu^b G_\nu^c, \quad (1.36)$$

Where f_{abc} are the structure constants of the group $SU(3)_c$. The covariant derivative associated with the gauge transformation is

$$D_\mu = \partial_\mu - igG_\mu^a t^a. \quad (1.37)$$

Ignoring the mass term and the θ -term (which is a minute quantity: $\theta_{QCD} < 10^{-9}$) in the Lagrangian give rise to a rather big symmetry group for the action. We write down as, assuming the three flavor of quarks for our case, $G_{QCD} \equiv SU(3)_c \times U(3)_R \times U(3)_L$ plus discrete symmetries: Parity (P), charge conjugation (C) and time reversal (T). More extensive discussions are provided in [3]. Now, let us break up the chiral symmetry group of the action into its simple subgroups. It then reads $SU(3)_R \times SU(3)_L \times U(1)_A \times U(1)_V$. The global $U(1)_V$ subgroup corresponds to the conservation of the baryon number. The subgroup $U(1)_A$, however, is broken at the loop level. The subgroup which is thus more relevant to our work is the global $SU(3)_R \times SU(3)_L$ chiral symmetry plus discrete symmetries. The QCD Lagrangian in the massless limit is then invariant under independent left-handed and right-handed quark field transformations

$$q_R \rightarrow \exp(-i\alpha_R \cdot \lambda) q_R \quad ; \quad q_L \rightarrow \exp(-i\alpha_L \cdot \lambda) q_L, \quad (1.38)$$

Where λ^a ($a = 1, 2, \dots, 8$) are the $SU(3)$ Gell-Mann matrices.

In general the symmetry of the action is not necessarily the one which is manifested in nature and this actually happens in QCD due to the strong interactions. This may happen via a well-known phenomenon namely, spontaneous symmetry breaking. Besides the gauge symmetry which is exact, the flavor chiral symmetry is not realized in nature. The absence of parity-doubling among low-lying hadronic excitations supports the postulation of the dynamical symmetry breaking of the strong Lagrangian. We therefore consider the following spontaneous chiral symmetry breaking (SCSB) pattern ¹

$$G \equiv SU(3)_R \times SU(3)_L \times U(1)_V \xrightarrow{SCSB} H \equiv SU(3)_V \times U(1)_V. \quad (1.39)$$

The particle spectrum consists of multiplets of the subgroup H which leaves the vacuum invariant. The octet of pseudo-Goldstone bosons ($\pi^\pm, \pi^0, K^\pm, K^0, \bar{K}^0, \eta$) are then one of these multiplets and the only massless particles in the chiral limit. In reality quarks have masses and this accounts for the small mass of the pseudo-scalar mesons. To address this issue we may split the Lagrangian into two parts as follows

$$\mathcal{L}_{QCD} = \mathcal{L}_0 + \mathcal{L}_1, \quad \mathcal{L}_1 = m_u \bar{u}u + m_d \bar{d}d + m_s \bar{s}s, \quad (1.40)$$

¹It should be noted that the symmetry $SU(3)_L \times SU(3)_R$ is also broken by the anomaly. This anomaly is associated with the coupling of quarks to photons. This “non-strong” effect is incorporated in the effective Wess-Zumino-Witten action[4, 5].

Where, \mathcal{L}_0 is invariant under chiral group $G \equiv SU(3)_L \times SU(3)_R$ and \mathcal{L}_1 breaks the chiral symmetry explicitly but is a small perturbation provided that the quark masses are much smaller than Λ_χ (the mass scale in which the SCSB occurs).

In the next sections I shall focus on the properties of the pseudo-scalar mesons and their dynamics within the framework of effective field theory.

1.5 Effective Field Theory

To study the properties of the strong interactions at low energy the underlying theory (QCD) proved to be difficult. In fact at low energy we observe bound states as mesons and baryons which we consider as dynamical variables. Pseudo-scalar mesons are the lightest particles in the physical spectrum. So it is our main task to find an effective field theory for QCD which captures the symmetry property of the original theory and contains the Goldstone mesons. In the following I shall discuss first the linear sigma model as an illustrating example and then Chiral Perturbation Theory as a promising low energy theory for QCD.

1.5.1 Sigma-model and Non-linear Effective Action

It is instructive to start with linear sigma model and its effective field theory. We consider, for the linear sigma model the Lagrangian

$$\mathcal{L} = \frac{1}{2} \partial_\mu \vec{\phi} \cdot \partial^\mu \vec{\phi}^T - \mu (\vec{\phi} \cdot \vec{\phi} - a^2)^2. \quad (1.41)$$

The vector field $\vec{\phi} = (\phi_1, \dots, \phi_N)$ is a N -component real scalar field. The global transformation of the vector field $\vec{\phi}$ under the N -dimensional rotation group $G \equiv O(N)$ leaves the Lagrangian invariant. It can be seen from the potential term in the Lagrangian that there is a non-zero vacuum expectation value for a set of fields that satisfy $\phi_0^2 = \phi_1^2 + \dots + \phi_N^2 = a^2$. This puts a non-linear constraint on the field configurations which give rise to the ground state of the theory. In fact there are infinite number of field transformations that satisfy the said relation. Now we assume that one of the ground states is picked up via a dynamical mechanism. In other words, the symmetry of the Lagrangian is spontaneously broken to the subgroup $H \equiv O(N-1)$. According to the Goldstone theorem this theory contains $N-1$ massless Goldstone bosons, denoted by π^i , where $N-1$ is equal to the broken generators. The Goldstone fields are thus the coordinates of the *coset space* $O(N)/O(N-1)$. Each orientation on the $N-1$ dimensional sphere corresponds to a new set of Goldstone fields. We may consider one simple field configuration for the vacuum to be

$\vec{\phi}_0 = (0, \dots, a)$. The vector field $\vec{\phi}$ can be expanded around $\vec{\phi}_0$ and we write it in terms of the pion fields and massive field σ assuming that $\sigma \ll a$. It is convenient to write $\vec{\phi}$ in the exponential representation form as

$$\phi^T = (a + \sigma) \exp(i\Pi/a) \phi_0^T/a, \quad \Pi = \sum_i \lambda^i \pi^i. \quad (1.42)$$

Where $\lambda^i (i = 1, \dots, N-1)$ denote the matrix representation for the broken generators. Let us now put ϕ in the Lagrangian and do the algebra, we obtain

$$\mathcal{L}(\sigma, \Pi) = \frac{1}{2} \partial_\mu \sigma \partial^\mu \sigma + \frac{1}{2} (a + \sigma)^2 \partial_\mu \Pi \partial^\mu \Pi - \mu (\sigma^2 + 2a\sigma)^2, \quad (1.43)$$

Where one reads for the mass of the heavy field, $m_\sigma = \sqrt{8\mu a}$, and the pions are massless. In the limit of vanishing sigma field, the Lagrangian in Eq. (1.43) is called nonlinear sigma model because of the non-linear relation $\vec{\phi}^2 = a^2$ imposed on the fields. Assuming that at very low energies the σ particle is absent we may then integrate out the sigma field and find an effective action where, only the pion fields are kept dynamically active. To this end one may employ the path integral procedure to remove the heavy field σ

$$\exp(iZ_{eff}(\Pi)) = \frac{\int [d\sigma] \exp(i \int d^4x \mathcal{L}(\sigma, \Pi))}{\int [d\sigma] \exp(i \int d^4x \mathcal{L}(\sigma, 0))}. \quad (1.44)$$

However, to reach our aim it suffices to do an approximation where we ignore the σ self-interaction terms and complete the square in σ field to get the Lagrangian in a form

$$\begin{aligned} \mathcal{L}(\sigma, \Pi) &= \mathcal{L}(\Pi) + \mathcal{L}'(\sigma, \Pi), \\ \mathcal{L}(\Pi) &= \frac{1}{2} a^2 \partial_\mu \Pi \partial^\mu \Pi, \\ \mathcal{L}'(\sigma, \Pi) &= -\frac{1}{2} \sigma (\partial^2 + m_\sigma^2) \sigma + a \sigma \partial_\mu \Pi \partial^\mu \Pi + \frac{1}{2} \partial(\sigma \cdot \partial \sigma). \end{aligned} \quad (1.45)$$

The total derivative term will drop out when we calculate the action. The first term in the Lagrangian $\mathcal{L}(\sigma, \Pi)$, contains only the pion fields and is the leading term in the effective action we are going to find. The σ field in the $\mathcal{L}'(\sigma, \Pi)$, should be integrated out and we carry out the procedure by changing the heavy field to $\sigma' = \sigma - K^{-1}J$, where, $K = \partial^2 + m_\sigma^2$ and $J = a \partial_\mu \Pi \partial^\mu \Pi$. We will get

$$\begin{aligned} \int \mathcal{L}'(\sigma, \Pi) d^4x &= -\frac{1}{2} \int d^4x [(\sigma - K^{-1}J)K(\sigma - K^{-1}J) - JK^{-1}J] \\ &\equiv -\frac{1}{2} \int d^4x (\sigma' K \sigma' - JK^{-1}J). \end{aligned} \quad (1.46)$$

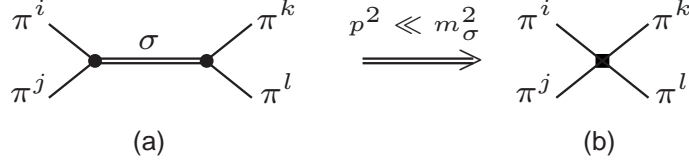


Figure 1.1: (a) shown is the tree level Feynman diagram for the $\sigma - \pi$ interaction, (b) The local effective vertex of the $\pi\pi$ interaction after σ field is integrated out.

Feynman propagator D_F is defined as $(\partial^2 + m_\sigma^2)D_F(x-y) = -\delta^4(x-y)$. This implies that $K^{-1}J(x) = -\int d^4y D_F(x-y)J(y)$. To perform the path integral in Eq. (1.44), the integral measure will change to $[d\sigma']$. Since the path integral spans over all the values of σ the field at each point of space-time we have $[d\sigma'] = [d\sigma]$.

$$\begin{aligned} \exp(iZ_{eff}(J)) &= \frac{\int [d\sigma'] \exp(i \int d^4x \mathcal{L}'(\sigma', J))}{\int [d\sigma] \exp(i \int d^4x \mathcal{L}(\sigma, 0))} \\ &= \frac{\int [d\sigma'] \exp(\frac{-i}{2} \int d^4x (\sigma' K \sigma' - J K^{-1} J))}{\int [d\sigma] \exp(i \int d^4x \sigma K \sigma)}, \end{aligned} \quad (1.47)$$

and finally we obtain

$$\begin{aligned} \exp(iZ_{eff}(J)) &= \exp\left(\frac{i}{2} \int d^4x (J K^{-1} J)\right) \\ &= \exp\left(-\frac{i}{2} \int \int d^4x d^4y J(x) D_F(x-y) J(y)\right). \end{aligned} \quad (1.48)$$

We can now find the next-to-leading term of the effective action. Since the heavy particles propagate only up to short distances at low energy it is possible to Taylor expand $J(y)$ around x as $J(y) = J(x) + (y-x) \cdot \partial J(y)_{y=x} + \dots$ with the first term dominating. The second term is of higher order in momentum which goes beyond the order we are interested in. We then only keep the first term and will obtain the local effective action as

$$\begin{aligned} Z_{eff}(J) &= -\frac{1}{2} \int \int d^4x d^4y J(x) D_F(x-y) J(y) \\ &\approx -\frac{1}{2m_\sigma^2} \int d^4x J(x) J(x) + \dots, \end{aligned} \quad (1.49)$$

Where we have used the approximation $D_F(x-y) \approx -\frac{1}{m_\sigma^2}$ for momentum $p^2 \ll m_\sigma^2$. The interesting observation here is the fact that the effect of the

heavy particle σ is nicely *decoupled* and only appears as an overall constant in the generating functional Z_{eff} . Now the effective action is sum of the Eq. (1.49) resulting from integrating out the σ term and the leading term given in Eq. (1.45)

$$\mathcal{L}_{eff} = \frac{1}{2}a^2\partial_\mu\Pi\partial^\mu\Pi - \frac{1}{2m_\sigma^2}(\partial_\mu\Pi\partial^\mu\Pi)^2 + \dots, \quad (1.50)$$

where ellipses denote the terms arising from propagation of the σ particle at higher orders of the inverse powers of m_σ . The effective Lagrangian in Eq. (1.50), exhibits a weakly interacting theory for the pions, with no interaction at $p^2 = 0$. That is because there are derivative interaction terms in the Lagrangian only. Fig. (1.1) depicts two tree level Feynman diagrams: when the heavy field is still active in the theory and when this field is integrated out based on the assumption that $p^2/m_\sigma^2 \ll 1$. Sigma model as well as non-linear Sigma model are discussed in many quantum field theory books and also particle physics books for which we refer to [1, 3]

1.5.2 Lowest Order Effective Lagrangian with Global Flavor Symmetry

Constructing an effective field theory (EFT) for QCD by integrating out the heavy degrees of freedom is not workable. At low energy one has to deal with an entirely different set of degrees of freedom, namely baryons and mesons, whereas quarks and gluons are the variables present in the QCD Lagrangian.² However, an inspection in the hadron spectrum indicates a mass gap such that the pseudo-scalar octet is sequestered from the rest of the hadrons. Here we say that there is a separation of mass scale. This together with the constraints from the Goldstone property of the pseudo-scalar mesons lead us to build an EFT containing pseudo-Goldstone mesons.

Let us assume the SCSB pattern given in Eq. (1.39) where symmetry group $G \equiv SU(3)_L \times SU(3)_R$ is dynamically broken to a diagonal subgroup $H \equiv SU(3)_V$. We take symmetry group G with $n_G = 16$ generators and group H with $n_H = 8$ generators. Goldstone's theorem then requires massless particle in the spectrum, as many as the number of broken generators. This implies the number of Goldstone particles $N_{GB} = n_G - n_H$. The eight Goldstone fields, denoted by $\phi^i(x) (i = 1, \dots, 8)$, are the coordinates in the coset space G/H and describe the local orientation of the vacuum for small deviation of the standard

²We remind the reader however, of the Lagrangian of the extended Nambu and Jona-Lasinio model where the gluons are integrated out and the resulting effective action is expanded in terms of local quark field operators.

vacuum say that with $\phi^i(x) = 0$.³ In order to find the chiral transformation property of the Goldstone fields we chose a matrix representative of the fields as $\xi(\phi) \equiv (\xi_L(\phi), \xi_R(\phi)) \in G$, where L and R are the $SU(3)_L$ and $SU(3)_R$ transformation respectively. The $\xi_{L,R}$ may be considered in the CCWZ prescription.⁴

For a group element $g(g_L, g_R) \in G$ and $h \in H$, we can write the chiral transformation of the Goldstone fields as

$$\xi_L \xrightarrow{G} g_L \xi_L h^\dagger(g, \phi), \quad \xi_R \xrightarrow{G} g_R \xi_R h^\dagger(g, \phi). \quad (1.51)$$

The compensating H transformation is necessary to put the $\xi(\phi)$ back into its original form. In our case the coset space G/H is curved and therefore H transformation is nonlinear. Since the vacuum is parity invariant, the same H transformation occurred in both left-handed and right-handed sectors. This allows to find a simpler representation for the Goldstone fields that transforms linearly under the chiral group. So we define $U(\phi) = \xi_R(\phi)\xi_L^\dagger(\phi)$. It is easy to check that the transformation of $U(\phi)$ under G is linear

$$U(\phi) \xrightarrow{G} g_R U(\phi) g_L. \quad (1.52)$$

We can now arbitrarily choose $\xi_L(\phi) = \xi_R^\dagger(\phi) = u(\phi)$ which results in $U(\phi) = u(\phi)^2$. The matrix $U \in SU(3)$ parameterizes the Goldstone bosons as

$$U(\phi) = \exp(i\sqrt{2}\phi/F_0), \quad (1.53)$$

where

$$\phi(x) = \begin{pmatrix} \frac{\pi^0}{\sqrt{2}} + \frac{\eta}{\sqrt{6}} & \pi^+ & K^+ \\ \pi^- & -\frac{\pi^0}{\sqrt{2}} + \frac{\eta}{\sqrt{6}} & K^0 \\ K^- & \bar{K}^0 & -\frac{2\eta}{\sqrt{6}} \end{pmatrix}. \quad (1.54)$$

The most general chiral Lagrangian which contains the pseudo-scalar mesons must be Lorentz invariant and also be symmetric under chiral transformation. The chiral perturbation theory in its modern form was first systematized by

³We refer to Ref.[14] and references therein for a detailed discussion on the existence of an isomorphic mapping between the coset space G/H and the Goldstone fields and related discussions.

⁴In this prescription which was put forward by Callan, Coleman, Wess and Zumino[6, 7], one picks $\xi = \exp(iB \cdot \phi(x))$ where B is a set of broken generators and the Goldstone fields are the $\phi^i(x)$.

Weinberg[8]. The full effective Lagrangian can be written in terms of sub-terms with a definite number of derivatives as

$$\mathcal{L}_{eff} = \sum_n \mathcal{L}_n, \quad (1.55)$$

Where n denotes the number of derivatives. The Lagrangian \mathcal{L}_n is of order p^n because it contains operators with n number of derivatives. We can then obtain the lowest order Lagrangian in the chiral limit, denote by \mathcal{L}_2 , taking into account the unitarity of the U matrix: $UU^\dagger = 1$,

$$\mathcal{L}_2 = \frac{F_0^2}{4} \langle \partial_\mu U^\dagger \partial^\mu U \rangle. \quad (1.56)$$

$\langle X \rangle$ denotes the trace of the matrix X . The constant F_0 is related to the pion decay constant. To prove this claim, Noether currents of the G symmetry are found

$$\begin{aligned} V_\mu^i &= -\frac{iF_0^2}{4} \langle \lambda^i (U^\dagger \partial_\mu U + U \partial_\mu U^\dagger) \rangle \\ A_\mu^i &= i\frac{F_0^2}{4} \langle \lambda^i (U^\dagger \partial_\mu U - U \partial_\mu U^\dagger) \rangle, \end{aligned} \quad (1.57)$$

Where, V_μ^i and A_μ^i are the vector and axial currents respectively and $i = 1, \dots, 8$. On the other hand, the pion decay constant is defined through the matrix element

$$\langle 0 | A_\mu^i | \pi^j(\mathbf{p}) \rangle = if_\pi p_\mu \delta^{ij}. \quad (1.58)$$

If we plug in the meson field $U(\phi)$ in the axial current given above, to leading order we find that

$$A_\mu^i = \frac{F_0}{\sqrt{2}} \langle \lambda^i \partial_\mu \phi \rangle. \quad (1.59)$$

Now by comparing Eq. (1.58) and Eq. (1.59) it can be read that F_0 is actually the pion decay constant. So far we have assumed that the chiral symmetry is exact. However, in reality the chiral symmetry is explicitly softly broken due to the small quark masses. This is induced by the mass term $\bar{q}_R \mathcal{M} q_L + \bar{q}_L \mathcal{M}^\dagger q_R$ in which $\mathcal{M} = \text{diag}(m_u, m_d, m_s)$ and m_i is the current quark mass.⁵ In order to incorporate the mass term in the chiral Lagrangian, the quark mass matrix has to be promoted to a spurion with the chiral transformation

$$\mathcal{M} \rightarrow g_R \mathcal{M} g_L^\dagger, \quad \mathcal{M}^\dagger \rightarrow g_L \mathcal{M}^\dagger g_R^\dagger. \quad (1.60)$$

⁵The current quark mass is QCD scale dependent and should not be confused with the constituent quark masses of the quark model.

This allows the inclusion of all the symmetry breaking operators to the effective Lagrangian in such a way that mass term is rendered chirally invariant. The leading order of such terms is $\langle U\mathcal{M}^\dagger + \mathcal{M}U^\dagger \rangle$, when added to Eq. (1.56) it gives rise to the leading order chiral Lagrangian

$$\mathcal{L}_2 = \frac{F_0^2}{4} (\langle \partial_\mu U^\dagger \partial^\mu U \rangle + 2B_0 \langle U\mathcal{M}^\dagger + \mathcal{M}U^\dagger \rangle). \quad (1.61)$$

The constant B_0 is related to the vacuum expectation value

$$\langle \bar{q}q \rangle = -F_0^2 B_0 (1 + \mathcal{O}(\mathcal{M})), \quad q = (u, d, s). \quad (1.62)$$

Quark masses are counted as $\mathcal{O}(p^2)$ because of the relation $m_{\pi^0}^2 = B_0(m_u + m_d)$ that we will shortly obtain. Even at the this order we are able to obtain interesting results on the relation among meson masses as well as the quark mass ratios. One needs to look at terms in the Lagrangian that have the form $\langle \phi^2 M \rangle$ from where we can read the meson masses in terms of quark masses and the effective constant B_0 . If we do so it will be found that there is an off-diagonal term involving the $\pi - \eta$ fields followed by the constant $m_d - m_u$. This then requires to diagonalize the mass matrix and consequently will bring in the lowest order mixing angle

$$\tan(2\epsilon) = \frac{\sqrt{3} m_d - m_u}{2 m_s - \hat{m}}, \quad \hat{m} = (m_u + m_d)/2. \quad (1.63)$$

We ignore here the explicit calculations and only present the result for meson masses at first order in $m_d - m_u$,

$$\begin{aligned} m_{\pi^0}^2 &= m_{\pi^\pm}^2 + \mathcal{O}((m_d - m_u)^2) = 2B_0\hat{m}, \\ m_{K^0}^2 &= B_0(m_s + \hat{m}) + B_0(m_d - m_u)/2, \\ m_{K^\pm}^2 &= B_0(m_s + \hat{m}) - B_0(m_d - m_u)/2, \\ m_\eta^2 &= 2B_0(\hat{m} + 2m_s)/3. \end{aligned} \quad (1.64)$$

The meson masses in Eq. (1.64) satisfy the Gell-Mann-Okubo (GMO) relation $m_\eta^2 = (2m_{K^+}^2 + 2m_{K^0}^2 - m_\pi^2)/3$. Using the physical masses for the mesons, it turns out that this relation is fulfilled up to about 10 per cent, arising from higher order corrections. From the relations for the meson masses given in Eq. (1.64) we can readily extract the quark mass ratio \hat{m}/m_s as

$$\frac{\hat{m}}{m_s} = \frac{m_\pi^2}{m_{K^+}^2 + m_{K^+}^2 - m_\pi^2}. \quad (1.65)$$

Using the physical values $m_\pi = 0.134$ GeV, $m_{K^+} = 0.493$ GeV and $m_{K^0} = 0.497$ GeV, we find for the quark mass ratio $\hat{m}/m_s \approx 1/27$. To obtain the

ratio m_u/m_d , requires some more efforts. Eq. (1.64) provides the mass splitting among kaons due to the strong interactions which is of the form $(m_{K^0}^2 - m_{K^+}^2)_{QCD} = B_0(m_d - m_u)$ and that for pions is $(m_{\pi^0}^2 - m_{\pi^+}^2)_{QCD} = \mathcal{O}((m_d - m_u)^2)$. The latter being of second order in $(m_d - m_u)$ is considered to be negligible. In addition, we have the relation $(m_{K^0}^2 - m_{K^+}^2)_{em} = (m_{\pi^0}^2 - m_{\pi^+}^2)_{em}$. This is in fact the Dashen's theorem which is correct to lowest order in electromagnetic effects and quark masses. Merging these relations together leads us to obtain the value of $B_0(m_d - m_u)$ in terms of measurable meson masses as

$$\begin{aligned} (m_{K^0}^2 - m_{K^+}^2)_{QCD} &= B_0(m_d - m_u) \\ &= m_{K^0}^2 - m_{K^+}^2 - m_{\pi^0}^2 + m_{\pi^+}^2. \end{aligned} \quad (1.66)$$

From this relation and with $m_\pi^2 = B_0(m_d + m_u)$, we arrive at

$$\frac{m_d - m_u}{m_d + m_u} = \frac{m_{K^0}^2 - m_{K^+}^2 - m_{\pi^0}^2 + m_{\pi^+}^2}{m_\pi^2}. \quad (1.67)$$

Pitting in the physical masses $m_{\pi^0} = 0.134$ GeV, $m_{\pi^+} = 0.139$ GeV along with kaon masses given above we get $m_u/m_d \approx 0.55$. It is important to notice that the absolute value of the quark masses cannot be extracted from chiral perturbation theory (ChPT) alone.

Before we finish this section it is worthwhile to briefly address the problem of elastic $\pi\pi$ scattering at leading order in ChPT. The S-matrix can be written for the scattering $\pi^i\pi^j \rightarrow \pi^k\pi^l$ as

$$S_{ij,kl} = \lim_{t \rightarrow \infty(1-i\epsilon)} \langle \pi^i(p_1)\pi^j(p_2) | T \left(\exp(i \int d^4x \mathcal{L}_2) \right) | \pi^k(p_3)\pi^l(p_4) \rangle. \quad (1.68)$$

The leading contribution to the non-trivial part of the S-matrix is then

$$T_{ij,kl} = \langle \pi^i(p_1)\pi^j(p_2) | T \left(\int d^4x \mathcal{L}_2 \right) | \pi^k(p_3)\pi^l(p_4) \rangle, \quad (1.69)$$

Where i,j,k and l stand for the isospin indices. Taking into account the crossing symmetry and isospin invariance of the T-matrix, the T-matrix can be written in terms of analytic function $A(s, t, u)$ as

$$T_{ij;kl}(s, t, u) = A(s, t, u)\delta_{ij}\delta_{kl} + A(t, s, u)\delta_{ik}\delta_{jl} + A(u, t, s)\delta_{il}\delta_{jk} \quad (1.70)$$

Where the Mandelstam variables are

$$s = (p_i + p_j)^2, \quad t = (p_i - p_k)^2, \quad u = (p_i - p_l)^2. \quad (1.71)$$

For our purpose, the relevant terms in \mathcal{L}_2 are those with at most four meson fields. For these we have obtained

$$\begin{aligned} \mathcal{L}_2 &= 1/3F_0^2(B_0\hat{m}\pi^0\pi^+\pi^-\pi^- - \pi^0\pi^0\partial_\mu\pi^+\partial^\mu\pi^- - \partial_\mu\pi^0\partial^\mu\pi^+\pi^-\pi^- \\ &\quad + \pi^0\partial_\mu\pi^0\partial^\mu\pi^+\pi^- + \pi^0\partial_\mu\pi^0\pi^+\partial^\mu\pi^-) + \dots, \end{aligned} \quad (1.72)$$

Where, ellipses stand for terms with higher number of fields. To evaluate the function $A(s,t,u)$, we consider the scattering $\pi^+\pi^- \rightarrow \pi^0\pi^0$. In Eq. (1.69), we use the Wick's theorem to reduce the T-product (Time-ordered product) to N-product (Normal-ordered product) of contractions. At tree-level all four fields are non-contracted and act on the initial and final-state particles. Note that each derivative brings out a factor of ip_i when acted on the initial or final-state with momentum p_i . After explicit calculations are done, we find for the scattering amplitude

$$M(p_1, p_2, p_3, p_4) = \frac{1}{3F_0^2}(2B_0\hat{m} + 2p_1.p_2 + 2p_3.p_4 + p_1.(p_3 + p_4) + p_2.(p_3 + p_4)). \quad (1.73)$$

Furthermore, it is possible to write the momenta in terms of one single Mandelstam variable. We have $s = (p_1 + p_2)^2 = (2p_1.p_2 + 2m_\pi^2)$ and also $s = (p_3 + p_4)^2 = (2p_3.p_4 + 2m_\pi^2)$. From here two products $p_1.p_2$ and $p_3.p_4$ can be eliminated in favor of s . Using the relation $m_\pi^2 = 2B_0\hat{m}$, we obtain

$$A(s, t, u) = \frac{1}{F_0^2}(s - m_\pi^2). \quad (1.74)$$

This is in full accord with the current algebra result obtained by Weinberg in the sixties[9].

1.5.3 Chiral Effective Lagrangian with Local Flavor Symmetry

To get more benefits out of the chiral Lagrangian, the method of external fields is introduced[10]. In this approach one incorporates the coupling of classical external fields to quarks along with a set of appropriate field transformations. This then allows the computation of Green functions of quark currents by the use of the effective Lagrangian. First let us consider the extended QCD Lagrangian

$$\begin{aligned} \mathcal{L}_{QCD} &= \mathcal{L}_{QCD}^0 + \bar{q}\gamma^\mu(v_\mu + \gamma_5 a_\mu)q - \bar{q}(s + ip)q, \\ \mathcal{L}_{QCD}^0 &= -\frac{1}{4}G_a^{\mu\nu}G_{\mu\nu}^a + \bar{q}_R i\gamma^\mu D_\mu q_R + \bar{q}_L i\gamma^\mu D_\mu q_L. \end{aligned} \quad (1.75)$$

The fields s, p, v_μ and a_μ are 3×3 Hermitian matrices in flavor space and denote the scalar, pseudo-scalar, vector and axial-vector external fields respectively. The external field approach allows the global flavor symmetry to be promoted to a local one. The set of appropriate field transformations under local chiral

symmetry are

$$\begin{aligned}
q_L &\rightarrow g_L(x)q_L, \\
q_R &\rightarrow g_R(x)q_R, \\
l_\mu &\equiv v_\mu - a_\mu \rightarrow g_L l_\mu g_L + i g_L \partial_\mu g_L^\dagger, \\
r_\mu &\equiv v_\mu + a_\mu \rightarrow g_R l_\mu g_R + i g_R \partial_\mu g_R^\dagger, \\
s + ip &\rightarrow g_R(s + ip)g_L^\dagger.
\end{aligned} \tag{1.76}$$

If we now regard these external fields also as external fields in the effective Lagrangian which we have already built in the last section, it then seems possible to write down the effective action with the *local* chiral symmetry. The fields a_μ and v_μ get involved in the covariant derivatives

$$D_\mu U = \partial_\mu U - ir_\mu U + iUl_\mu, \quad D_\mu U^\dagger = \partial_\mu U^\dagger + iU^\dagger r_\mu - il_\mu U^\dagger, \tag{1.77}$$

and also through the field strength tensors

$$F_L^{\mu\nu} = \partial^\mu l^\nu - \partial^\nu l^\mu - i[l^\mu, l^\nu], \quad F_R^{\mu\nu} = \partial^\mu r^\nu - \partial^\nu r^\mu - i[r^\mu, r^\nu]. \tag{1.78}$$

Given all these, generalization of the Lagrangian \mathcal{L}_2 obtained in Eq. (1.61) can be done by changing the derivatives to covariant derivatives as

$$\mathcal{L}_2 = \frac{F_0^2}{4} (\langle D_\mu U^\dagger D^\mu U \rangle + \langle U \chi^\dagger + \chi U^\dagger \rangle). \tag{1.79}$$

Where $\chi = 2B_0(s + ip)$. The quark masses are involved in the scalar external field s , so that $s = \mathcal{M} + s_{ext}$. We can also attribute physical gauge fields to the vector and axial-vector external fields. In terms of left-handed and right-handed external fields we have

$$\begin{aligned}
r_\mu &= e\mathcal{Q}A_\mu + r_\mu ext, \\
l_\mu &= e\mathcal{Q}A_\mu + \frac{e}{\sqrt{2}\sin(\theta_W)}(W_\mu^\dagger T_+ + h.c.) + l_\mu ext,
\end{aligned} \tag{1.80}$$

Where, A_μ is the photon field and W^+ stands for the electroweak gauge boson field. θ_W is the Weinberg mixing angle. \mathcal{Q} denotes the quark-charge matrix and T_+ is a 3×3 unitary matrix containing the relevant quark-mixing angles of the full Cabibbo-Kobayashi-Maskawa (CKM) matrix:

$$\mathcal{Q} = \begin{pmatrix} \frac{2}{3} & 0 & 0 \\ 0 & -\frac{1}{3} & 0 \\ 0 & 0 & -\frac{1}{3} \end{pmatrix}, \quad T_+ = \begin{pmatrix} 0 & V_{ud} & V_{us} \\ 0 & 0 & 0 \\ 0 & 0 & 0 \end{pmatrix}. \tag{1.81}$$

Physical observables defined as various correlation functions can be obtained by taking functional derivatives of generating functional with respect to

the external fields. The generating functional are defined in the path integral formalism. At very low energy we *assume*

$$\begin{aligned} e^{iZ(s,p,v,a)} &= \frac{1}{Z_0} \int \mathcal{D}q \mathcal{D}\bar{q} \mathcal{D}G_\mu \exp\left(i \int d^4x \mathcal{L}_{QCD}(x)\right) \\ &= \frac{1}{Z_0} \int \mathcal{D}U \exp\left(i \int d^4x \mathcal{L}_{ChPT}(x)\right). \end{aligned} \quad (1.82)$$

For example, the expectation value of the quark condensate can be achieved by varying the generating functional with respect to the scalar external field as

$$\langle \bar{q} \lambda^a q \rangle = \frac{1}{Z_0} \left(-i \frac{\delta}{\delta s^a} \right) \exp(iZ(s,p,v,a))|_{s=p=v=a=0}, \quad (1.83)$$

Where s^a are defined via $s = s^0 + \sum_{a=1}^8 \lambda^a s^a$ and the λ^a stand for the Gell-Mann matrices and s^0 may be regarded as the matrix \mathcal{M} , the quark mass matrix. In section (1.9) we will work out as an example, the expectation value of quark condensate up to one-loop order in chiral perturbation theory.

1.6 Higher Order Chiral Lagrangians

The main motivation for the construction of the chiral Lagrangians of higher orders is that they are essential for the inclusion of the quantum effects. In doing the loop computations by using the vertices from Lagrangian \mathcal{L}_2 , it turns out that the divergences have the form that can not be absorbed by renormalizing the coupling constants or doing the field redefinitions in \mathcal{L}_2 only. Here we have a non-renormalizable theory in that the divergences can only be absorbed by terms or *counter-terms* from those one finds in \mathcal{L}_4 . The most general effective Lagrangian at order p^4 consistent with Lorentz invariance, chiral symmetry and parity was written down by Gasser and Leutwyler[11] as

$$\begin{aligned} \mathcal{L}_4 &= L_1 \langle D_\mu U^\dagger D^\mu U \rangle^2 + L_2 \langle D_\mu U^\dagger D_\nu U \rangle \langle D^\mu U^\dagger D^\nu U \rangle \\ &+ L_3 \langle D^\mu U^\dagger D_\mu U D^\nu U^\dagger D_\nu U \rangle + L_4 \langle D^\mu U^\dagger D_\mu U \rangle \langle \chi^\dagger U + \chi U^\dagger \rangle \\ &+ L_5 \langle D^\mu U^\dagger D_\mu U (\chi^\dagger U + U^\dagger \chi) \rangle + L_6 \langle \chi^\dagger U + \chi U^\dagger \rangle^2 \\ &+ L_7 \langle \chi^\dagger U - \chi U^\dagger \rangle^2 + L_8 \langle \chi^\dagger U \chi^\dagger U + \chi U^\dagger \chi U^\dagger \rangle \\ &- i L_9 \langle F_{\mu\nu}^R D^\mu U D^\nu U^\dagger + F_{\mu\nu}^L D^\mu U^\dagger D^\nu U \rangle \\ &+ L_{10} \langle U^\dagger F_{\mu\nu}^R U F^{L\mu\nu} \rangle + H_1 \langle F_{\mu\nu}^R F^{R\mu\nu} + F_{\mu\nu}^L F^{L\mu\nu} \rangle + H_2 \langle \chi^\dagger \chi \rangle. \end{aligned} \quad (1.84)$$

The unitary matrix $U \in SU(3)$ contains the pseudo-scalar mesons. $\langle X \rangle$ stands for the trace of matrix X. The equation of motion has been used to remove

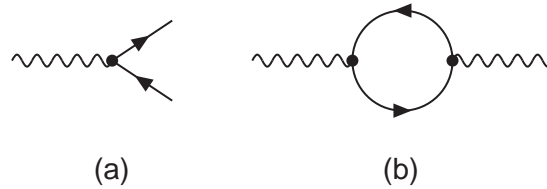


Figure 1.2: (a) Shown the basic photon-electron vertex which shows up in QED and is of order e (electron charge). (b) Feynman diagram of the photon polarization which is of order e^2

dependent terms. There are 10+2 low-energy constants (LECs) in the Lagrangian. The last two terms in the Lagrangian contain only the external fields and are not relevant for low energy physics. The LECs are free parameters which encode the effects of heavy degrees of freedom and get no constraints from chiral symmetry. These LECs, however, can be determined using experimental data. Chiral Lagrangian has been worked out to Next-to-Next-to-leading order[12]. At this order the number of LECs rapidly grows to 94+4.

1.7 Power counting scheme

Power-counting in renormalizable theories is pretty simple, i.e. QED and QCD at high energies. The reason is that for that there is a unique coupling constant attributed to a basic vertex which can be used to determine the strength of a generic Feynman diagram in a perturbative expansion. Fig (1.2a) depicts a vertex of a renormalizable theory, i.e QED with strength e (e is the electron charge). The power-counting of an arbitrary Feynman diagram like that given in Fig (1.2b) is then simply done by counting the number of times the basic vertex in Fig (1.2a) shows up in the graph. So the graph in Fig (1.2b) is of order e^2 .

This, however, is not the case for a non-renormalizable theory like ChPT. At lowest order there is a vertex of order p^2 and the next-to-leading Lagrangian provides order p^4 tree level vertex and so forth. A generic Feynman diagram can then be built out of a combination of various vertices, coming from different orders, hooked up to meson propagators. This implies that a power-counting scheme is a necessary ingredient for a non-renormalizable theory to be able for collecting all the relevant Feynman diagrams of a given chiral order. In Fig. (1.3) we show as an example vertices from chiral Lagrangian of order p^2 and order p^4 and the question is then how to determine the dimensionality of

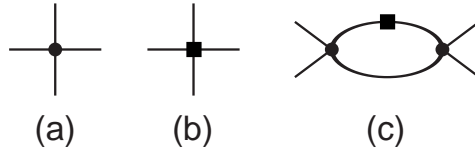


Figure 1.3: (a)-(b) The tree Feynman diagrams taken from chiral Lagrangians \mathcal{L}_2 and \mathcal{L}_4 respectively. (c) A generic Feynman graph which is built out of vertices (a) and (b) and is of order p^6 .

the Feynman diagram in Fig. (1.3c) consisting of vertices of order p^2 and p^4 and meson propagators. Here we consider a generic case and write a Feynman integral which has dimension p^D as

$$\mathcal{A}_D = \int (d^4p)^{N_L} \frac{1}{(p^2)^{N_I}} \prod_n p^{nV_n}, \quad (1.85)$$

Where, N_L is the number of loops, N_I is the number of internal lines and V_n is the number of vertices of order p^n . From Eq. (1.85) we find for D the following relation

$$D = 4N_L - 2N_I + \sum_i nV_n. \quad (1.86)$$

Moreover, there is an identity which links the number of loops and internal lines to the sum of the all vertices in the graph according to

$$N_L - N_I + \sum_n V_n = 1. \quad (1.87)$$

We apply the relation above to eliminate N_I in Eq. (1.86) and thus obtain the dimensionality of a Feynman graph of general form as

$$D = 2 + 2N_L + \sum_n (n-2)V_n. \quad (1.88)$$

In chiral perturbation theory the lowest order is of order p^2 , so $n \geq 2$. It can easily be seen that for a given D, there is only a limited number of graphs that satisfy Eq. (1.88) and this proves that renormalization of a non-renormalizable theory is possible order by order in perturbative expansion. Nevertheless, It should be noted that by going to higher orders, the number of graphs grow rapidly. We discuss the matter of regularization and renormalization in the next section.

1.8 Regularization and Renormalization

Feynman integrals have ultra-violet divergences. We thus need to modify the momentum integrals in such a way that it becomes possible to keep the finite part and the infinite part of the integral separately. By readjusting the bare coupling constants properly, the divergent part can be removed. For this purpose two steps are needed. First, one regularizes the Feynman graphs and then the sum of the regularized graphs should be renormalized.

Dimensional regularization for the computation of the Feynman diagrams, in chiral perturbation theory, is known as a practical choice. It preserves the chiral symmetry and therefore the Ward identities remain valid and no symmetry violating counter-terms are needed.

In this scheme, integrating in dimension $d = 4 - 2\epsilon$ of space-time for sufficiently small ϵ , makes the momentum integral converge. When we Laurent expand the momentum integral in ϵ , the results begin by terms like $\frac{1}{\epsilon^L}$ along with terms accompanied by positive powers of ϵ . L is the number of loops in the integral. In the limit $\epsilon \rightarrow \infty$ these terms are infinite. For example, if we perform a two loop momentum integration, terms with negative powers in ϵ as $\frac{1}{\epsilon^2}$ and $\frac{1}{\epsilon}$ appear in the result. Doing a one-loop integration in dimensional regularization, the divergent part is found to occur in the form

$$\frac{1}{16\pi^2} \left(-\frac{1}{\bar{\epsilon}} + \frac{1}{2} \log(M^2/\mu^2) + \mathcal{O}(\epsilon) \right), \quad (1.89)$$

Where $1/\bar{\epsilon} = 1/\epsilon + \log(4\pi) + 1 - \gamma_E$. Where γ_E is the Euler constant. Through the renormalization procedure we need counter-terms with adjustable coupling constants to remove the pieces proportional to $1/\bar{\epsilon}$. The bare coupling constants L_i should therefore be split into two parts as

$$L_i = L_i^r(\mu) - \frac{\Gamma_i}{32\pi^2} \left(\frac{1}{\bar{\epsilon}} \right) + \mathcal{O}(\epsilon). \quad (1.90)$$

L_i^r s are measurable quantities and can be determined phenomenologically. If Γ_i s are found so that the divergences of the one loop Green functions plus divergences of the tree level diagrams of \mathcal{L}_4 vanish then we say that the amplitude is renormalized at this order. Gasser and Leutwyler applied the background field method and heat kernel technique to compute the divergences at one-loop level. Its result for the Γ^i s are given in Tab.1.1. After renormalization is done, ϵ should be sent to zero. Doing so, we obtain the finite part of the given amplitude which is independent of the regularization parameter ϵ . At first sight it seems that the amplitude is renormalization scale dependent, since both chiral logarithm and L_i^r depend on the subtraction point μ . However, the physical

i	Γ_i [11]	$10^3 L_i^r$ [11]	$10^3 L_i^r$ [19]	Source
1	3/32	0.9 ± 0.3	0.43 ± 0.12	K_{e4} and $\pi\pi$ scattering
2	3/16	1.7 ± 0.7	0.73 ± 0.12	K_{e4} and $\pi\pi$ scattering
3	0	-4.4 ± 2.5	-2.35 ± 0.37	K_{e4} and $\pi\pi$ scattering
4	1/8	0 ± 0.5	0	Zweig rule
5	3/8	2.2 ± 0.5	0.97 ± 0.11	$F_K : F_\pi$
6	11/144	0 ± 0.3	0	Zweig rule
7	0	-0.4 ± 0.15	-0.31 ± 0.14	Gell-Mann-Okubo, L_5, L_8
8	5/48	1.1 ± 0.3	0.6 ± 0.18	$M_{K^0} - M_{K^+}, L_5, \frac{(m_s - \tilde{m})}{(m_d - m_u)}$
9	1/4	7.4 ± 0.7	5.93 ± 0.43 [20]	$\langle r^2 \rangle_{em}^\pi$
10	-1/4	-0.6 ± 0.7		$\pi \rightarrow e\nu\gamma$

Table 1.1: The phenomenological values for the low energy constants L_i^r at the subtraction point $\mu = m_\eta$ [11] and at $\mu = m_\rho$ [19, 20]. The last column indicates the experimental or theoretical sources used to determine the LECs.

observables must be renormalization scale invariance. This will result in the renormalization group equation for the low energy constants (LECs) L_i^r

$$\mu \frac{dL_i^r(\mu)}{d\mu} = -\frac{\Gamma_i}{16\pi^2}. \quad (1.91)$$

Solving the differential equation above gives rise to

$$L_i^r(\mu_2) = L_i^r(\mu_1) + \frac{\Gamma_i}{16\pi^2} \log\left(\frac{\mu_1}{\mu_2}\right). \quad (1.92)$$

In Tab. 1.1 we have collected the values for the LECs and the experimental or theoretical sources where they have been obtained from.

At two-loop level or order p^6 , computations become more involved because now besides the *local* divergences which can be removed by those from counter-terms of order p^6 , there is another type of divergences which are called *nonlocal* divergences. The non-local divergences, however, always cancel in a local quantum field theory. Local divergences of order p^6 can be found in [21].

1.9 Quark-Antiquark Vacuum Expectation Value at One-loop Order

In section (1.5.3) we explained that the introduction of external field technique enlarges the domain of the ChPT applications. Here we have intended to do some detailed calculations regarding the order parameter of the quantum chromo dynamics. To this aim, we use Eq. (1.83) to find $\langle \bar{q}q \rangle$ in terms of \mathcal{L}_{ChPT}

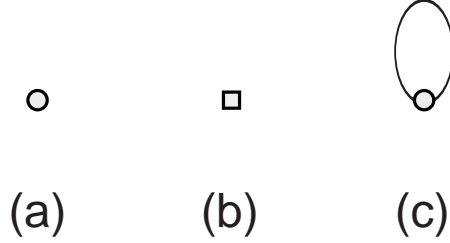


Figure 1.4: (a) The $\langle \bar{q}q \rangle$ insertion of order p^2 , (b) The $\langle \bar{q}q \rangle$ insertion of order p^4 and (c) is the so-called tadpole or one-loop Feynman diagram of order p^4 .

first. We find relations below among various expectation values in the isospin limit

$$\begin{aligned}\langle \bar{q}\lambda^0 q \rangle &= 2\langle \bar{u}u \rangle + \langle \bar{s}s \rangle \equiv \frac{\delta L_{eff}}{\delta s_0}, \\ \langle \bar{q}\lambda^8 q \rangle &= \frac{2}{\sqrt{3}} (\langle \bar{u}u \rangle - \langle \bar{s}s \rangle) \equiv \frac{\delta L_{eff}}{\delta s_8},\end{aligned}\quad (1.93)$$

Where, $L_{eff} = \int d^4x \mathcal{L}_{eff}$ and $\mathcal{L}_{eff} = \mathcal{L}_2 + \mathcal{L}_4 + \dots$. We solve the coupled equations given above for $\langle \bar{u}u \rangle$ and $\langle \bar{s}s \rangle$ in terms of partial derivatives of the chiral Lagrangian.

$$\begin{aligned}\langle \bar{u}u \rangle &= \frac{1}{3} \frac{\delta L_{eff}}{\delta s_0} + \frac{\sqrt{3}}{6} \frac{\delta L_{eff}}{\delta s_8}, \\ \langle \bar{s}s \rangle &= \frac{1}{3} \frac{\delta L_{eff}}{\delta s_0} - \frac{1}{\sqrt{3}} \frac{\delta L_{eff}}{\delta s_8}.\end{aligned}\quad (1.94)$$

To do one-loop order calculations, we need vertices from \mathcal{L}_2 to construct loop diagrams and also tree level vertices from \mathcal{L}_4 as counter-terms. The relevant Feynman diagrams for this quantity up to order p^4 are presented in Fig. (1.4). To construct the tadpole diagram shown in Fig. (1.4c) the relevant terms in \mathcal{L}_2 are those with at most two pion fields and one scalar external field. The kinetic term in \mathcal{L}_2 is free from such terms and only the second term can give the needed terms. We Taylor expand the $U(\phi)$ field and only keep terms with at most two fields, for the relevant term we find

$$\begin{aligned}\mathcal{L}_2 &= -F_0^2/4 \langle (\chi + \chi^\dagger)(1 - \phi^2/F_0^2) \rangle + \dots, \\ &= -F_0^2 B_0 \langle s - s\phi^2/F_0^2 \rangle + \dots,\end{aligned}\quad (1.95)$$

Where, in the last equation we have replaced $\chi = 2B_0(s + ip)$ and only kept the relevant terms. The first term in the Eq. (1.95) gives rise to the leading

order value for the vacuum expectation value. We thus find $\langle \bar{u}u \rangle = \langle \bar{s}s \rangle = -F^2 B_0$. The second term can be written out in terms of pseudo-scalar fields. To calculate the tadpole contribution we construct the matrix element below and plug in the Lagrangian in terms of meson fields

$$\begin{aligned} \langle \bar{q}q \rangle_{tadpole} &= \left\langle \pi | i \int d^4x \mathcal{L}_{ChPT}(x) | \pi \right\rangle, \\ \mathcal{L}_{ChPT}|_{\bar{u}u} &= -iB_0/2 (\pi^0 \pi^0 + 2\pi^+ \pi^- + 1/3 \eta \eta + K^+ K^- + \bar{K}^0 K^0), \\ \mathcal{L}_{ChPT}|_{\bar{s}s} &= -i2B_0 (1/3 \eta \eta + 1/2 K^+ K^- + 1/2 \bar{K}^0 K^0). \end{aligned} \quad (1.96)$$

Here, to proceed we do field contractions for each pair and taking into account the momentum conservation in the vertex and following Feynman rules, we end up having momentum integrals with final results as

$$\begin{aligned} \langle \bar{u}u \rangle_{tadpole} &= (-B_0/2) \int \frac{d^d k}{(2\pi)^d} \left(\frac{3}{k^2 - m_\pi^2} + \frac{1/3}{k^2 - m_\eta^2} + \frac{2}{k^2 - m_K^2} \right), \\ \langle \bar{s}s \rangle_{tadpole} &= (-2B_0) \int \frac{d^d k}{(2\pi)^d} \left(\frac{1/3}{k^2 - m_\eta^2} + \frac{1}{k^2 - m_K^2} \right). \end{aligned} \quad (1.97)$$

To perform the integrals, dimensional regularization is implemented and we have found

$$\begin{aligned} \langle \bar{u}u \rangle_{tadpole} &= B_0/16\pi^2 ((3/2m_\pi^2 + 1/6m_\eta^2 + m_K^2)/\bar{\epsilon} \\ &\quad - 3/2m_\pi^2 \log(m_\pi^2/\mu^2) - 1/6m_\eta^2 \log(m_\eta^2/\mu^2) \\ &\quad - m_K^2 \log(m_K^2/\mu^2)), \end{aligned} \quad (1.98)$$

$$\begin{aligned} \langle \bar{s}s \rangle_{tadpole} &= B_0/16\pi^2 ((2/3m_\eta^2 + 2m_K^2)/\bar{\epsilon} \\ &\quad - 2/3m_\eta^2 \log(m_\eta^2/\mu^2) - 2m_K^2 \log(m_K^2/\mu^2)), \end{aligned} \quad (1.99)$$

Where, $1/\bar{\epsilon} = 1/\epsilon - \gamma_E + 1 + \log(4\pi)$. The last piece to be computed is counter-terms (CTs) with vertices taken from \mathcal{L}_4 as shown in Fig. (1.4b). These are necessary ingredients to be able to remove the infinities we encountered. At this order, we collect terms with at most two powers of the scalar external field and no pion field is necessary. Our final results for the counter-term contribution read

$$\begin{aligned} \langle \bar{u}u \rangle_{CT} &= B_0^2 (32(2\hat{m} + m_s)L_6 + 16\hat{m}L_8 + 8\hat{m}H_2), \\ \langle \bar{s}s \rangle_{CT} &= B_0^2 (32(2\hat{m} + m_s)L_6 + 16m_s L_8 + 8m_s H_2). \end{aligned} \quad (1.100)$$

Meson masses to leading order are given in Eq. (1.64). We use these relations to replace the quark masses, and we find

$$\begin{aligned} \langle \bar{u}u \rangle_{CT} &= B_0 ((16m_\pi^2 + 32m_K^2)L_6 + 8m_\pi^2 L_8 + 4m_\pi^2 H_2), \\ \langle \bar{s}s \rangle_{CT} &= B_0 ((16m_\pi^2 + 32m_K^2)L_6 + (16m_K^2 - 8m_\pi^2)L_8 \\ &\quad + (8m_K^2 - 4m_\pi^2)H_2). \end{aligned} \quad (1.101)$$

The infinities we found in the one-loop integrals can be removed by renormalizing the LECs in the counter-terms. We replace the bare LECs by those given below

$$\begin{aligned}
L_6 &= L_6^r - \frac{\Gamma_6}{32\pi^2} \frac{1}{\bar{\epsilon}}, & \Gamma_6 &= 11/144, \\
L_8 &= L_8^r - \frac{\Gamma_8}{32\pi^2} \frac{1}{\bar{\epsilon}}, & \Gamma_8 &= 5/48, \\
H_2 &= H_2^r - \frac{\Delta_2}{32\pi^2} \frac{1}{\bar{\epsilon}}, & \Delta_2 &= 5/24.
\end{aligned} \tag{1.102}$$

At the end, we write the expectation value up to order p^4 normalized to lowest order (LO) value, $\langle \bar{u}u \rangle_{LO} = \langle \bar{u}u \rangle_{LO} = -F_0^2 B_0$. We find

$$\begin{aligned}
\langle \bar{u}u \rangle / \langle \bar{u}u \rangle_{LO} &= 1 - 1/F_0^2 (3/2 \bar{A}_\pi + 1/6 \bar{A}_\mu + \bar{A}_K \\
&\quad + 16 m_\pi^2 L_6^r + 8 m_\pi^2 L_8^r + 32 m_K^2 L_8^r + 4 m_K^2 H_2^r).
\end{aligned} \tag{1.103}$$

$$\begin{aligned}
\langle \bar{s}s \rangle / \langle \bar{s}s \rangle_{LO} &= 1 - 1/F_0^2 (2/3 \bar{A}_\mu + 2 \bar{A}_K + 16 m_\pi^2 L_6^r + 32 m_K^2 L_6^r \\
&\quad - 8 m_\pi^2 L_8^r + 16 m_K^2 L_8^r + 16 m_K^2 H_2^r - 4 m_\pi^2 H_2^r).
\end{aligned} \tag{1.104}$$

Where, $\bar{A}_N = -(m_N^2/16\pi^2) \log(m_N^2/\mu^2)$. As can be seen, at one-loop level the vacuum expectation value cannot be defined unambiguously, since it depends on the subtraction constant H_2^r . At leading order however, this was not the case.

1.10 Kaon Semi-leptonic Decays and V_{us}

The unitary 3×3 Cabibbo-Kobayashi-Maskawa (CKM) matrix relates the quark weak eigenstates to mass eigenstates. The quark mixing phenomenon occurs in the weak charged interactions of quarks in the Standard model. Its matrix elements are

$$V_{CKM} = \begin{pmatrix} V_{ud} & V_{us} & V_{ub} \\ V_{cd} & V_{cs} & V_{cb} \\ V_{td} & V_{ts} & V_{tb} \end{pmatrix}. \tag{1.105}$$

The matrix elements are free parameters in the Standard model and can be extracted from experimental data. For the case with two generation the CKM matrix reduces to the Cabibbo matrix with only one parameter, namely Cabibbo angle θ_C . Moreover the CKM matrix can be written in terms of Wolfenstein parameters (λ, A, ρ, η) as

$$V_{CKM} = \begin{pmatrix} 1 - \lambda^2/2 & \lambda & A\lambda^3(\rho - i\eta) \\ -\lambda & 1 - \lambda^2/2 & A\lambda^2 \\ A\lambda^3(1 - \rho - i\eta) & -A\lambda^2 & 1 \end{pmatrix}. \tag{1.106}$$

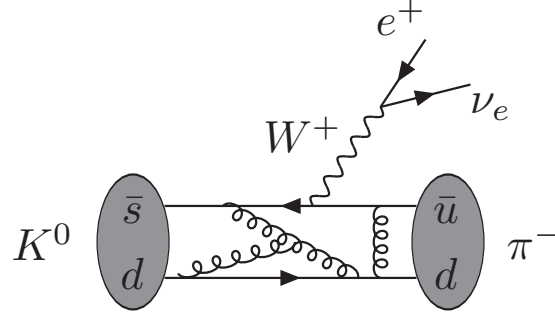


Figure 1.5: The semi-leptonic kaon decay is shown. The solid lines represent the quarks and the wiggly lines stand for the gluons. The propagation of the weak boson is shown by curly line.

Unitarity of the CKM matrix in the first row implies the following constraint on three matrix element

$$|V_{ud}|^2 + |V_{us}|^2 + |V_{ub}|^2 = 1. \quad (1.107)$$

Any deviation from unitary found is in conflict with the Standard model and may signal a potential new physics. From Particle Data Group it reads: $V_{ud} = 0.97383$, $V_{us} = 0.2272$ and $V_{ub} = 0.00396$. Our focus is on the determination of the matrix element V_{us} . Hyperon and semi-leptonic kaon decays are the main sources to determine V_{us} . However, the Hyperon decays are disfavored because of larger theoretical uncertainties associated with the SU(3) breaking calculations. The semi-leptonic kaon decays are known as $K \rightarrow \pi l \nu_l$, namely, $K^0 \rightarrow \pi^- l^+ \nu_l$ and $K^+ \rightarrow \pi^0 l^+ \nu_l$ where the final state lepton can be an electron or a muon. Figure. (1.5) depicts a schematic Feynman diagram of kaon decay via weak charged interaction. As shown in this interaction both non perturbative strong interactions and the electroweak interactions are involved. The hadronic matrix element can be parameterized in terms of two formfactors

$$\begin{aligned} \langle \pi^-(p_\pi) | \bar{s} \gamma_\mu u | K^0(p_K) \rangle &= (p_K + p_\pi) f_+^{K^0 \pi^-}(t) + (p_K - p_\pi) f_-^{K^0 \pi^-}(t), \\ \langle \pi^0(p_K) | \bar{s} \gamma_\mu u | K^+(p_\pi) \rangle &= \frac{1}{\sqrt{2}} \left((p_K + p_\pi) f_+^{K^+ \pi^0}(t) + (p_K - p_\pi) f_-^{K^+ \pi^0}(t) \right). \end{aligned} \quad (1.108)$$

The formfactors in two processes are related due to the isospin. This implies that $f_\pm^{K^0 \pi^-} = f_\pm^{K^+ \pi^0}$. The decay rate is given in the master formula below where the effects of the strong interactions and weak interactions are factorized

into the calculable quantities

$$\Gamma(K^0 \rightarrow \pi^- e^+ \nu_e) = \frac{G_F^2 S_{EW} m_K^2}{192\pi^3} |V_{us} f_+^{K^0\pi^-}(0)|^2 I_{e^+} (1 + 2\Delta_{EM}), \quad (1.109)$$

Where S_{EW} is the short distance radiative corrections. Δ_{EM} stands for the model dependent long-distance QED corrections. The phase space integral is denoted by I_{e^+} which is a function of the slope parameters of the formfactors. Besides the slope parameters needed in the phase space integral, the only piece which is responsible of long distance strong interaction is encoded in the vector formfactor $f_+^{K^0\pi^-}$ at zero momentum transfer. To extract the value of V_{us} with high precision, precise theoretical evaluations of the quantities defined above are demanding. Among these, determination of the vector form-factor $f_+(0)$ has been further studied in the last paper including the isospin breaking effects to this quantity. At leading chiral order the vector form-factors are normalized to unity, $f_+^{K^0\pi^-}(0) = f_+^{K^+\pi^0}(0) = 1$. According to the Ademollo-Gatto's theorem, deviation of $f_+^{K^0\pi^-}(0)$ from unity is of order $(m_s - \hat{m})^2$ or SU(3) symmetry breaking while that for $f_+^{K^+\pi^0}(0)$ can gain corrections of first order in SU(2) symmetry breaking, namely of order $(m_d - m_u)$.

1.11 The Papers

A brief summary for each paper is provided in this section. All works are done within the framework of the chiral perturbation theory. The evaluation of the quantum effects via the application of the Feynman diagrammatic approach is the main technology employed in all works. The analytical results are typically very long at two loop order and this requires systematic calculations and many cross-checks.

Paper I

In this article we have investigated the finite volume corrections to the vacuum expectation value $\langle \bar{q}q \rangle$ in SU(3) chiral perturbation theory (ChPT) at two loop order accuracy. We have then confronted the ChPT calculations with that obtained from an extended Lüscher formula for the said quantity. Although Lattice *QCD* computations can now be performed with fairly small quark masses, extrapolation to the physical masses is still essential. The finite size effects come about as a modification in the propagators since the finite size of the lattice leads to the momentum discretization and this in effect develops a different type of infrared singularities. The boundary conditions imposed on the lattice, however is not going to alter the ultra-violet infinities, because at

very large energy the discretized momenta tends to the continuous limit. In an interesting article Lüscher found an asymptotic formula in which the physical mass shift due to the finite volume is related to the elastic scattering amplitude evaluated in infinite volume. An important outcome in Lüscher's article concerning the mass shift was that in the leading large L (The lattice size) the relevant Feynman diagrams contribute with only one propagator which has to be evaluated in finite volume. The computation of these Feynman diagrams led him to drive his asymptotic formula. In this paper, an asymptotic formula is found for the quark condensate. On the other hand, the finite volume corrections are evaluated by directly performing the Feynman integrals in finite-volume.

Paper II

Here I sketch out the results concerning the eta decay to three pions presented in the second paper.

For this process, the strong interaction is dominated and the electromagnetic effects are safely negligible. Chiral perturbation theory (ChPT) is employed for this study. This decay is an $\Delta I = 1$ transition and therefore the decay width is proportional to the value $m_d - m_u$. In order to pull out the overall mixing angle we do a Taylor expansion of the loop integrals involving two charged kaons around the neutral kaon mass. In principle this decay provides an exceptional tool for the estimation of the value $m_d - m_u$. The decay rate at tree level is known since the sixties and it is badly in conflict with the experiment. In this work we have done a full next-to-next-leading order (NNLO) calculation in the same line as the one loop corrections (NLO) was done by Gasser and Leutwyler some years back. On the basis of the dispersion analysis, its result also account on the large quantum correction. We have also addressed the question of convergence in this study. we find somewhat larger correction in comparison with the dispersive analysis but the convergence is reasonably acceptable.

We have also compared the Dalitz plot distribution in $\eta \rightarrow \pi^0\pi^+\pi^-$ with the experiment where we have used a standard parameterization for the Dalitz plot as $|M|^2 = M_0^2(1+ay+by^2+dx^2+fy^3+gx^2y+...)$ and $|\bar{M}|^2 = \bar{M}_0^2(1+2\alpha z+...)$. The changes in the Dalitz parameters in going from NLO to NNO is mild but the change in the overall factor, M_0^2 , is sizable. We find the Dalitz plot parameters for the decay $\eta \rightarrow \pi^0\pi^+\pi^-$ as $M_0^2 = 538 \pm 18$, $a = -1.271 \pm .0075$, $b = .394 \pm .102$, $d = .055 \pm .057$, $f = .025 \pm .160$. and for the decay $\eta \rightarrow \pi^0\pi^0\pi^0$ as $\bar{M}_0^2 = 4790 \pm 160$ and $\alpha = .013 \pm .032$. Our theoretical result for the Dalitz plot parameters near the experimental values less than expected and this is puzzling to us because using the same input parameters has given rise to a good result for the $\pi\pi$ scattering length where the S-wave scattering makes up the main effects as in the case of η decay.

Our result for the ratio of the decay rates $r = \frac{\Gamma(\eta \rightarrow \pi^0 \pi^0 \pi^0)}{\Gamma(\eta \rightarrow \pi^0 \pi^+ \pi^-)}$ reads $r_{NNLO} = 1.47$ which is in very good agreement with experimental result $r_{exp} = 1.49 \pm .06$.

For the decay width at NNLO we obtain $\Gamma(\eta \rightarrow \pi^0 \pi^+ \pi^-) = \sin^2 \epsilon 2.33 MeV$. Using the experimental result $\Gamma_{exp}(\eta \rightarrow \pi^0 \pi^+ \pi^-) = 296 \pm 15 eV$ we obtain $R = 42.2$ where we have defined $\sin(\epsilon) = \frac{\sqrt{3}}{4} \frac{m_d - m_u}{m_s - \hat{m}} = \frac{\sqrt{3}}{4} \frac{1}{R}$.

Paper III

In this paper we have studied the vector and scalar form factors of the semi-leptonic kaon decays. As improvements the isospin breaking effects are included. This is done for four different processes. Two weak charged kaon decays namely $K^+ \rightarrow \pi^0 l \nu_l$ and $K^0 \rightarrow \pi^- l \nu_l$ as well as two rare weak kaon decays, namely $K \rightarrow \pi l l$ and $K \rightarrow \pi \nu \nu$. We have defined a set of form-factor ratios which are sensitive to the isospin breaking effects. We have also computed the vector formfactor $f_+(t)$ and scalar form-factor $f_+(t)$ at $t = 0$ and also its behavior by varying the momentum transfer t . Finally we have computed corrections to the Callen-Treiman relation for the four process mentioned above.

References

- [1] Michael E. Peskin, Daniel V. Schroeder, An Introduction to Quantum Field Theory, Westview press 1995
- [2] Lewis H. Ryder, Quantum Field Theory, Cambridge University press 1996
- [3] John F. Donoghue, Eugene Golowich and Barry R. Holstein, Dynamics of the Standard Model, Cambridge University Press 1992
- [4] J. Wess and B. Zumino, Phys. Lett. B **37** (1971) 95.
- [5] E. Witten, Nucl. Phys. B **223** (1983) 422.
- [6] S. R. Coleman, J. Wess and B. Zumino, Phys. Rev. **177** (1969) 2239.
- [7] C. G. Callan, S. R. Coleman, J. Wess and B. Zumino, Phys. Rev. **177** (1969) 2247.
- [8] S. Weinberg, Physica A **96** (1979) 327.
- [9] S. Weinberg, Phys. Rev. Lett. **17** (1966) 616.
- [10] J. Gasser and H. Leutwyler, Annals Phys. **158** (1984) 142.
- [11] J. Gasser and H. Leutwyler, Nucl. Phys. B **250** (1985) 465.

-
- [12] J. Bijnens, G. Colangelo and G. Ecker, *Annals Phys.* **280** (2000) 100 [arXiv:hep-ph/9907333].
 - [13] H. Leutwyler, arXiv:hep-ph/0008124.
 - [14] S. Scherer, *Adv. Nucl. Phys.* **27** (2003) 277 [arXiv:hep-ph/0210398].
 - [15] A. V. Manohar, arXiv:hep-ph/9606222.
 - [16] S. R. Coleman and E. Witten, *Phys. Rev. Lett.* **45** (1980) 100.
 - [17] S. A. Gottlieb, W. Liu, D. Toussaint, R. L. Renken and R. L. Sugar, *Phys. Rev. D* **35** (1987) 3972.
 - [18] J. Bijnens, J. Prades and E. de Rafael, *Phys. Lett. B* **348** (1995) 226 [arXiv:hep-ph/9411285].
 - [19] G. Amoros, J. Bijnens and P. Talavera, *Nucl. Phys. B* **602** (2001) 87 [arXiv:hep-ph/0101127].
 - [20] J. Bijnens and P. Talavera, *JHEP* **0203**, 046 (2002) [arXiv:hep-ph/0203049].
 - [21] J. Bijnens, G. Colangelo and G. Ecker, *JHEP* **9902** (1999) 020 [arXiv:hep-ph/9902437].

Acknowledgments

I would like to thank my advisor Hans Bijnens, for many fruitful discussions and encouragements especially for the last two years since we embarked on research. It was a great opportunity to work with him and learn a great deal of perturbative calculations and analysis of a non-perturbative nature. I wish to thank Gösta Gustafson for a very kind hospitality he extended to me on my arrival to Lund. I was engaged in interesting discussions with Gösta Gustafson, Leif Lönnblad and Torbjörn Sjöstrand, so I would like to thank them. Parsa and Claudia, we had a great time in Lund. Thank you for coming all the way to Sweden.

Finite Volume Dependence of the
Quark-antiquark Vacuum
Expectation Value

Paper I

LU TP 06-11
hep-lat/0602019
Revised March 2006

Finite Volume Dependence of the Quark-Antiquark Vacuum Expectation Value¹

Johan Bijnens and Karim Ghorbani

Department of Theoretical Physics, Lund University
Sölvegatan 14A, SE 22362 Lund, Sweden

Abstract

A general formula is derived for the finite volume dependence of vacuum expectation values analogous to Lüscher's formula for the masses. The result involves no integrals over kinematic quantities and depends only on the matrix element between pions at zero momentum transfer thus presenting a new way to calculate the latter, i.e. pion sigma terms.

The full order p^6 correction to the vacuum condensate $\langle \bar{q}q \rangle$ is evaluated and compared with the result from the Lüscher formula. Due to the size of the p^6 result no conclusion about the accuracy of the Lüscher formula can be drawn.

¹Reprinted with permission from Physics Letters B 636 (2006). Copyright (2006) Elsevier B.V.

2.1 Introduction

Quantum Chromo Dynamics (QCD) at low energy remains a difficult problem. One of the ways to deal with this problem is to numerically evaluate the functional integral of QCD. This approach, known as lattice QCD, has now reached the stage where realistic calculations with fairly light quark masses are now possible. One side effect of this is that finite volume corrections are becoming more important. Luckily in many cases these corrections can be evaluated analytically using Chiral Perturbation Theory (ChPT) [1, 2]. The application of ChPT to finite volume was started by Gasser and Leutwyler [3]. A review of recent work in this area can be found in [4]. Note that ChPT is applicable to finite volume as soon as the typical momenta that are relevant are small enough. This imposes a size restriction on the volume as

$$F_\pi L > 1. \quad (2.1)$$

Here F_π is the pion decay constant and L is the linear size of the volume. This paper is concerned with the p -regime. This is the regime where the volume is large enough such that the zero momentum fluctuations of the meson fields can be treated perturbatively. This is the regime with in addition the requirement that

$$m_\pi^2 F_\pi^2 V \gg 1. \quad (2.2)$$

These finite volume corrections have been evaluated for many quantities up to one-loop order. This is the order where the first nontrivial dependence on the volume shows up. One purpose of this paper is to calculate the full two-loop finite volume corrections to the vacuum condensate $\langle \bar{q}q \rangle$. This is the one of the calculations of finite volume effects to this order² The vacuum condensate at finite volume has been studied at one-loop in Ref. [6].

An alternative approach to finite volume corrections was introduced by Lüscher where the leading part of the finite volume corrections was derived to all orders in perturbation theory for the mass in terms of a scattering amplitude [7, 8]. This was extended to the finite volume corrections for the pion decay constant in [9]. The other purpose of this paper is to extend the Lüscher formula also to vacuum expectation values. This will in general connect the finite volume corrections of an operator to the zero-momentum transfer matrix element of that operator between pion states as shown in Eq. (2.5). This allows for new ways to calculate sigma terms from the finite volume variation of vacuum condensates.

Note that all our formulas are for the case of an infinite extension in the time direction but a finite volume in the three spatial directions. The formulas

²Ref. [5] with another calculation appeared essentially simultaneously. There the pion mass at finite volume was studied at two-loop order.

can be easily extended to a small fourth direction as well by replacing the integrals with the expressions for that case.

2.2 A Lüscher Formula for the Vacuum Condensate

It turns out to be straightforward to extend Lüscher's formula for the mass to the case of the vacuum condensate. In fact the formula has an even simpler structure than the one for the mass or the decay constant [9]. The underlying observation of Lüscher's method is that the leading finite volume corrections come from one of the propagators feeling the finite volume effects only. We write the finite volume propagator $G_V(q)$ as

$$G_V(q) = \sum_{\vec{n}} e^{-iq_i n_i L_i} G_\infty(q). \quad (2.3)$$

Here the sum is over a vector of integers and L_i is the length of the volume in the i -th direction. The term with $\vec{n} = \vec{0}$ gives the infinite volume case. Lüscher then kept only the term with one of the $n_i = \pm 1$ since this is parametrically leading. As suggested in [10] one can also easily keep the entire series, thus keeping part of the subleading corrections. The remainder of the Lüscher's analysis goes by taking the component of \vec{q} parallel to \vec{n} , q_n and distorting the integration contour along that direction to $q_n \rightarrow q_n - is$. In the limit of $s \rightarrow \infty$ the contribution from that integral vanishes and only the parts coming from the singularities encountered while deforming the contour remain. These happen when relevant propagators can go on-shell. A pedagogical introduction can be found in [8].

The difficulty in proving this is that it needs to be done to all orders in perturbation theory, this was done in [7]. Here we only sketch the lines of reasoning. Of the three types of contributions shown in Fig. 4 of [7] only one is relevant here and is shown in Fig. 2.1(b). The case of operators with contributions of the type shown in diagram (a) is not relevant for ChPT, one can always add the parity-conjugate operator to remove the contribution from diagram (a).

One difference with the case of the mass or decay constant here is that when the singularity is encountered, there is no freedom left in the relevant matrix element and the integral over the momentum of the propagator can be fully done. In the case of the mass and decay constant there is an external momentum available, p_{ext} , this leaves after putting the deformed q on-shell a freedom in $q \cdot p_{ext}$ which results in the final integration over ν . Here there is no external momentum and hence there is no such freedom left.

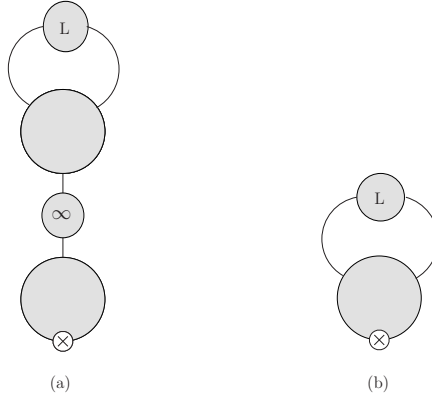


Figure 2.1: The two types of diagrams giving the leading finite volume corrections

The formula after putting everything on-shell becomes

$$\langle O \rangle_V - \langle O \rangle_\infty = - \sum_{\vec{n} \neq \vec{0}} \frac{1}{16\pi^2} \int_0^\infty \frac{dq^2 q^2}{\sqrt{m_0^2 + q^2}} e^{-\sqrt{\vec{n}^2(m_0^2 + q^2)}L^2} \langle \phi | O | \phi \rangle, \quad (2.4)$$

for a real boson with infinite volume mass m_0 and the matrix element on the right hand side should be taken at zero momentum transfer. The integral can now be done explicitly in terms of the generalized Bessel function K_1 . It also only depends on $k = \vec{n}^2$ which is also integer. The number of times in the sum that $\vec{n}^2 = k$ we call $x(k)$. We obtain

$$\langle O \rangle_V - \langle O \rangle_\infty = - \sum_{k=1, \infty} \frac{x(k)}{16\pi^2} \frac{m_0^2}{\sqrt{\zeta(k)}} K_1(\zeta(k)) \langle \phi | O | \phi \rangle, \quad (2.5)$$

with $\zeta(k) = \sqrt{k} m_0 L$. Note that the above formula is for the case of one real scalar. The multiplicity factors for complex scalars can be trivially taken into account. Note that we have left the sum over all modes in as suggested for the mass in [11].

In particular for the case of $\langle \bar{q}q \rangle$ the relevant matrix element is the sigma term. The finite volume corrections to the vacuum condensate thus are another option to calculate the pion sigma term. This can then be compared with the direct calculation of the sigma term via the matrix element $\langle \pi | \bar{q}q | \pi \rangle$ or via the Feynman-Hellman theorem from $\partial m_\pi^2 / \partial m_q$.

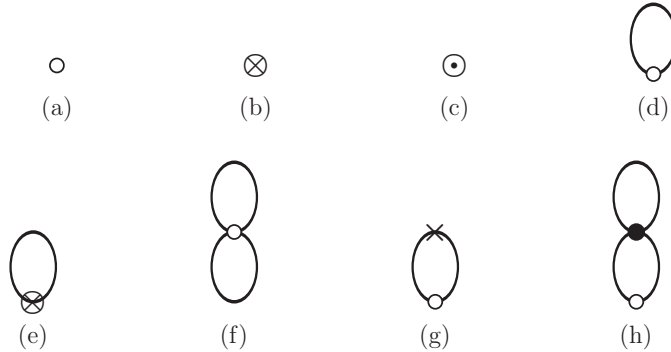


Figure 2.2: The diagrams up to order p^6 for $\langle \bar{q}q \rangle$. The lines are meson propagators and the vertices are: \circ a p^2 insertion of $\bar{q}q$, \otimes a p^4 insertion of $\bar{q}q$, \odot a p^6 insertion of $\bar{q}q$, \bullet a p^2 vertex and \times a p^4 vertex.

2.3 The finite volume vacuum condensate at two-loops

The vacuum condensate at two-loop was calculated in [12], here we repeat that calculation taking into account the finite volume effects. The calculation in terms of the lowest order meson masses is straightforward and proceeds exactly as in [12]. The details of calculation of two loops in ChPT can be found in [12]. The diagrams that contribute are shown in Fig. 2.2.

In infinite volume the loop diagrams contain the integrals

$$\begin{aligned}
 A(m^2) &= \frac{1}{i} \int \frac{d^d p}{(2\pi)^d} \frac{1}{p^2 - m^2}, \\
 B(m^2) &= \frac{1}{i} \int \frac{d^d p}{(2\pi)^d} \frac{1}{(p^2 - m^2)^2}.
 \end{aligned} \tag{2.6}$$

These are expanded in terms of $\epsilon = (4 - d)/2$ as

$$\begin{aligned}
 A(m^2) &= \frac{m^2}{16\pi^2} \left(\frac{1}{\epsilon} - \gamma_E + \log(4\pi) + 1 \right) + \bar{A}(m^2) + \epsilon A^\epsilon(m^2) + \mathcal{O}(\epsilon^2), \\
 B(m^2) &= \frac{1}{16\pi^2} \left(\frac{1}{\epsilon} - \gamma_E + \log(4\pi) + 1 \right) + \bar{B}(m^2) + \epsilon B^\epsilon(m^2) + \mathcal{O}(\epsilon^2),
 \end{aligned} \tag{2.7}$$

with a similar expansion for $B(m^2)$. At finite volume the integrals over momenta get replaced by sums over the finite possible momenta. In this paper

we only keep three of the four dimensions at the same finite length L . Their principle of evaluation can be found in Refs. [3, 13] and explicit expressions are at finite volume. After renormalization the divergent parts cancel and the finite parts become subtraction-scale μ dependent. The needed explicit expressions are

$$\begin{aligned}\bar{A}(m^2) &= -\frac{m^2}{16\pi^2} \log\left(\frac{m^2}{\mu^2}\right) - \frac{1}{16\pi^2} \sum_{k=1,\infty} x(k) \frac{4m^2}{\lambda_k} K_1(\lambda_k) \\ \bar{B}(m^2) &= -\frac{1}{16\pi^2} \log\left(\frac{m^2}{\mu^2}\right) - \frac{1}{16\pi^2} + \frac{1}{16\pi^2} \sum_{k=1,\infty} x(k) 2K_0(\lambda_k)\end{aligned}\quad (2.8)$$

with $\lambda_k = \sqrt{k} mL$. The functions K_1 and K_2 are modified Bessel functions and the integer quantity $x(k)$ is the number of times the sum of squares $\vec{k}^2 = k_1^2 + k_2^2 + k_3^2$ is equal to k when k_1, k_2, k_3 are varied over all positive and negative integers. For large L the Bessel functions lead to an exponential fall-off with the finite size.

We have checked explicitly that at two-loop order the contributions containing A^ϵ and B^ϵ cancel, so we do not need to evaluate these at finite volume. That this cancellation happens follows from the cancellations of nonlocal divergences but in the calculation of [12] this calculation was not explicitly checked. We have also reperformed the full calculation since in [12] the relation $\bar{A}(m^2) = m^2 (\bar{B}(m^2) + 1/(16\pi^2))$ was used, which is no longer true at finite volume. In Ref. [12] the result was expressed in terms of the physical mass and decay constant. This can be done here as well but since we must then distinguish between the integrals at finite volume and those at infinite volume the formula is shorter if we leave meson masses and decay constants in their unrenormalized form.

The result, in three flavour ChPT, uses the p^4 low-energy constants (LECs) L_i^r from Ref. [2] and the C_i^r from [14]. The latter drop out when comparing finite and infinite volume corrections and the values of the L_i^r only contribute to that difference at NNLO. We also suppress the μ dependence of all quantities. The lowest order masses for the pions, kaons and eta we denote by χ_π , χ_K and χ_η respectively and in term of the average up and down quark-mass \hat{m} and strange quark-mass m_s they are

$$\chi_\pi = 2B_0\hat{m}, \quad \chi_K = B_0(\hat{m} + m_s) \quad \chi_\eta = 2B_0(\hat{m} + 2m_s)/3. \quad (2.9)$$

We define the quantities

$$\langle \bar{u}u \rangle = -B_0 F_0^2 \left(1 + \frac{v_4^u}{F_0^2} + \frac{v_6^u}{F_0^4} \right), \quad \langle \bar{s}s \rangle = -B_0 F_0^2 \left(1 + \frac{v_4^s}{F_0^2} + \frac{v_6^s}{F_0^4} \right). \quad (2.10)$$

The calculation gives

$$\begin{aligned}
v_4^u &= \bar{A}(\chi_\pi) \left(3/2 \right) + \bar{A}(\chi_K) + \bar{A}(\chi_\eta) \left(1/6 \right) + 16 \chi_\pi L_6^r + 8 \chi_\pi L_8^r \\
&\quad + 4 \chi_\pi H_2^r + 32 \chi_K L_6^r, \\
v_4^s &= \bar{A}(\chi_K) \left(2 \right) + \bar{A}(\chi_\eta) \left(2/3 \right) + 16 \chi_\pi L_6^r + 4 (2\chi_K - \chi_\pi) (2L_8^r + H_2^r) \\
&\quad + 32 \chi_K L_6^r, \\
v_6^u &= \bar{A}(\chi_\pi)^2 \left(-3/8 \right) + \bar{A}(\chi_\pi) \bar{A}(\chi_\eta) \left(1/4 \right) + \bar{A}(\chi_\pi) \bar{B}(\chi_\pi) \left(-3/4 \chi_\pi \right) \\
&\quad + \bar{A}(\chi_\pi) \bar{B}(\chi_\eta) \left(1/12 \chi_\pi \right) + \bar{A}(\chi_K) \bar{A}(\chi_\eta) \left(-1/3 \right) \\
&\quad + \bar{A}(\chi_K) \bar{B}(\chi_\eta) \left(-2/9 \chi_K \right) + \bar{A}(\chi_\eta)^2 \left(1/72 \right) + \bar{A}(\chi_\eta) \bar{B}(\chi_\pi) \left(1/4 \chi_\pi \right) \\
&\quad + \bar{A}(\chi_\eta) \bar{B}(\chi_K) \left(-1/3 \chi_K \right) + \bar{A}(\chi_\eta) \bar{B}(\chi_\eta) \left(-7/108 \chi_\pi + 4/27 \chi_K \right) \\
&\quad + \bar{A}(\chi_\pi) \left(-36 \chi_\pi L_4^r - 24 \chi_\pi L_5^r + 72 \chi_\pi L_6^r + 48 \chi_\pi L_8^r - 24 \chi_K L_4^r \right. \\
&\quad \left. + 48 \chi_K L_6^r \right) + \bar{A}(\chi_K) \left(-8 \chi_\pi L_4^r + 16 \chi_\pi L_6^r - 48 \chi_K L_4^r - 16 \chi_K L_5^r \right. \\
&\quad \left. + 96 \chi_K L_6^r + 32 \chi_K L_8^r \right) + \bar{A}(\chi_\eta) \left(4/3 \chi_\pi L_4^r + 8/9 \chi_\pi L_5^r - 8/3 \chi_\pi L_6^r \right. \\
&\quad \left. + 64/3 \chi_\pi L_7^r + 16/3 \chi_\pi L_8^r - 40/3 \chi_K L_4^r - 32/9 \chi_K L_5^r + 80/3 \chi_K L_6^r \right. \\
&\quad \left. - 64/3 \chi_K L_7^r \right) + \bar{B}(\chi_\pi) \left(-24 \chi_\pi \chi_K L_4^r + 48 \chi_\pi \chi_K L_6^r - 12 \chi_\pi^2 L_4^r \right. \\
&\quad \left. - 12 \chi_\pi^2 L_5^r + 24 \chi_\pi^2 L_6^r + 24 \chi_\pi^2 L_8^r \right) + \bar{B}(\chi_K) \left(-8 \chi_\pi \chi_K L_4^r \right. \\
&\quad \left. + 16 \chi_\pi \chi_K L_6^r - 16 \chi_K^2 L_4^r - 8 \chi_K^2 L_5^r + 32 \chi_K^2 L_6^r + 16 \chi_K^2 L_8^r \right) \\
&\quad + \bar{B}(\chi_\eta) \left(-8/9 \chi_\pi \chi_K L_4^r + 32/27 \chi_\pi \chi_K L_5^r + 16/9 \chi_\pi \chi_K L_6^r \right. \\
&\quad \left. - 128/9 \chi_\pi \chi_K L_7^r - 64/9 \chi_\pi \chi_K L_8^r + 4/9 \chi_\pi^2 L_4^r - 4/27 \chi_\pi^2 L_5^r \right. \\
&\quad \left. - 8/9 \chi_\pi^2 L_6^r + 64/9 \chi_\pi^2 L_7^r + 8/3 \chi_\pi^2 L_8^r - 32/9 \chi_K^2 L_4^r \right. \\
&\quad \left. - 64/27 \chi_K^2 L_5^r + 64/9 \chi_K^2 L_6^r + 64/9 \chi_K^2 L_7^r + 64/9 \chi_K^2 L_8^r \right) \\
&\quad + 192 \chi_\pi \chi_K C_{21}^r + 8 \chi_\pi \chi_K C_{94}^r + 48 \chi_\pi^2 C_{19}^r + 80 \chi_\pi^2 C_{20}^r + 48 \chi_\pi^2 C_{21}^r \\
&\quad - 4 \chi_\pi^2 C_{94}^r + 64 \chi_K^2 C_{20}^r + 192 \chi_K^2 C_{21}^r, \\
v_6^s &= +\bar{A}(\chi_\pi) \bar{B}(\chi_\eta) \left(1/3 \chi_\pi \right) + \bar{A}(\chi_K) \bar{A}(\chi_\eta) \left(-2/3 \right) \\
&\quad + \bar{A}(\chi_K) \bar{B}(\chi_\eta) \left(-8/9 \chi_K \right) + \bar{A}(\chi_\eta)^2 \left(2/9 \right) \\
&\quad + \bar{A}(\chi_\eta) \bar{B}(\chi_K) \left(-2/3 \chi_K \right) + \bar{A}(\chi_\eta) \bar{B}(\chi_\eta) \left(-7/27 \chi_\pi + 16/27 \chi_K \right) \\
&\quad + \bar{A}(\chi_\pi) \left(-24 \chi_\pi L_4^r + 48 \chi_\pi L_6^r \right) + \bar{A}(\chi_K) \left(-16 \chi_\pi L_4^r + 32 \chi_\pi L_6^r \right. \\
&\quad \left. - 64 \chi_K L_4^r - 32 \chi_K L_5^r + 128 \chi_K L_6^r + 64 \chi_K L_8^r \right)
\end{aligned}$$

$$\begin{aligned}
& +\bar{A}(\chi_\eta) \left(-8/3 \chi_\pi L_4^r + 32/9 \chi_\pi L_5^r + 16/3 \chi_\pi L_6^r - 128/3 \chi_\pi L_7^r \right. \\
& -64/3 \chi_\pi L_8^r - 64/3 \chi_K L_4^r - 128/9 \chi_K L_5^r + 128/3 \chi_K L_6^r + 128/3 \chi_K L_7^r \\
& \left. +128/3 \chi_K L_8^r \right) + \bar{B}(\chi_K) \left(-16 \chi_\pi \chi_K L_4^r + 32 \chi_\pi \chi_K L_6^r - 32 \chi_K^2 L_4^r \right. \\
& -16 \chi_K^2 L_5^r + 64 \chi_K^2 L_6^r + 32 \chi_K^2 L_8^r \left. \right) + \bar{B}(\chi_\eta) \left(-32/9 \chi_\pi \chi_K L_4^r \right. \\
& +128/27 \chi_\pi \chi_K L_5^r + 64/9 \chi_\pi \chi_K L_6^r - 512/9 \chi_\pi \chi_K L_7^r - 256/9 \chi_\pi \chi_K L_8^r \\
& +16/9 \chi_\pi^2 L_4^r - 16/27 \chi_\pi^2 L_5^r - 32/9 \chi_\pi^2 L_6^r + 256/9 \chi_\pi^2 L_7^r + 32/3 \chi_\pi^2 L_8^r \\
& -128/9 \chi_K^2 L_4^r - 256/27 \chi_K^2 L_5^r + 256/9 \chi_K^2 L_6^r + 256/9 \chi_K^2 L_7^r \\
& \left. +256/9 \chi_K^2 L_8^r \right) - 192 \chi_\pi \chi_K C_{19}^r - 64 \chi_\pi \chi_K C_{20}^r + 192 \chi_\pi \chi_K C_{21}^r \\
& +48 \chi_\pi^2 C_{19}^r + 16 \chi_\pi^2 C_{20}^r + 48 \chi_\pi^2 C_{21}^r + 4 \chi_\pi^2 C_{94}^r \\
& +192 \chi_K^2 C_{19}^r + 192 \chi_K^2 C_{20}^r + 192 \chi_K^2 C_{21}^r .
\end{aligned} \tag{2.11}$$

These results agree analytically with those of Ref. [12]. In Ref. [12] numerical results were presented. Using the formulas above one obtains much smaller numerical corrections at NNLO than were obtained there. This effect is mainly due to the rewriting of the $1/F_0^2$ into $1/F_\pi^2$ and to a lesser extent of rewriting the masses in terms of the physical masses.

Numerical results are presented in terms of the ratio

$$R_q = \frac{\langle \bar{q}q \rangle_V - \langle \bar{q}q \rangle_\infty}{\langle \bar{q}q \rangle_\infty} \tag{2.12}$$

where we calculate both numerator and denominator to NLO or NNLO in ChPT. As input parameters for F_0 and the L_i^r we use the values obtained in fit 10 of Ref. [15]. In addition, we have set $H_2^r = 0$. The results for both R_u and R_s are shown in Fig. 2.3 for $\chi_K = (450 \text{ MeV})^2$ and three values of the lowest order pion mass $\chi_\pi = (100 \text{ MeV})^2$, $(250 \text{ MeV})^2$ and $(450 \text{ MeV})^2$. The finite volume corrections to the strange quark vacuum expectation value are always small. The light quark vacuum expectation value can have sizable finite volume corrections for the smaller pion mass.

2.4 Comparison and conclusions

The sigma terms in infinite volume are known to two-loop order in ChPT. Either directly [16] or via the derivative of the meson mass to the quark mass [12, 17]. The sigma terms are also known for two-flavour case [18, 19, 20].

A major motivation for this work was to test the accuracy of the Lüscher type of finite volume formulas. So, how well do the two approaches compare.

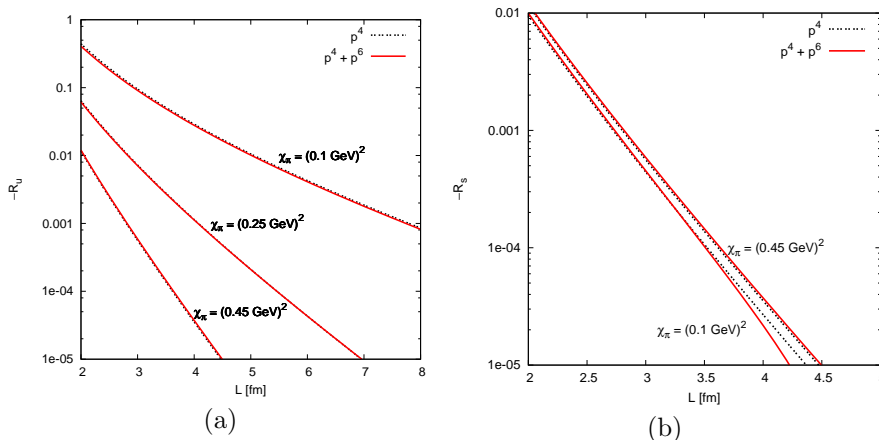


Figure 2.3: (a) The ratio R_u for three values of the input lowest order pion mass and $\chi_K = (450 \text{ MeV})^2$ (b) The same for R_s , with $\chi_K = (450 \text{ MeV})^2$ and $\chi_\pi = (100 \text{ MeV})^2$, and $(450 \text{ MeV})^2$.

At one-loop the comparison is rather trivial since at most one-propagator can show up in the relevant one-loop diagrams. We can also apply the formula (2.5) for the different species of meson separately and thus construct the exact one loop ChPT formula. At one loop the only test possible is thus how fast the sum over k converges and how quickly it converges to an exponential. This was already studied in [11] and the convergence to the leading exponential is rather slow while the sum over k converges faster. We find the same conclusions. The extended Lüscher formula agrees analytically with the full one-loop expressions and is thus fully accurate.

At two loop level the two formulas have a different behaviour. There are diagrams now allowing two propagators simultaneously to feel the effect of the finite volume. A small complication that needs to be taken into account here is that the Lüscher formula is with the infinite volume mass at one loop. Thus when changing from the lowest order mass to the physical mass in the one loop formulas this needs to be done with the infinite volume expressions. But, even after doing this, the corrections are very small. The two-loop calculation as plotted in Fig. 2.3 is obviously very small. In addition, it is dependent on precisely how one defines the one-loop order. E.g., there are ambiguities in using the the physical pion decay constant or the lowest order one, and how much one uses the Gell-Mann-Okubo relation in the one-loop expression. With these changes the two-loop calculation can be changed significantly but remains mostly small. The Lüscher formula at this order has also small corrections since the sigma terms have small corrections at one-loop. We have not plotted it since

it will essentially be on top of the other curves in Fig. 2.3.

Both the extended Lüscher formula and the full two-loop calculations thus indicate small two-loop order corrections. The actual numerical results of the two-loop expressions depends strongly on the inherent ambiguities in defining it. So, both approaches give comparable results at this order, but we cannot draw conclusions on the accuracy of the extended Lüscher formula.

The extended Lüscher formula allows also to include effects from even higher orders by using the sigma terms at higher orders. This quantity is known to NNLO but its numerical value depends strongly on the input parameters chosen [16]. There might thus be sizable effects at higher orders but there need not be.

In conclusion, we have derived an extended Lüscher formula for the finite volume effects on the quark vacuum condensate. We have also calculated these effects to two-loop order in ChPT. At one-loop order the extended Lüscher formula is exactly equal to the full ChPT calculation. At two-loop order, the latter includes extra effects, but both approaches indicate very small corrections. The difference is within the inherent uncertainty of the full ChPT calculation at that order and we thus cannot conclude if the difference is due to the inherent uncertainty in the two-loop order result or to the effects not captured by the Lüscher formula.

Acknowledgements

We thank Gilberto Colangelo and Christoph Haefeli for discussions. This work is supported by the European Union TMR network, Contract No. HPRN-CT-2002-00311 (EURIDICE) and by the European Community-Research Infrastructure Activity Contract No. RII3-CT-2004-506078 (HadronPhysics). KG acknowledges a fellowship from the Iranian Ministry of Science.

References

- [1] S. Weinberg, *PhysicaA* **96** (1979) 327.
- [2] J. Gasser and H. Leutwyler, *Annals Phys.* **158** (1984) 142; *Nucl. Phys. B* **250** (1985) 465.
- [3] J. Gasser and H. Leutwyler, *Nucl. Phys. B* **307** (1988) 763.
- [4] G. Colangelo, *Nucl. Phys. Proc. Suppl.* **140** (2005) 120 [arXiv:hep-lat/0409111].
- [5] Authors: Gilberto Colangelo and Christoph Haefeli, *Finite volume effects for the pion mass at two loops*, hep-lat/0602017.
- [6] S. Descotes-Genon, *Eur. Phys. J. C* **40** (2005) 81 [arXiv:hep-ph/0410233].

-
- [7] M. Lüscher, Commun. Math. Phys. **104** (1986) 177.
 - [8] M. Lüscher, DESY 83/116 *Lecture given at Cargese Summer Inst., Cargese, France, Sep 1-15, 1983*
 - [9] G. Colangelo and C. Haefeli, Phys. Lett. B **590** (2004) 258 [arXiv:hep-lat/0403025].
 - [10] G. Colangelo, S. Durr and C. Haefeli, Nucl. Phys. B **721** (2005) 136 [arXiv:hep-lat/0503014].
 - [11] G. Colangelo and S. Durr, Eur. Phys. J. C **33** (2004) 543 [arXiv:hep-lat/0311023].
 - [12] G. Amorós, J. Bijnens and P. Talavera, Nucl. Phys. B **585** (2000) 293 [Erratum-ibid. B **598** (2001) 665] [arXiv:hep-ph/0003258].
 - [13] P. Hasenfratz and H. Leutwyler, Nucl. Phys. B **343** (1990) 241.
 - [14] J. Bijnens, G. Colangelo and G. Ecker, JHEP **9902** (1999) 020 [arXiv:hep-ph/9902437]; Annals Phys. **280** (2000) 100 [arXiv:hep-ph/9907333].
 - [15] G. Amorós, J. Bijnens and P. Talavera, Nucl. Phys. B **602** (2001) 87 [arXiv:hep-ph/0101127].
 - [16] J. Bijnens and P. Dhonte, JHEP **0310** (2003) 061 [arXiv:hep-ph/0307044].
 - [17] G. Amorós, J. Bijnens and P. Talavera, Nucl. Phys. B **568**, 319 (2000) [arXiv:hep-ph/9907264].
 - [18] U. Bürgi, Nucl. Phys. B **479**, 392 (1996) [arXiv:hep-ph/9602429]; Phys. Lett. B **377**, 147 (1996) [arXiv:hep-ph/9602421].
 - [19] J. Bijnens, G. Colangelo, G. Ecker, J. Gasser and M. E. Sainio, Nucl. Phys. B **508**, 263 (1997) [Erratum-ibid. B **517**, 639 (1998)] [arXiv:hep-ph/9707291]; Phys. Lett. B **374**, 210 (1996) [arXiv:hep-ph/9511397].
 - [20] J. Bijnens, G. Colangelo and P. Talavera, JHEP **9805**, 014 (1998) [arXiv:hep-ph/9805389].

$\eta \rightarrow 3\pi$ at Two Loops In Chiral
Perturbation Theory

Paper II

$\eta \rightarrow 3\pi$ at Two Loop In Chiral Perturbation Theory

Johan Bijnens¹ and Karim Ghorbani²

Department of Theoretical Physics, Lund University,
Sölvegatan 14A, S 223-62 Lund, Sweden

abstract We calculate the decay $\eta \rightarrow 3\pi$ at next-to-next-to-leading order or order p^6 in Chiral Perturbation Theory. The corrections are somewhat larger than was indicated by dispersive estimates. We present numerical results for the Dalitz plot parameters, the ratio r of the neutral to charged decay and the total decay rate. The latter lead to central values for the isospin breaking quantities $R = 42.2$ and $Q = 23.2$ from $\Gamma(\eta \rightarrow \pi^+\pi^-\pi^0)$.

PACS:11.30.Rd, 12.39.Fe, 13.25.Jx, 14.40.Aq.

¹Electronic Address: bijnens@thep.lu.se

²Electronic Address: karim.ghorbani@thep.lu.se

3.1 Introduction

Since its discovery, the eta particle has been under tense scrutiny, fairly recent reviews are [1, 2]. The eta decay to three pions is particularly interesting. It can only happen due to isospin breaking. This implies that the decay rate vanishes in the limit of equal of up and down quark-masses, ignoring electromagnetic effects. The very first attempts to explain the decay [3, 4], considering it to be an electromagnetic decay, resulted in an almost zero decay rate which was in flat disagreement with experiment.

Later on, a combination of current algebra technique in $SU(3)$ and partially conserved axial-vector current (PCAC) hypothesis could make a better prediction [5, 6]. This, however, underestimated the observed decay rate by a factor of a few. PCAC and current algebra were generalized into Chiral Perturbation Theory (ChPT) and brought into a modern form [7, 8, 9]. The lowest order for $\eta \rightarrow 3\pi$ was calculated in [5, 6] and the next-to-leading order (NLO) in [10]. The main goal of this paper is to obtain next-to-next-to-leading-order (NNLO) expression for this decay.

We give now a short overview of the present situation, closely following the discussion in [11].

The well-known tree-level result for this decay channel can be derived from current algebra or ChPT and has the structure

$$A(s, t, u) = \frac{B_0(m_u - m_d)}{3\sqrt{3}F_\pi^2} \left(1 + \frac{3(s - s_0)}{m_\eta^2 - m_\pi^2} \right). \quad (3.1)$$

The prefactor $m_u - m_d$ shows that the decay is isospin violating or $SU(2)_V$ -violating. The magnitude of $m_u - m_d$ determines the size of the isospin symmetry breaking coming from the strong interaction itself. A precise determination of this quantity is in principle possible here because its size has a direct impact on the decay rate.

Using Dashen's theorem this factor can be obtained from the physical meson masses by removing electromagnetic effects to lowest order. Following the line of the argument outlined in Dashen's theorem [12] one arrives at

$$B(m_d - m_u) = m_{K^0}^2 - m_{K^+}^2 - m_{\pi^0}^2 + m_{\pi^+}^2. \quad (3.2)$$

Under these circumstances, the theoretical decay width is 66 eV to be compared with 295 eV from experiment [13]. One may consider three potential sources for this discrepancy. First, the violation of the Dashen's theorem due to the electromagnetic interferences increases the value of $m_d - m_u$ [14, 15] and therefore the decay width, but this is not sufficient as will be discussed more in the discussion section. Secondly, electromagnetic corrections of the decay amplitude which are of higher order, order $e^2 p^2$, are safely negligible in comparison with the strong interactions as pointed out in [16] where the analysis of [3, 4] was brought to NLO.

Finally the contribution of the higher order chiral effects must be taken into account. Especially since the strong $\pi\pi$ rescattering in the S -wave channel may develop a significant correction, see e.g. [17, 18]. The NLO corrections were obtained in [10]. The unitarity correction at one-loop level is about half of the total NLO effects. This, of course, confirmed the fact that by virtue of a large eta mass, significant rescattering effects in the S -wave can occur. The vertex corrections and tree graphs make up the rest of the NLO contribution. The coupling constants involved at this level can be rewritten in terms of meson masses except for L_3^r . In [8, 10] L_3^r was estimated by invoking the OZI (Okubo-Zweig-Iizuka) rule and comparing with $\pi\pi$ scattering lengths. Their finding for the decay rate of $\eta \rightarrow 3\pi$ is 160 ± 50 which is still far from the experimental value, however with a large theoretical error.

Given the importance of the unitarity correction at NLO, it was deemed necessary to estimate this part of the corrections to higher order. This can be done using dispersive methods. In [19], extended Khuri-Treiman equations are used to evaluate the two-pion rescattering to the decay $\eta \rightarrow \pi\pi\pi$. They achieve a moderate modification, an increase of about 14% per cent in the amplitude at the center of the Dalitz plot. Moreover, another analysis, based on a somewhat different dispersive method, but also restricting itself to two-pion rescattering, represented in [20] suggests also a mild enhancement to the real part of the amplitude in the physical region. A more model-dependent analysis of dispersive corrections appeared recently [21] relying on combining $U(3) \times U(3)$ ChPT and a relativistic coupled-channels method, finds agreement with data.

Given all these, our motivation to perform a full NNLO computation is twofold. First, due to a relatively large strange quark-mass, the convergence of three-flavour or $SU(3)$ ChPT is an a priori question. The reason hinges on the fact that the ratio M_K^2/M_ρ^2 is much larger than M_π^2/M_ρ^2 and there are possibly large effects as a result of strange quark loops. Three-flavour ChPT is probably less convergent than two-flavour ChPT, see e.g. [22] for a discussion. In general, one needs to have several terms available in order to check convergence. The situation at present is not fully clear, The result for the vector form factor, $K_{\ell 4}$ and $\pi\pi$ -scattering have an acceptable convergence, while the result for the masses and πK -scattering, seem to converge slower, see [23] and references therein. Therefore we would like to check explicitly whether one may treat the strange quark-mass perturbatively for this process, namely $\eta \rightarrow 3\pi$. In addition, at NLO the unitarity correction provided only half of the total correction. It is therefore also of interest to know if the other corrections are important at NNLO as well. This is known to be the case for $K_{\ell 4}$ by comparing [24] and [25].

Our finding shows that the full amplitude up to and including order p^6 corrections converges reasonably acceptably but we find larger corrections than

in [19, 20].

In this paper, we perform the full NNLO calculation of $\eta \rightarrow 3\pi$ in standard three-flavour ChPT. We do this to first order in the isospin breaking quantity $m_u - m_d$. In addition, we perform a first numerical analysis with this expression. We have therefore also estimated the order p^6 coupling constants C_i^r , using a resonance chiral Lagrangian, assuming that vector and scalar mesons saturate the C_i^r . In addition, we derive an inequality between the slope parameters.

The layout of this article is as following. In Sect. 3.2 a brief introduction to Chiral Perturbation Theory is provided. Sect. 3.3 describes how to calculate the $\eta \rightarrow 3\pi$ amplitude in the presence of mixing, the kinematics for the decay and the form of the amplitude at NNLO. We also show the Feynman diagrams and provides references to how we deal with the loop integrals and renormalization. A short discussion on our analytic results is given in Sect. 3.4 followed by our estimate of order p^6 low energy constants in Sect. 3.5. A main part of the manuscript is the numerical results and comparison with experiment given Sect. 3.6. We first present a discussion on the amplitude level, Sect. 3.6.1, then compare with the earlier dispersive results, Sect. 3.6.2. The main comparison with experiment is done in Sect. 3.6.3 for the Dalitz plot distributions and in Sect. 3.6.4 for the ratio of amplitudes. We present the results for the value of R and Q in Sect. 3.6.5. The App. 3.A contains a discussion on the cancellations inherent in α and the derivation of the inequality between the slope parameters. The remaining appendices present our NLO expression and the dependence on the order p^6 low energy constants.

3.2 Chiral Perturbation Theory

One approach to address Quantum Chromodynamics (QCD) at low energy is the application of effective field theories. In [26] and references therein some basic concepts and a few interesting examples can be found for this method. As an effective field theory, ChPT is constructed based on the approximate chiral symmetry of the underlying theory (QCD) and is an expansion in external momenta and quark-masses, momenta and meson masses are generically denoted by p and the expansion is in powers of these. The dynamical degrees of freedom i.e. pseudo-Goldstone particles, are manifested as a result of the spontaneous chiral symmetry breaking of QCD. Weinberg [7] systematized the use of effective field theory as an alternative to the current algebra formalism, incorporating naturally the chiral logarithms. Gasser and Leutwyler in two elegant papers presented this expansion including terms of order p^4 and introduced the external field method [8]. They also formulated the extension to three light flavours [9]. They found a substantial correction to the $\pi\pi$ scattering lengths and effective ranges at this order. Reviews of ChPT at order p^4 are [27, 28]. This line of work has been further developed to include p^6 corrections,

see the review [23]. A more introductory recent review is [29].

The full action consists of subterms with a definite number of derivatives or powers of quark-masses as shown below

$$\mathcal{L}_{eff} = \mathcal{L}_2 + \mathcal{L}_4 + \mathcal{L}_6 + \dots \quad (3.3)$$

The subscript indicates the chiral order. Quark masses are counted as order p^2 using the lowest order relation $m_\pi^2 = B_0(m_u + m_d)$. The lowest order chiral Lagrangian incorporates two parameters and has the form

$$\mathcal{L}_2 = \frac{F_0^2}{4} (\langle D_\mu U D^\mu U^\dagger \rangle + \langle \chi U^\dagger + U \chi^\dagger \rangle) \quad (3.4)$$

and the next-to-leading Lagrangian or order p^4 Lagrangian is given as[9]

$$\begin{aligned} \mathcal{L}_4 = & L_1 \langle D_\mu U^\dagger D^\mu U \rangle^2 + L_2 \langle D_\mu U^\dagger D_\nu U \rangle \langle D^\mu U^\dagger D^\nu U \rangle \\ & + L_3 \langle D^\mu U^\dagger D_\mu U D^\nu U^\dagger D_\nu U \rangle + L_4 \langle D^\mu U^\dagger D_\mu U \rangle \langle \chi^\dagger U + \chi U^\dagger \rangle \\ & + L_5 \langle D^\mu U^\dagger D_\mu U (\chi^\dagger U + U^\dagger \chi) \rangle + L_6 \langle \chi^\dagger U + \chi U^\dagger \rangle^2 \\ & + L_7 \langle \chi^\dagger U - \chi U^\dagger \rangle^2 + L_8 \langle \chi^\dagger U \chi^\dagger U + \chi U^\dagger \chi U^\dagger \rangle \\ & - i L_9 \langle F_{\mu\nu}^R D^\mu U D^\nu U^\dagger + F_{\mu\nu}^L D^\mu U^\dagger D^\nu U \rangle \\ & + L_{10} \langle U^\dagger F_{\mu\nu}^R U F^{L\mu\nu} \rangle + H_1 \langle F_{\mu\nu}^R F^{R\mu\nu} + F_{\mu\nu}^L F^{L\mu\nu} \rangle + H_2 \langle \chi^\dagger \chi \rangle. \end{aligned} \quad (3.5)$$

The matrix $U \in SU(3)$ parameterizes the octet of light pseudo-scalar mesons with its exponential representation given in terms of mesonic fields matrix as

$$U(\phi) = \exp(i\sqrt{2}\phi/F_0), \quad (3.6)$$

where

$$\phi(x) = \begin{pmatrix} \frac{\pi_3}{\sqrt{2}} + \frac{\eta_8}{\sqrt{6}} & \pi^+ & K^+ \\ \pi^- & -\frac{\pi_3}{\sqrt{2}} + \frac{\eta_8}{\sqrt{6}} & K^0 \\ K^- & \bar{K}^0 & -\frac{2\eta_8}{\sqrt{6}} \end{pmatrix}. \quad (3.7)$$

The covariant derivative and the field strength tensor are defined as

$$D_\mu U = \partial_\mu U - i r_\mu U + i U l_\mu, \quad F_{\mu\nu}^L = \partial_\mu l_\nu - \partial_\nu l_\mu - i [l_\mu, l_\nu], \quad (3.8)$$

and a similar definition for the right-handed field strength. Here l_μ and r_μ represents the left-handed and right-handed chiral currents respectively. χ is parameterized in terms of scalar (s) and pseudo scalar (p) external densities as $\chi = 2B_0(s + ip)$. In the process discussed in this article we have set $s = \text{diag}(m_u, m_d, m_s)$ and $p = l_\mu = l_\nu = 0$. Finally, the notation $\langle A \rangle = \text{Tr}_F(A)$,

the trace over flavours. The $SU(3)$ chiral Lagrangian of order p^6 contains 94 operators. For its explicit form we refer to [30].

To carry out any practical calculation in a non-renormalizable effective field theory we need two things. First, a power counting scheme is necessary in order to organize all the contributing operators to the amplitude in a given chiral order. For ChPT this is essentially dimensional counting. The dimensionality of a Feynman graph contributing to the matrix element can be obtained by using the well-known formula[7]

$$D = 2 + 2N_L + \sum_d N_d (d - 2) \quad (3.9)$$

where N_L is the number of loops and N_d is the number of vertices taken from Lagrangian of order d in chiral order. For the implementation of the renormalization program, described below, a dimensional regularization scheme is considered a practical method, particularly when higher order loops are concerned, since it respects chiral symmetry [8] and it only requires one regulator for all loops.

Tree diagrams using only vertices from the Lagrangian \mathcal{L}_2 , provide the lowest order term in the expansion. In general, tree-level diagrams make up the semi-classical part of the unitarity of the S-matrix. We thus ought to include loop effects. The infinities which arise from one loop diagrams with vertices taken from \mathcal{L}_2 can not be absorbed by renormalizing F_0 and B_0 or rescaling the fields since these contribute at tree level at a *different* order in p^2 from the one-loop diagrams. This is the property that characterizes the non-renormalizability of the Lagrangian. The most general Lagrangian at next-to-leading order, \mathcal{L}_4 of (3.5), incorporates 10+2 operators with corresponding low-energy coupling constants (LECs), namely L_i , H_1 and H_2 . The \mathcal{L}_4 provides counter-terms polynomial in external momenta and masses which are appropriate for the cancellation of the ultraviolet divergences of the regularized graphs which show up at one-loop level. We thus split the L_i into an infinite and finite L_i^r part, [7, 8, 9]. By applying the same argument, the construction of the next-to-next-leading Lagrangian is needed in order to extend our calculation to two-loop order. This was carried out in [30]. Renormalization at higher orders contains many subtleties. The procedure used here is discussed extensively in [31, 32]. The full divergence structure at order p^4 [8, 9] and p^6 [32] is known. For our calculation, the cancellation of the divergences is an important cross-check. The nontrivial predictions of ChPT, the so called chiral logarithms, are due to infrared singularities in the chiral limit due to the (pseudo)-Goldstone boson intermediate states. Lattice QCD computations support this logarithmic behavior when compared with ChPT results evaluated in finite volume [33].

The part not determined by ChPT, the L_i^r and higher order LECs, C_i^r at order p^6 , encode the information about higher scale physics which has no

dynamical role in our effective field theory and they gain no constraints from the imposed chiral symmetry. They are thus the full freedom allowed by the chiral symmetry Ward identities. For many processes it is turned out that the chiral logarithms do not saturate the amplitude, making the determination of the LECs, an important task. The predictivity of ChPT is limited by the determination of these unknown parameters. Fixing the free parameters in the theory gives rise to a unique low-energy theory for QCD. To this end both theoretical, including Lattice QCD, and phenomenological approaches are needed. Often used is the large N_c limit in the form of Zweig's rule which requires suppression for the NLO LECs $2L_1^r - L_2^r, L_4^r$ and L_6^r . This together with the $\pi\pi$ scattering analysis determine the L_1^r, L_2^r and L_3^r and has been tested in the more accurate determination of these constants from $K_{\ell 4}$. The LECs L_5^r, L_7^r and L_8^r are involved in the higher order corrections to the decay constants, meson masses and Gell-Man-Okubo relation and therefore directly related to quantities which are experimentally obtainable. Moreover, the electromagnetic charge radius of pion and radiative leptonic decay of pion fix the value of L_9^r and L_{10}^r respectively. Detailed discussion on determination of p^4 LECs are given in [9] at order p^6 in [23, 25, 34].

On the other hand, systematic extension to effective field theories incorporating the resonance fields may provide a profound theoretical ground to ultimately underpin the values of the LECs. Resonance field methodology takes its original form in Sakurai's hypothesis of vector meson dominance. It was worked out at order p^4 by [35]. We will only use it for order p^6 LECs in the simplified form discussed in Sect. 3.5. More systematic approaches at order p^6 exist [36] but there are also caveats to be observed from short-distance constraints, both positive and negative [37, 38].

3.3 Eta decay amplitude: formalism

3.3.1 Matrix-elements in the presence of mixing

In this section we explain how to calculate matrix-elements by the use of the Lehmann-Symanzik-Zimmermann (LSZ) reduction formula in the present of mixing. This is a generalization of the discussion in [34] Sect. 2, to the case needed here. The scattering amplitude is basically the residue of the Fourier transformed Green function in the limit where all the outgoing particles go on-shell.

For the case of $\eta \rightarrow \pi^+\pi^-\pi^0$, the mixing occurs in the two external legs involving neutral particles pion and eta as illustrated in Fig. 3.1. For the decay $\eta \rightarrow \pi^0\pi^0\pi^0$ mixing is relevant in all four external legs. In [34] two-point functions were analyzed in all generality as well as amplitudes where one external leg could undergo mixing. Here, we reiterate some basic ingredients

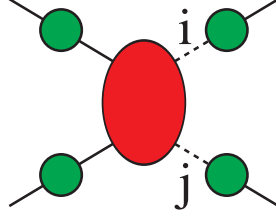


Figure 3.1: The full four-point Green function is represented. The Oval stands for the amputated four-point Green function and circles indicate the full two-point functions. The solid lines are external mesons and the dashed lines labeled by i and j , indicate the sum over states implied in the two external legs where mixing occurs.

introduced there and will lead to derive a general formula that relates the amputated four-point Green function to the scattering amplitude order by order in perturbative expansion of $\eta \rightarrow \pi^+\pi^-\pi^0$. In the ChPT calculation we only retain terms to first order in isospin breaking, we therefore can use the relation (3.29) and do not need a more general formula for $\eta \rightarrow \pi^0\pi^0\pi^0$ to all orders in the mixing.

The amplitude or matrix-element for a process with n ingoing and outgoing particles can be expressed in the form

$$\mathcal{A}_{i_1 \dots i_n} = \left(\frac{(-i)^n}{\sqrt{Z_{i_1} \dots Z_{i_n}}} \right) \prod_{i=1}^n \lim_{k_i^2 \rightarrow m_i^2} (k_i^2 - m_i^2) G_{i_1 \dots i_n}(k_1, \dots, k_n). \quad (3.10)$$

The function $G_{i_1 \dots i_n}(k_1, \dots, k_n)$ is the exact n -point Green function³ and the coefficients Z_i are defined as

$$G_{ii}(p^2 \approx m_{i \text{ phys}}^2) = \frac{iZ_i}{p^2 - m_{i \text{ phys}}^2}. \quad (3.11)$$

These are often called field-strength or wave-function renormalization factors.

We begin by decomposing the full four-point function into the amputated four-point function and four full propagators or two-point functions for the external legs.

$$\begin{aligned} G_{1238} &= G_{11}(p^2 \approx m_{1 \text{ phys}}^2) G_{22}(p^2 \approx m_{2 \text{ phys}}^2) \\ &\quad G_{3i}(p^2 \approx m_{3 \text{ phys}}^2) G_{8j}(p^2 \approx m_{8 \text{ phys}}^2) \mathcal{G}_{12ij}. \end{aligned} \quad (3.12)$$

³We consider as operators that are in the Green functions the fields as present in the Lagrangian. The formula is valid for all operators with a nonzero coupling to single-particle states.

Note that by definition Π only starts at NLO in the chiral expansion.

We now have all the ingredients to put in (3.10) and perform the chiral expansion for the amplitude. We obtain using $Z_{11} = Z_{22}$ and $\Pi_{38}(p^2) = \Pi_{83}(p^2)$ up to order p^6 :

$$\mathcal{A}_{1238} = \mathcal{A}_{1238}^{(2)} + \mathcal{A}_{1238}^{(4)} + \mathcal{A}_{1238}^{(6)} + \dots, \quad (3.18)$$

$$\mathcal{A}_{1238}^{(2)} = \mathcal{G}_{1238}^{(2)}, \quad (3.19)$$

$$\mathcal{A}_{1238}^{(4)} = \mathcal{G}_{1238}^{(4)} - \left(Z_{11}^{(4)} + \frac{1}{2} Z_{33}^{(4)} + \frac{1}{2} Z_{88}^{(4)} \right) \mathcal{G}_{1238}^{(2)} - \frac{\Pi_{38}^{(4)}}{\Delta m_1^2} \mathcal{G}_{1288}^{(2)} - \frac{\Pi_{38}^{(4)}}{\Delta m_2^2} \mathcal{G}_{1233}^{(2)}, \quad (3.20)$$

$$\begin{aligned} \mathcal{A}_{1238}^{(6)} &= \mathcal{G}_{1238}^{(6)} - \frac{1}{2} \left(2Z_{11}^{(6)} + Z_{33}^{(6)} + Z_{88}^{(6)} \right) \mathcal{G}_{1238}^{(2)} \\ &\quad - \frac{1}{2} \left(2Z_{11}^{(4)} + Z_{33}^{(4)} + Z_{88}^{(4)} \right) \mathcal{G}_{1238}^{(4)} \\ &\quad + \frac{3}{8} \left(\left(Z_{33}^{(4)} \right)^2 + \left(Z_{88}^{(4)} \right)^2 \right) \mathcal{G}_{1238}^{(2)} + \left(Z_{33}^{(4)} \right)^2 \mathcal{G}_{1238}^{(2)} \\ &\quad + \left(\frac{1}{4} Z_{33}^{(4)} Z_{88}^{(4)} + \frac{1}{2} Z_{11}^{(4)} Z_{11}^{(4)} + \frac{1}{2} Z_{11}^{(4)} Z_{11}^{(4)} \right) \mathcal{G}_{1238}^{(2)} \\ &\quad - \frac{\Pi_{38}^{(3)}(4)}{\Delta m_1^2} \mathcal{G}_{1288}^{(4)} - \frac{\Pi_{38}^{(8)}(4)}{\Delta m_2^2} \mathcal{G}_{1233}^{(4)} - \frac{\Pi_{38}^{(3)}(6)}{\Delta m_1^2} \mathcal{G}_{1288}^{(2)} \\ &\quad - \frac{\Pi_{38}^{(8)}(6)}{\Delta m_2^2} \mathcal{G}_{1233}^{(2)} + \frac{\Pi_{38}^{(3)}(4) \Pi_{88}^{(3)}(4)}{\Delta m_1^2} \mathcal{G}_{1288}^{(2)} + \frac{\Pi_{38}^{(8)}(4) \Pi_{88}^{(3)}(4)}{\Delta m_2^2} \mathcal{G}_{1233}^{(2)} \\ &\quad + \frac{1}{2} \left(Z_{33}^{(4)} \frac{\Pi_{38}^{(3)}(4)}{\Delta m_1^2} + Z_{88}^{(4)} \frac{\Pi_{38}^{(3)}(4)}{\Delta m_1^2} + Z_{11}^{(4)} \frac{\Pi_{38}^{(3)}(4)}{\Delta m_1^2} \right) \mathcal{G}_{1288}^{(2)} \\ &\quad + \frac{1}{2} \left(Z_{33}^{(4)} \frac{\Pi_{38}^{(8)}(4)}{\Delta m_2^2} + Z_{88}^{(4)} \frac{\Pi_{38}^{(8)}(4)}{\Delta m_2^2} + Z_{11}^{(4)} \frac{\Pi_{38}^{(8)}(4)}{\Delta m_2^2} \right) \mathcal{G}_{1233}^{(2)}. \quad (3.21) \end{aligned}$$

We defined the abbreviations $\Delta m_1^2 = m_\pi^2 - m_{\eta_0}^2$ and $\Delta m_2^2 = m_\eta^2 - m_{\pi_0}^2$ with first a physical mass and the second term the lowest order mass. $\Pi_{ij}^{(k)}(I)$ are evaluated at the physical π^0 mass for $I = 3$ and at the physical η mass for $I = 8$. The $\mathcal{G}_{12ij}^{(n)}$ are evaluated at the physical charged pion mass for the legs with indices 1 or 2 and at the physical π^0 mass for the leg labeled i and at the physical η mass at the leg labeled j . The set of terms are shown at the different orders.

3.3.2 Kinematics and isospin

We write the amplitude for the decay $\eta(p_\eta) \rightarrow \pi^+(p_+)\pi^-(p_+)\pi^0(p_0)$ using the Mandelstam variables

$$\begin{aligned} s &= (p_+ + p_-)^2 = (p_\eta - p_0)^2, \\ t &= (p_+ + p_0)^2 = (p_\eta - p_-)^2, \\ u &= (p_- + p_0)^2 = (p_\eta - p_+)^2. \end{aligned} \quad (3.22)$$

These are linearly dependent

$$s + t + u = m_{\pi^0}^2 + m_{\pi^-}^2 + m_{\pi^+}^2 + m_\eta^2 \equiv 3s_0. \quad (3.23)$$

Due to the $SU(2)_V$ symmetry breaking the isospin basis and physical basis in the π^0 - η subset do not coincide. To diagonalize the mass matrix and consequently the two-point functions at *leading order* we perform the following transformation and find the corresponding *lowest order* mixing angle

$$\begin{aligned} \pi_3 &= \pi \cos(\epsilon) - \eta \sin(\epsilon) \\ \eta_8 &= \pi \sin(\epsilon) + \eta \cos(\epsilon) \end{aligned} \quad (3.24)$$

The lowest order mixing angle is

$$\begin{aligned} \tan(2\epsilon) &= \frac{\sqrt{3} m_d - m_u}{2 m_s - \hat{m}}, \\ \hat{m} &= (m_u + m_d)/2. \end{aligned} \quad (3.25)$$

G-parity requires the amplitude to vanish at the limit $m_u = m_d$ and therefore it must inevitably be accompanied by an overall factor of $m_u - m_d$ which we have chosen to be in the form of $\sin(\epsilon)$.

$$A(\eta \rightarrow \pi^+ \pi^- \pi^0) = \sin(\epsilon) M(s, t, u) \quad (3.26)$$

Since the amplitude is invariant under charge conjugation we have

$$M(s, t, u) = M(s, u, t). \quad (3.27)$$

Note that the isospin breaking factor which is pulled out is different in different references, [10] and [39] use different quantities. We have chosen $\sin(\epsilon)$ since it is the factor that naturally shows up at lowest order.

For the eta decay to three neutral pions, the amplitude must be symmetric under the exchange of pions (Bose symmetry) and this together with isospin symmetry and using the fact that the decay is caused by the $\Delta I = 1$ operator $(1/2)(m_u - m_d)(\bar{u}u - \bar{d}d)$ implies

$$A(\eta \rightarrow \pi^0 \pi^0 \pi^0) = \sin(\epsilon) \overline{M}(s, t, u) \quad (3.28)$$

with

$$\overline{M}(s, t, u) = M(s, t, u) + M(t, u, s) + M(u, s, t). \quad (3.29)$$

This relation is only true when isospin breaking in the amplitude is taken into account to first order only. $M(s, t, u)$ and $\overline{M}(s, t, u)$ are treated in the isospin limit. We will work in this limit in the remainder of the paper.

3.3.3 A simplified form for the amplitude to order p^6

The scattering amplitude can be represented in terms of components with definite isospin assignments as[20]

$$M(s, t, u) = M_0(s) + (s - u)M_1(t) + (s - t)M_1(u) + M_2(t) + M_2(u) - \frac{2}{3}M_2(s). \quad (3.30)$$

The function $M_I(x = s, t, u)$ indicates scattering in the kinematic x -channel with total isospin I . Analyticity, unitarity and crossing symmetry as imposed on the S-matrix, give rise to this exceptionally useful representation. For the derivation and detailed discussion for the case of $\pi\pi$ we refer to [40]. This relation only holds up to $\mathcal{O}(p^8)$.

The argument is based on the fact that nonpolynomial dependence on s, t, u is related to an absorptive part via unitarity. Up to order p^6 there are only absorptive parts in the two-pion S and P -waves and then using isospin one derives the form (3.30).

It is important to note that the polynomial part of the amplitude cannot be split uniquely into M_I functions since the relation $s + t + u = 3s_0$ allows a different redistribution of the said part to the M_I s. A list of the equivalent redefinitions for the case of $K \rightarrow 3\pi$ can be found in App. A of [41]. The choice we made is to remove as much as possible first out of M_2 and then out of M_1 .

Eq. (3.30) makes the formidable task of handling two loop expressions much more manageable and we indeed confirmed explicitly the validity of Eq. (3.30) for the decay $\eta \rightarrow \pi^0\pi^+\pi^-$ at $\mathcal{O}(p^6)$.

Note that the neutral decay amplitude can also be expressed directly in terms of the $M_I(t)$,

$$\overline{M}(s, t, u) = M_0(s) + M_0(t) + M_0(u) + \frac{4}{3}(M_2(s) + M_2(t) + M_2(u)). \quad (3.31)$$

when using the isospin relation (3.29).

3.3.4 Feynman Graphs

We have collected all the amputated Feynman diagrams needed for this process according to the ChPT power counting scheme introduced in Sect. 3.2. In these figures a filled circle denotes a vertex of order p^2 , a filled square a vertex of order p^4 and the grey filled square a vertex of order p^6 .

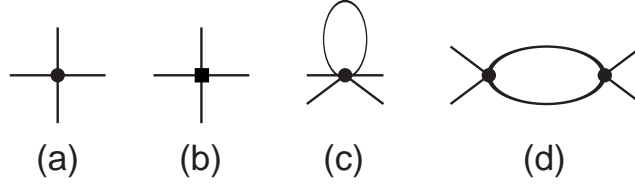


Figure 3.2: The Feynman diagrams of order p^2 , (a) and of order p^4 , (b)-(d).

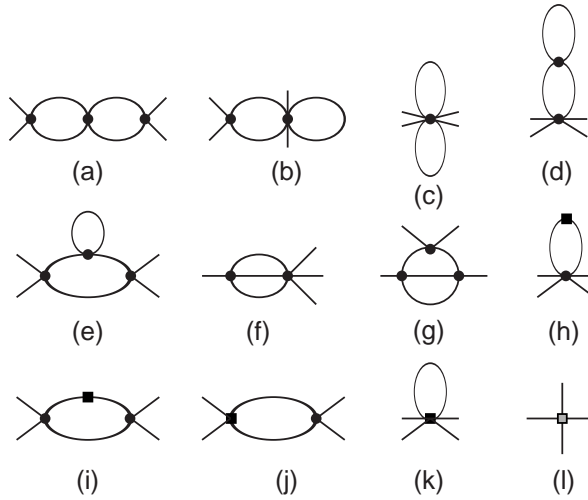


Figure 3.3: Feynman diagrams of order p^6 .

3.3.5 Regularization, renormalization and integrals

As a regularization method we use dimensional integration. The regularization method is described in detail in [31, 32].

The one-loop functions needed are defined in many places. We use the definitions as given in [42, 25, 43]. The two-loop integrals we evaluate numerically using the methods described in [42] for the sunset integrals and in [43] for the vertex integrals.

In addition to the integrals given there, we also need derivatives w.r.t. one of the masses in order to be able to pull out the overall isospin breaking factor in the amplitudes. For all the one-loop integrals needed, these derivatives can be derived exactly. An example of a relation we derived, needed to obtain

agreement with the order p^4 result of [10] is

$$\begin{aligned} \overline{C}(m^2, m^2, m^2, p^2) &= \left. \frac{\partial}{\partial m_1^2} \overline{B}(m_1^2, m_2^2, p^2) \right|_{m_1^2=m_2^2=m^2} \\ &= -\frac{2}{p^2 - 4m^2} \left(\overline{B}(m^2, m^2, p^2) - \overline{B}(m^2, m^2, 0) - \frac{2}{16\pi^2} \right). \end{aligned} \quad (3.32)$$

For the two-loop integrals, we have taken the derivatives numerically.

3.4 Analytical results

3.4.1 Order p^2

At leading order there is one tree graph from \mathcal{L}_2 to compute since we have already diagonalized the fields in the lowest order Lagrangian. The lowest order decay amplitude takes on the form

$$M^{(2)}(s) = \frac{1}{F_\pi^2} \left(\frac{4}{3} m_\pi^2 - s \right) \quad (3.33)$$

using the identity $s + t + u = 3s_0$. F_π and m_π are the physical pion decay constant and the physical pion mass respectively, which involve corrections of order p^4 and p^6 . The higher order corrections due to the redefinition of the parameters are carried to the respective amplitude of order p^4 and p^6 . This agrees with the known lowest order results [5, 6, 10] but is written in a somewhat different form. We have chosen this form since it brings out the Adler zero explicitly.

3.4.2 Order p^4

At this order we obtain vertices from \mathcal{L}_2 to construct the tadpole, Fig. 3.2(c) and the so-called unitarity graphs Fig. 3.2(d) and in addition, the tree diagram from \mathcal{L}_4 , Fig. 3.2(b). These are the diagrams contributing to $\mathcal{G}_{1238}^{(4)}$ of (3.20). The second set of terms in $\mathcal{A}_{1238}^{(4)}$ in (3.20) is from what is usually called wave function renormalization. The final two terms in $\mathcal{A}_{1238}^{(4)}$ of (3.18) are what are called the mixing corrections⁵.

The sum of all the contributions described in Eq. (3.20) gives the full one-loop amplitude. G-parity requires the amplitude to be proportional to $\sin(\epsilon)$ as was the case at leading order. This does not occur explicitly at order p^4 ,

⁵In our calculations, lowest order mixing is dealt with exactly. The mixing at higher orders is dealt with perturbatively.

because now isospin is broken in the meson loops. In order to pull out an overall mixing angle we then carry out a Taylor expansion of the loop integrals involving two charged kaons around the neutral kaon mass. The amplitude is written as

$$M^{(4)}(s, t, u) = \frac{1}{F_\pi^4} \left[M_0^{(4)}(s) + (s-u)M_1^{(4)}(t) + (s-t)M_1^{(4)}(u) + M_2^{(4)}(t) + M_2^{(4)}(u) - \frac{2}{3}M_2^{(4)}(s) \right]. \quad (3.34)$$

The full expression at $\mathcal{O}(p^4)$ for the $M^{(4)}(t)$ can be found in App. 3.B. There, all the masses and the pion decay constant are the physical ones. We have taken the expressions at lowest order and one-loop order and added the correction terms needed at the higher orders to bring them into the form we show in (3.33) and App. 3.B. and are corrected up to order p^6 . We retain all the p^4 effective constants in our expression, in contrast to [10] where all but L_3 are eliminated in favor of measurable quantities. We have also found our analytical results in full accord with that in [10].

3.4.3 Order p^6

We again split the amplitude as in (3.30).

$$M^{(6)}(s, t, u) = \frac{1}{F_\pi^6} \left[M_0^{(6)}(s) + (s-u)M_1^{(6)}(t) + (s-t)M_1^{(6)}(u) + M_2^{(6)}(t) + M_2^{(6)}(u) - \frac{2}{3}M_2^{(6)}(s) \right]. \quad (3.35)$$

However, the order p^6 expression is extremely long. The dependence on the order p^6 LECs is given in App. 3.C. We split the result in several parts

$$M_I^{(6)}(t) = M_I^C(t) + M_I^{LL}(t) + M_I^T(t). \quad (3.36)$$

$M_I^C(t)$ contains the contributions from the order p^6 LECs, $M_I^{LL}(t)$ contains the contributions that involve the order p^4 LECs and $M_I^T(t)$ is the pure two-loop contribution, only dependent on the masses of the pseudo-scalars. $M_I^T(t)$ itself we split in the parts coming from vertex-integrals, sunset-integrals and the rest. The latter split is definitely not unique. It depends on how many of the relations between the various integrals are actually used and we observe strong numerical cancellations between its different parts. We therefore only quote numerical results for $M_I^T(t)$ as a whole.

The calculation has been performed independently by each of the authors, the divergences agree with those of the general calculation [32] and nonlocal

divergences cancel as required. We have also checked explicitly that the amplitudes can be brought into the form (3.30). The numerical results are also done twice and we have checked that they agree. Finally, μ -independence has been checked numerically and found to be satisfactory. The latter is not exact, since we have expressed the order p^4 and p^6 in the physical masses and there is a residual p^8 μ dependence left over. We do observe a strong cancellation between the order p^4 and p^6 μ -dependence as expected.

3.5 Resonance estimates of the p^6 LECs and the inclusion of the η'

Chiral symmetry imposes no constraints on the values of the low energy constants, nevertheless these constants do depend on the parameters of the underlying theory, QCD, namely the masses of the heavy quarks and the scale Λ_{QCD} . Hence, all the LECs may be determined from first principles employing the Lattice QCD technique. At order p^4 , most of the LECs have been determined phenomenologically and some of them are checked numerically by the use of the Lattice QCD [44]. At the present time, only very few of the order p^6 LECs are estimated using available data[23]. In this section, we will discuss briefly how to do an approximate estimation of the LECs within the framework of the resonance effective field theories. In the limit $N_c \rightarrow \infty$, the matching of the QCD and ChPT might become feasible since now, an infinite tower of massive narrow hadronic states emerge. With these states one can construct a chiral invariant Lagrangian incorporating both Goldstone mesons and resonance fields. In practice one has to do a truncation on the hadronic spectrum and limit the resonance multiplets to low-lying excitations. The construction of the p^4 resonance Lagrangian is discussed in the pioneering works[35, 37]. The extension of the earlier works to $\mathcal{O}(p^6)$ is presented in [36]. In the following we present a resonance Lagrangian at order p^6 with the vector realization of the vector fields, [35, 36] use the antisymmetric tensor formulation. The exchange of axial-vector resonances does not contribute to the process $\eta \rightarrow 3\pi$ and they are not discussed here. We do, in addition to the lowest vector nonet, include the pseudo-scalar singlet and a scalar nonet.

The building blocks one needs for the construction of the Lagrangian take the form

$$\begin{aligned} u^\mu &= iu^\dagger D^\mu U u^\dagger \quad \text{with} \quad u^2 = U, \\ \chi_\pm &= u^\dagger \chi u^\dagger \pm u \chi^\dagger u. \end{aligned} \tag{3.37}$$

These transform as an octet under $SU(3)_V$ using the general CCWZ construction⁶.

⁶See Refs. [35, 36] for a more extensive discussion and references

The resonance fields are counted as order 1 in the chiral counting. We do not include the complete possible list of terms here but restrict to a smaller subset which contains the lowest order interactions of the resonances in our chosen representation for them. This is the same subset of possible terms used in most of the work on NNLO ChPT. We only show the terms relevant for $\eta \rightarrow 3\pi$ here. For the vector fields we use as Lagrangian

$$\mathcal{L}_V = -\frac{1}{4}\langle V_{\mu\nu}V^{\mu\nu}\rangle + \frac{1}{2}m_V^2\langle V_\mu V^\mu\rangle - \frac{ig_V}{2\sqrt{2}}\langle V_{\mu\nu}[u^\mu, u^\nu]\rangle + f_\chi\langle V_\mu[u^\mu, \chi_-]\rangle. \quad (3.38)$$

$V_{\mu\nu} = \nabla_\mu V_\nu - \nabla_\nu V_\mu$ and the matrix content of the vector field reads in terms of the more familiar observed particles

$$V_\mu = \begin{pmatrix} \frac{\rho^0}{\sqrt{2}} + \frac{\omega}{\sqrt{2}} & \rho^+ & K^{*+} \\ \rho^- & -\frac{\rho^0}{\sqrt{2}} + \frac{\omega}{\sqrt{2}} & K^{*0} \\ K^{*-} & \bar{K}^{*0} & \phi \end{pmatrix}_\mu. \quad (3.39)$$

The singlet component does not contribute to order p^6 for $\eta \rightarrow 3\pi$. For the scalar meson nonet, the matrix of fields S , we consider

$$\mathcal{L}_S = \frac{1}{2}\langle \nabla^\mu S \nabla_\mu S - M_S^2 S^2 \rangle + c_d \langle S u^\mu u_\mu \rangle + c_m \langle S \chi_+ \rangle \quad (3.40)$$

At tree level integrating out the heavy fields is equivalent to applying the equation of motion for the elimination of the heavy fields. To solve the equation of motion we perform a perturbative expansion of the resonance field with coefficients in increasing powers of $1/M_R$ (M_R , the resonance mass) and then solve the equation of motion recursively. We obtain for the Vector V^μ and Scalar S resonance field

$$\begin{aligned} V^\mu &= -\frac{ig_V}{\sqrt{2}M_V^2}\nabla_\nu[u^\nu, u^\mu] - \frac{1}{M_V^2}f_\chi[u^\mu, \chi_-] + \dots \\ S &= \frac{c_d}{M_S^2}(u_\mu u^\mu) + \frac{c_m}{M_S^2}(\chi_+) + \frac{c_d}{2M_S^4}\nabla^\nu\nabla_\nu(u_\mu u^\mu) + \frac{c_m}{2M_S^4}(\nabla^\mu\nabla_\mu\chi_+) + \dots \end{aligned} \quad (3.41)$$

Substitution of (3.41) in the Lagrangians (3.38) and (3.40) we obtain the effective action from V, S -exchange[31, 25]

$$\mathcal{L}_V = -\frac{1}{4M_V^2}\left\langle\left(ig_V\nabla_\mu[u^\nu, u^\mu] - f_\chi\sqrt{2}[u^\nu, \chi_-]\right)^2\right\rangle \quad (3.42)$$

$$\mathcal{L}_S = \frac{1}{2M_S^4}\left\langle(c_d\nabla^\nu(u_\mu u^\mu) + c_m\nabla^\nu\chi_+)^2\right\rangle \quad (3.43)$$

The resonance couplings were determined in [31, 25, 35]. The values we use are

$$f_\chi = -0.025, \quad g_V = 0.09, \quad c_m = 42 \text{ MeV}, \quad c_d = 32 \text{ MeV}, \quad (3.44)$$

and for the masses we use

$$m_V = m_\rho = 0.77 \text{ GeV}, \quad m_S = 0.98 \text{ GeV}. \quad (3.45)$$

The η' plays a significant role in processes involving η due to the $\eta - \eta'$ mixing. Within the quark model, η' and η mix because of the $SU(3)$ symmetry breaking. In the chiral limit the pseudo-scalar octet becomes massless but the η' has a residual mass as a result of the axial $U(1)$ anomaly. In the combined chiral and large N_c limit, however, a nonet of Goldstone particles emerge and this provides a perturbative framework to investigate the dynamical interplay between η' and Goldstone particles, see e.g. [45, 46].

One important result is the saturation of the low energy constant L_7 by the η' exchange[9]

$$L_7^{\eta'} = -\frac{\tilde{d}_m^2}{2M_{\eta'}^2} \quad (3.46)$$

We therefore perceive the η' dynamical effects at order p^4 through its contribution to the effective constant L_7 . In the light of this realization, the $\eta - \eta'$ mixing effect on the C_i involved in the decay $\eta \rightarrow 3\pi$ can be obtained by constructing an appropriate $U(3)$ Lagrangian at order p^6 . That $\eta - \eta'$ mixing can be treated perturbatively for the decay $\eta \rightarrow 3\pi$ is discussed extensively in [45]. We take for the singlet degree of freedom P_1 the simple Lagrangian

$$\mathcal{L}_{\eta'} = \frac{1}{2} \partial_\mu P_1 \partial^\mu P_1 - \frac{1}{2} M_{\eta'}^2 P_1^2 + i \tilde{d}_m P_1 \langle \chi_- \rangle. \quad (3.47)$$

Integrating out P_1 leads to the order p^4 term with L_7 of (3.46) and the order p^6 Lagrangian

$$\mathcal{L}_{\eta'} = -\frac{\tilde{d}_m^2}{2M_{\eta'}^4} \partial_\mu \langle \chi_- \rangle \partial^\mu \langle \chi_- \rangle \text{ with } \tilde{d}_m = 20 \text{ MeV}. \quad (3.48)$$

The latter can be rewritten in general in terms of the basis of operators of [30]. The result is⁷

$$\begin{aligned} \partial_\mu \langle \chi_- \rangle \partial_\mu \langle \chi_- \rangle &= O_{18} + \frac{2}{9} O_{19} - \frac{1}{3} O_{20} + \frac{1}{3} O_{21} + 2O_{27} + \frac{2}{3} O_{31} - \frac{1}{3} O_{32} \\ &\quad + \frac{1}{3} O_{33} - 2O_{35} + O_{37} - \frac{8}{3} O_{94}. \end{aligned} \quad (3.49)$$

⁷This was derived by the authors of [25] but not included in the final manuscript. It agrees with the expression shown by Kaiser[47].

i	$\frac{F_0^2 g_V^2}{M_V^2}$	$\frac{F_0^2 g_V f_X}{\sqrt{2}M_V^2}$	$\frac{F_0^2 f_X^2}{M_V^2}$	$\frac{F_0^2 c_d^2}{M_S^4}$	$\frac{F_0^2 c_d c_m}{M_S^4}$	$\frac{F_0^2 c_m^2}{M_S^4}$	$\frac{F_0^2 \tilde{d}_m^2}{M_{P_1}^4}$
1	1/8			-1/4			
4	1/8						
5					1/2		
8					1/2		
10					-1		
12					-1/2		
18							-1/2
19					1/27		-1/9
20					-1/18		1/6
22	1/16	1/2		1/8			
24	1/12			-1/6			
25	-3/8	-1		1/4			
26	7/36	1	1	-5/36	-1/2	-1/4	
27	-1/36			1/18	1/3		-1
28	1/72			-1/36			
29	-11/72	-1	-1	1/18	-1/2	-1/4	
31					-7/18		-1/3
32					-1/18		1/6
33					2/9		-1/6

Table 3.1: The resonance exchange estimates of C_i contributing to $\eta \rightarrow 3\pi$. The vector exchange results are taken from [48] scalar exchange from [36]. For the singlet eta contribution, see text. The result for the C_i^r is the top row multiplied by the coefficients given in the table. Only nonzero coefficients that also contribute to $\eta \rightarrow 3\pi$ are given. We use here the dimensionless version of the C_i^r . Only terms relevant for $\eta \rightarrow 3\pi$ are shown.

We have derived the contribution to $\eta \rightarrow 3\pi$ in different ways. An option is to evaluate explicitly the resonance exchange directly from the Lagrangians with resonances. The second method is as described above, to evaluate the exchange in general in terms of an effective Lagrangian of the pseudo-scalars only and then calculate with that one. The third option is to rewrite the contributions from vector and resonance exchange in terms of the order p^6 ChPT Lagrangian [32]. The latter can be done for the scalar octet using the results of [36], for the vector nonet using [48] and the pseudo-scalar singlet using (3.49). We have checked that the first method also gives the Lagrangians (3.42) and (3.43) and that the 2nd and third method in the end give the same contribution to $\eta \rightarrow 3\pi$. The results for the C_i are quoted in Tab. 3.1. In the numerical estimates we have used $F_0 = F_\pi$.

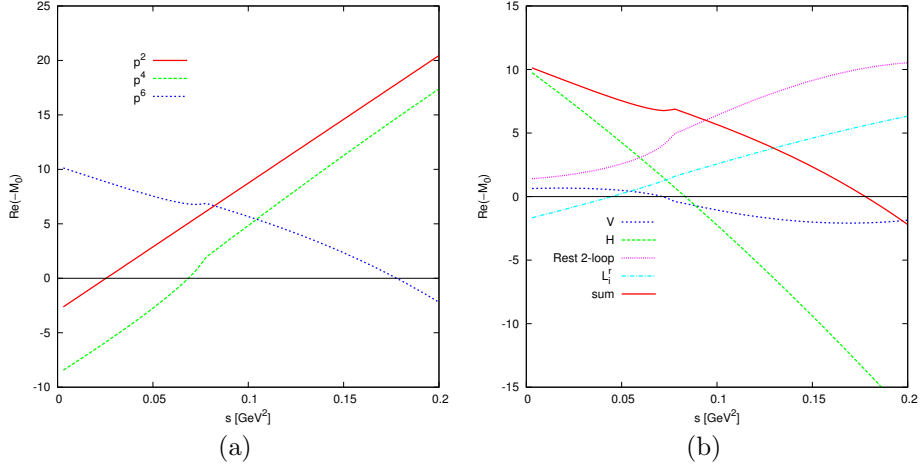


Figure 3.4: (a) The order p^2 , p^4 and p^6 contribution to $-ReM_0(s)$. (b) The order p^6 contribution to $-M_0(t)$ split into its parts, the contribution from vertex-integrals (V), sunsetintegrals (H) and the remaining pure two-loop part as well as the L_i^r -dependent part.

3.6 Numerical results

3.6.1 A first look

In this section we present some plots of the amplitude to give a first impression of how the higher orders look like. We start with figures showing different contributions to $M_{0,1,2}(s)$. It should be noted that since terms can be moved around between the $M_I(s)$ these figures cannot be used to check whether we have convergence or not. They are shown for illustration only. We have actually plotted the negative of the quantities defined earlier, this makes the size of the corrections easier to judge.

The input values we use are the physical eta mass, $m_\eta = 543.7$ MeV, the average Kaon mass removing electromagnetic effects, $m_K = 494.53$ MeV and a pion mass such that $s+t+u = m_\eta^2 + 3m_\pi^2$ is satisfied for the charged and neutral decay. So we use $3m_\pi^2 = 2m_{\pi^+}^2 + m_{\pi^0}^2$ for the charged decay and $m_\pi^2 = m_{\pi^0}^2$ for the neutral decay. More general plots were always done with the mass as for the charged decay. The order p^4 LECs are set to the values for fit 10 of [34] and we have set the order p^6 LECs equal to zero. The subtraction scale is $\mu = 770$ MeV.

In Fig. 3.4(a) we show the contributions of order p^2 , p^4 and p^6 to $M_0(t)$. One sees an acceptable convergence in the physical domain for the decay. In Fig. 3.4(b) we show how the different parts contribute. As one can see, there

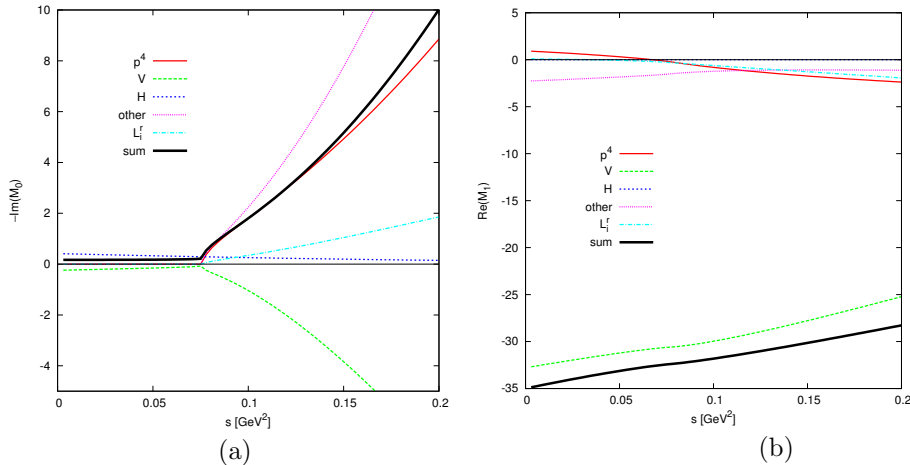


Figure 3.5: (a) The order p^2 , p^4 and p^6 contribution to $-\text{Im}M_0(s)$. (b) The order p^4 and p^6 contribution to $-\text{Re}M_1(s)$.

are sizable cancellations in the order p^6 contribution. In Fig. 3.5(a) we show the various contribution to the absorptive part of $M_0(s)$. We see that the total p^6 is about the same size as the order p^4 one. To be noted is the three particle cut that contributes first at order p^6 . This allowed $M_0(s)$ to have an absorptive part also below the two-pion threshold. This cut gets contributions from the vertex- and the sunset-integrals, diagrams in Fig. 3.3(f) and (g). As expected, this cut gives a rather small contribution. We also show a case where the convergence looks bad, $M_1(s)$ shown in Fig. 3.5(b). When we look at the full amplitude this large correction is not visible. It seems to be tempered sufficiently when all the different $M_I(s)$ are summed as in (3.30).

To see this, let us look at the amplitude along the line $u = t$ as a function of s for the full amplitude. Here we plot first our full result. In Fig. 3.6 we show the order p^2 , the sum of order p^2 and p^4 and finally the sum of order p^2 , p^4 and order p^6 . Note the shift in the Adler zero in going from order p^2 to order p^4 .

As a final part here we show the dependence on the subtraction constant μ . As mentioned above, our full result is μ -independent to the order it should be with a cancellation between the variation at NLO and NNLO. The μ -dependence creeps in via the estimate of the C_i^r and at which scale μ it is applied. In Fig. 3.8 we plot the real part of the amplitude to NLO and NNLO at $\mu = 0.6, 0.77$ and 0.9 GeV. The variation with μ is fairly small.

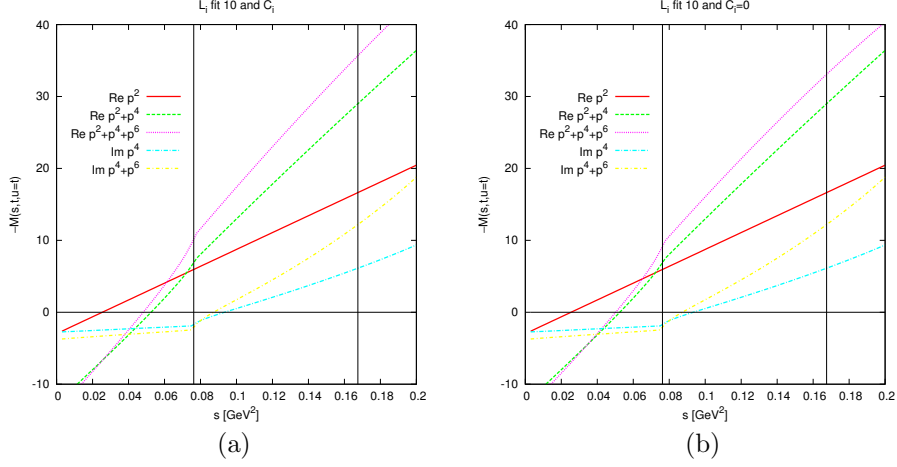


Figure 3.6: The amplitude $M(s, t, u)$ along the line $t = u$. The vertical lines indicate the physical region. (a) Shown are the real and imaginary parts with all parts summed up to the given order. (b) Same plot but the contribution from the C_i^T has been removed.

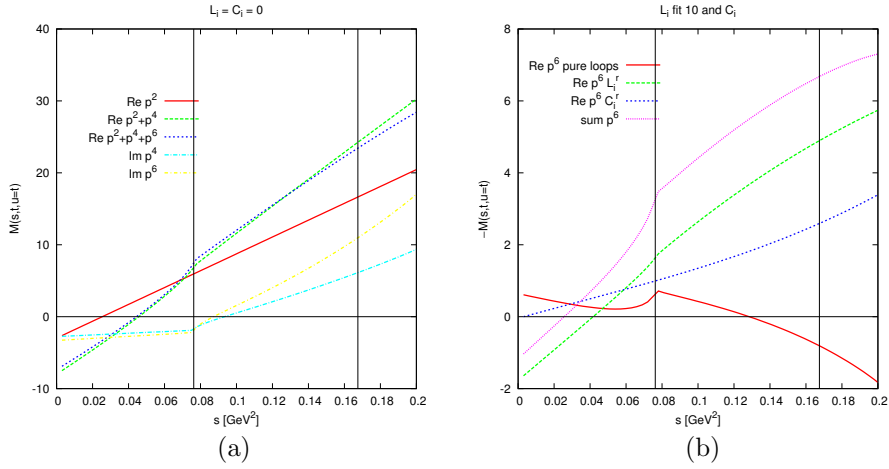


Figure 3.7: The amplitude $M(s, t, u)$ along the line $t = u$. The vertical lines indicate the physical region. (a) Shown are the real and imaginary parts with all parts summed up to the given order but the contribution from the L_i^T and C_i^T have been removed. (b) Same plot but showing the various parts.

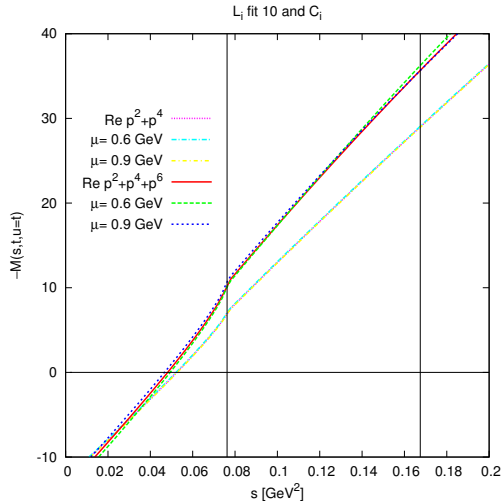


Figure 3.8: The amplitude $M(s, t, u)$ along the line $t = u$ to NLO and NNLO order for three choices of the subtraction point μ , i.e. three choices at which the estimate of the $C_i^r(\mu)$ is applied.

3.6.2 Comparison with the dispersive result

Since long ago it has been known that the decay amplitude of $\eta \rightarrow \pi\pi\pi$ receives a sizable enhancement due to the loop correction at $\mathcal{O}(p^4)$ [10]. In fact it turned out that a large part of this correction comes from $\pi\pi$ rescattering in the final state as expected [17, 18]. This has prompted two different analyses using dispersive methods. They both restrict themselves to $\pi\pi$ -rescattering but differ in how the subtraction constants are determined and in how the dispersion theory is used. Ref. [19] used the Khuri-Treiman equations and fixed the subtraction constants by comparing with the one-loop expression at various kinematical points. Ref. [20] generalized the reasoning behind [40] to obtain a series of dispersion relations for the $M_I(t)$ defined in (3.30). Their predictions on the decay width are in agreement within the quoted uncertainties, [20] finds $\Gamma = 219 \pm 22$ eV and [19] obtain $\Gamma = 209 \pm 20$ eV. Both used Dashen's theorem and the then known value of L_3^r to fix the overall constant. These, however, must be compared with $\Gamma_{exp} = 295$ eV which provides a check on Dashen's theorem [39]. On the other hand, as emphasized in [11, 49], they have a rather different behaviour in the phase space distributions. This is shown in Fig. 3.9. It can be seen that the slope in [19] is smaller than the order p^4 results while [20] has a larger slope than the one-loop result. The latter also follows from the very simplified dispersive analysis performed in [11] shown in Fig. 3.10(a). The

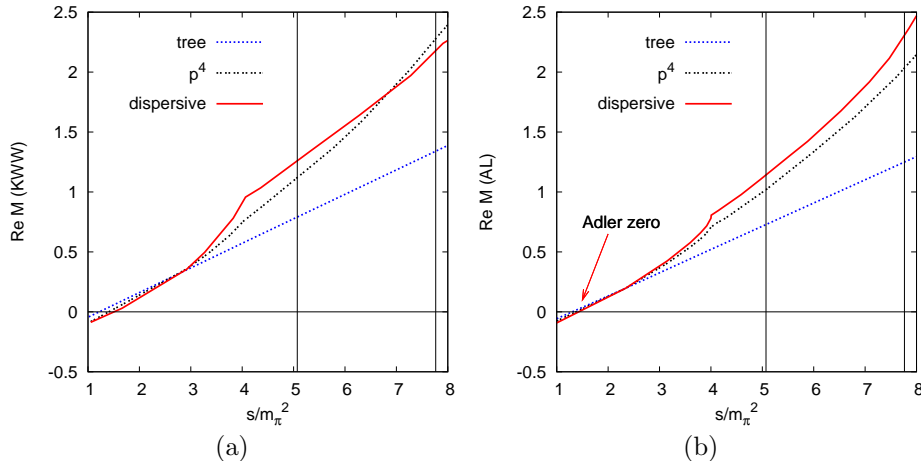


Figure 3.9: (a) Decay amplitude obtained by use of extended Khuri-Treiman equations[19] along the line $s = u$. (b) Alternative dispersive analysis for the decay amplitude[20]. Figs. from [49], adapted from [19, 20].

general feature of the result of [20] seems to be robust against small changes. One motivation for the present work is to check these predictions and see if other effects could be important as well, at order p^4 only about half the correction came from the unitarity correction.

We can now compare the same plot coming from our full NNLO calculation shown in Fig. 3.10(b). The total order p^6 correction is somewhat larger than observed in [19, 20] but the trend is definitely in better agreement with [20].

In [20] the fact that the position of the Adler zero did not change much from LO to NLO was used to determine the subtraction constants. In Fig. 3.11 we show a blowup of the region around the Adler zero. As can be seen, the position of the zero in the real part varies a bit by going from LO to NLO and then almost moves back at NNLO. This is not incompatible with the observation of [20], we use a slightly different version of NLO than the one in [10] and use different input parameters resulting from the order p^6 determination of LECs [34]. The current algebra prediction for the Adler zero⁸ is $s = \frac{4}{3}m_\pi^2$, independent of t . The NLO effect produces a t dependent shift in the zero for the real part. A fairly large positive shift occurs along the line $t = u$ going from LO to NLO and a smaller negative shift from NLO to NNLO as can be seen in Fig. 3.7(a). Along the line $s = u$, a smaller positive shift appears from LO to NLO at $s = 1.70 m_\pi^2$ shifting to $s = 1.17 m_\pi^2$ at NNLO. The effects on the slopes can be judged from Figs. 3.7(a) and Fig. 3.11.

⁸We take here the zero of the real part of the amplitude as the Adler zero.

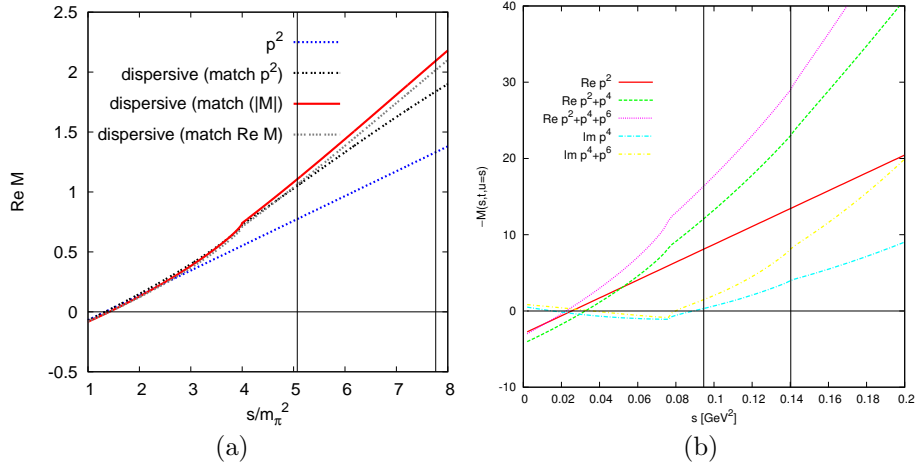


Figure 3.10: (a) The simplified analysis of [11] which shows the same general behaviour as the result of [20] shown in Fig. 3.9(b). (b) Our result for $M(s, t, u)$ at $s = u$.

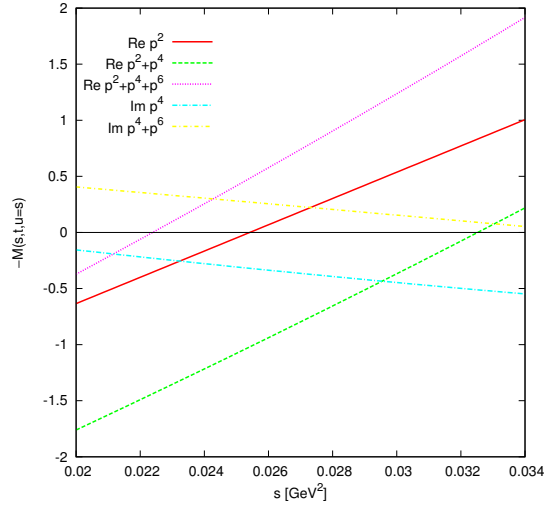


Figure 3.11: $M(s, t, u)$ along the line with $s = u$ concentrated along the Adler zero.

3.6.3 Dalitz Plot Parameters

In general we use the data averages of the particle data group (PDG)[13]. For the distributions in the Dalitz plot the PDG presents no averages. This

Exp.	a	b	d
KLOE [50]	$-1.090 \pm 0.005^{+0.008}_{-0.019}$	$0.124 \pm 0.006 \pm 0.010$	$0.057 \pm 0.006^{+0.007}_{-0.016}$
Crystal Barrel [51]	-1.22 ± 0.07	0.22 ± 0.11	0.06 ± 0.04 (input)
Layter et al. [52]	-1.08 ± 0.014	0.034 ± 0.027	0.046 ± 0.031
Gormley et al. [53]	-1.17 ± 0.02	0.21 ± 0.03	0.06 ± 0.04

Table 3.2: Measurements of the Dalitz plot distributions in $\eta \rightarrow \pi^+\pi^-\pi^0$. The parameters are defined in Eq. (3.51). The KLOE result [50] for f is $f = 0.14 \pm 0.01 \pm 0.02$. None of the others determined f . The Crystal Barrel used d as input, but remarked that a and b varied very little within the range of d used.

distribution is usually described in terms of the variables

$$\begin{aligned}
 x &= \sqrt{3} \frac{T_+ - T_-}{Q_\eta} \\
 y &= \frac{3T_0}{Q_\eta} - 1 \\
 Q_\eta &= m_\eta - 2m_{\pi^+} - m_{\pi^0}
 \end{aligned} \tag{3.50}$$

for the charged decay. T^i is the kinetic energy of pion π^i in the final state. The standard parameterization of the Dalitz plot is (up to third order)

$$|M|^2 = A_0^2 (1 + ay + by^2 + dx^2 + fy^3 + gx^2y + \dots) . \tag{3.51}$$

Odd terms in x are forbidden by charge conjugation, all experimental results find them compatible with zero and since all most precise experiments have presented fits with the odd terms set to zero we use those. f has only been measured by KLOE [50] and no experiment has attempted to determine g . Earlier experiments that only determined a and b are not included. The results are shown in Tab. 3.2. There are discrepancies among data which are hard for us to discuss since correlations are important. There is however a clear discrepancy between KLOE[50] and Gormley et al.[53] for a , KLOE[50], Gormley et al.[53] and Layter et al.[52] have three rather incompatible numbers for b . The results for d are all compatible.

Similarly the neutral decay is parameterized by

$$|\overline{M}|^2 = \overline{A}_0^2 (1 + 2\alpha z + \dots) . \quad z = \frac{2}{3} \sum_{i=1,3} \left(\frac{3E_i - m_\eta}{m_\eta - 3m_\pi^0} \right)^2 . \tag{3.52}$$

E_i is the energy of the i th pion in the final state. The parameter α has been measured by several experiments. There are two recent high precision measurements but they are in disagreement, however, KLOE published a new analysis

Exp.	α
KLOE [54]	$-0.027 \pm 0.004^{+0.004}_{-0.006}$
KLOE (prel)[55]	$-0.014 \pm 0.005 \pm 0.004$
Crystal Ball [56]	-0.031 ± 0.004
WASA/CELSIUS [57]	$-0.026 \pm 0.010 \pm 0.010$
Crystal Barrel [58]	$-0.052 \pm 0.017 \pm 0.010$
GAMS2000 [59]	-0.022 ± 0.023
SND [60]	$-0.010 \pm 0.021 \pm 0.010$

Table 3.3: Measurements of the Dalitz plot distribution in $\eta \rightarrow \pi^0\pi^0\pi^0$. The parameter α is defined in Eq. (3.52).

very recently. Let us now discuss how to extract the Dalitz parameters in chiral perturbation theory. First for the charged decay. The Dalitz plot variables x and y are related to the kinetic energy of the outgoing particles. In terms of Mandelstam parameters they are given as,

$$\begin{aligned}
 x &= \frac{\sqrt{3}}{2m_\eta Q_\eta}(u-t) \\
 y &= \frac{3}{2m_\eta Q_\eta}((m_\eta - m_{\pi^0})^2 - s) - 1 \stackrel{\text{iso}}{=} \frac{3}{2m_\eta Q_\eta}(s_0 - s). \quad (3.53)
 \end{aligned}$$

The first equality is valid in general, the second only in the isospin limit. Our amplitudes are in the isospin limit, with a common pion mass everywhere. The physical value gives $Q_\eta = m_\eta - 2m_{\pi^+} - m_{\pi^0} = 0.13318$. For the pion mass we used, $3m_\pi^2 = 2m_{\pi^+}^2 + m_{\pi^0}^2$, we get $Q_\eta = 0.13313$ MeV. So the value of Q_η is fine. In the isospin limit, $x = y = 0$ and $s = t = u = s_0$ coincide. In the physical case there is a small difference, $s = t = u = s_0$ corresponds to $y = -0.052$.

We evaluate the decay amplitude $M(s, t, u)$ in the s - t plane over the physical region. Since only two variables s and t are independent the relation $s+t+u = m_\eta^2 + 2m_{\pi^+}^2 + m_{\pi^0}^2$ is used to eliminate the third Mandelstam variable u in the amplitude. We then fit (3.51) to the amplitude $|M|^2 = |M^{(2)} + M^{(4)} + M^{(6)}|^2$ with as error $\Delta = \text{Re}M^{(6)}\text{Re}(M^{(2)} + M^{(4)} + M^{(6)}) + \text{Im}M^{(6)}\text{Im}(M^{(2)} + M^{(4)} + M^{(6)})$. This is half of the NNLO contribution. The fitting error quoted in the result (3.54) is from this error, not from errors in the input values of the C_i^r and other LECs. For y we used the second expression in (3.53). The fits have been performed to $|M^{(2)}|^2$, $|M^{(2)} + M^{(4)}|^2$ and $|M^{(2)} + M^{(4)} + M^{(6)}|^2$ labeled LO, NLO and NNLO respectively. In NNLO we have studied the effect of setting the $C_i^r = 0$ and setting $L_i^r = C_i^r = 0$ and in NLO for $L_i^r = 0$. In addition, we have checked how much changing y from the second to the first expression in (3.53) changes the results, labeled NNLOp as well as including the g term and

	A_0^2	a	b	d	f
LO	120	-1.039	0.270	0.000	0.000
NLO	314	-1.371	0.452	0.053	0.027
NLO ($L_i^r = 0$)	235	-1.263	0.407	0.050	0.015
NNLO	538	-1.271	0.394	0.055	0.025
NNLOp	574	-1.229	0.366	0.052	0.023
NNLOq	535	-1.257	0.397	0.076	0.004
NNLO ($\mu = 0.6$ GeV)	543	-1.300	0.415	0.055	0.024
NNLO ($\mu = 0.9$ GeV)	548	-1.241	0.374	0.054	0.025
NNLO ($C_i^r = 0$)	465	-1.297	0.404	0.058	0.032
NNLO ($L_i^r = C_i^r = 0$)	251	-1.241	0.424	0.050	0.007
dispersive[19]	—	-1.33	0.26	0.10	—
tree dispersive[11]	—	-1.10	0.33	0.001	—
absolute dispersive[11]	—	-1.21	0.33	0.04	—

Table 3.4: Theoretical estimate of the Dalitz plot distributions in $\eta \rightarrow \pi^+\pi^-\pi^0$. The parameters are defined in Eq. (3.51). The line labeled NNLO is our central result.

the terms with x^4, x^2y^2, y^4 , labeled NNLOq. The results are given in Tab. 3.4. The changes in going from NLO to NNLO are rather modest, the main change is the overall normalization A_0^2 . The linear slope a is lowered somewhat but not enough to reach the most recent experimental value. The same comment applies to the quadratic slope b . d is in agreement with the experimental values. f is always much smaller than the measured value of KLOE. The results from the dispersive calculations using Khuri-Treiman[19]⁹ and the simplified analysis of [11] with two different boundary conditions are also shown in the table. [21] used these parameters as input and we have therefore not shown their result. As final result we take the NNLO result of Tab. 3.4 with the MINUIT errors with inputs as above.

$$\begin{aligned}
A_0^2 &= 538 \pm 18, \\
a &= -1.271 \pm 0.075, \\
b &= 0.394 \pm 0.102, \\
d &= 0.055 \pm 0.057, \\
f &= 0.025 \pm 0.160.
\end{aligned} \tag{3.54}$$

The fitting results for the neutral decay are shown in Tab. 3.5. Again we

⁹Note that there exists an analysis [61] using the method of [19] fitting the preliminary KLOE results. However, their final normalization depends on the allowed ranges of parameters given by [19]. This is why we do not quote their numbers below.

	\overline{A}_0^2	α
LO	1090	0.000
NLO	2810	0.013
NLO ($L_i^r = 0$)	2100	0.016
NNLO	4790	0.013
NNLOq	4790	0.014
NNLO ($C_i^r = 0$)	4140	0.011
NNLO ($L_i^r = C_i^r = 0$)	2220	0.016
dispersive[19]	—	—(0.007—0.014)
tree dispersive[11]	—	—0.0065
absolute dispersive[11]	—	—0.007
[21]	—	—0.031

Table 3.5: Theoretical estimates of the Dalitz plot distribution in $\eta \rightarrow \pi^0\pi^0\pi^0$. The parameter α is defined in Eq. (3.52). The line labeled NNLO is the main result.

have fitted LO, NLO, NNLO and removed the contributions from C_i^r and L_i^r to see their effects. The one labeled NNLOq is the same fit as NNLO but with the next two terms in the expansion around $s = t = u = s_0$ included in the fit. As in the case of the charged decay, one sees that going from NLO to NNLO does not seem to change much in the Dalitz plot distributions but changes mainly the overall normalization. It should be mentioned that because of the three terms in (3.29) large cancellations happen in the amplitude for $\eta \rightarrow 3\pi^0$. This, as well as an inequality between the slope parameters is derived in App. 3.A. The inequality is always satisfied by our results and the equality which results under additional assumptions is reasonably well satisfied. Assuming the error on the NNLO result to be one half the NNLO contribution as we did for the charged case leads to

$$\begin{aligned}\overline{A}_0^2 &= 4790 \pm 160 \\ \alpha &= 0.013 \pm 0.032.\end{aligned}\tag{3.55}$$

The results from the dispersive calculations using Khuri-Treiman[19] and the simplified analysis of [11] with two different boundary conditions are also shown in the table. No theoretical prediction comes near the experimental results of KLOE[54] and Crystal Ball[56] except for the result¹⁰ of [21].

It is clear from these results that further study on possible variations of input parameters of ChPT is needed. One puzzling observation is however

¹⁰That reference combines a Chiral Lagrangian including the η' and a model for unitary resummations. Their good agreement with data is remarkable but should also be understood using more controlled approximations.

that the main effect in the dispersive calculations is S -wave rescattering and the input parameters used here give a very good prediction for the scattering length a_0^0 [62].

3.6.4 The ratio r and decay rates

We can now proceed to calculate the various decay rates from our amplitude. Since the evaluation of the NNLO terms is very slow we have used the following procedure. The actual shape of the allowed s, t, u region in the physical charged decay is somewhat different from the one allowed with an equal pion mass. We therefore perform the integration over the physically allowed values of s, t, u for the neutral and charged case.

The matrix-element $|M|^2$ is dealt with similar to the previous subsection. First we fit $|M|^2$ with an expansion in x and y up to fourth order in x and y for the charged and neutral case. The values for x and y are calculated using the values for s, t, u with the formulas of the isospin limit with the pion mass as defined above.

Doing that leads to the decay widths for the decays where we have indicated the various orders

$$\begin{aligned}
 \Gamma(\eta \rightarrow \pi^+ \pi^- \pi^0) &= \sin^2 \epsilon \cdot 0.572 \text{ MeV} && \text{LO}, \\
 &\sin^2 \epsilon \cdot 1.59 \text{ MeV} && \text{NLO}, \\
 &\sin^2 \epsilon \cdot 2.68 \text{ MeV} && \text{NNLO}, \\
 &\sin^2 \epsilon \cdot 2.33 \text{ MeV} && \text{NNLO } C_i^r = 0, \\
 \Gamma(\eta \rightarrow \pi^0 \pi^0 \pi^0) &= \sin^2 \epsilon \cdot 0.884 \text{ MeV} && \text{LO}, \\
 &\sin^2 \epsilon \cdot 2.31 \text{ MeV} && \text{NLO}, \\
 &\sin^2 \epsilon \cdot 3.94 \text{ MeV} && \text{NNLO}, \\
 &\sin^2 \epsilon \cdot 3.40 \text{ MeV} && \text{NNLO } C_i^r = 0. \quad (3.56)
 \end{aligned}$$

The numbers in (3.56) can be used to calculate the ratio of decay rates

$$r \equiv \frac{\Gamma(\eta \rightarrow \pi^0 \pi^0 \pi^0)}{\Gamma(\eta \rightarrow \pi^+ \pi^- \pi^0)}. \quad (3.57)$$

To lowest order and neglecting the differences in phase space this ratio is expected to be exactly 1.5. The correct treatment of phase space and the slightly different pion mass used lead to

$$r_{\text{LO}} = 1.54. \quad (3.58)$$

At higher orders a significant change is found with

$$\begin{aligned} r_{\text{NLO}} &= 1.46. \\ r_{\text{NNLO}} &= 1.47. \\ r_{\text{NNLO } C_i=0} &= 1.46. \end{aligned} \tag{3.59}$$

The small changes from NLO to NNLO is because the higher order corrections mainly change the overall size of the amplitude, not its shape.

This should be compared with the experimental result[13] of

$$\begin{aligned} r &= 1.49 \pm 0.06 \quad \text{our average.} \\ r &= 1.43 \pm 0.04 \quad \text{our fit,} \end{aligned} \tag{3.60}$$

The different results are from the direct measurements or from the global fit to eta decays. Our results agree excellently with each value.

3.6.5 Discussion and the values of R and Q

One of the prime reasons to study the hadronic eta decay to pions is the direct determination of the double quark mass ratio, Q^2 defined as[39]

$$Q^2 = \frac{m_s^2 - \hat{m}^2}{m_d^2 - m_u^2} \tag{3.61}$$

The reason for considering this quantity is that it is to first order independent of a shift in the quark masses of the form

$$\begin{aligned} m_u &\rightarrow m_u + \alpha m_d m_s, \\ m_d &\rightarrow m_d + \alpha m_s m_u, \\ m_s &\rightarrow m_s + \alpha m_u m_d. \end{aligned} \tag{3.62}$$

Within the framework of standard ChPT such a change is unobservable, it can always be compensated by a change in the values of the LECs up to order p^8 effects. This was observed to order p^4 in [63] but the generalization to higher orders is obviously true. In our case, we are implicitly using assumptions on the values of the constants such that this shift is fixed as discussed in [34]. That is one of the reasons we pulled out an overall factor of $\sin(\epsilon)$ rather than Q^{-2} out of the eta decay amplitude. To first order in isospin breaking we have

$$\sin(\epsilon) = \epsilon = \frac{\sqrt{3}}{4} \frac{m_d - m_u}{m_s - \hat{m}} = \frac{\sqrt{3}}{4} \frac{1}{R}, \tag{3.63}$$

where the last equality defines the ratio R .

	LO	NLO	NNLO	NNLO ($C_i^r = 0$)
$R(\eta)$	19.1	31.8	42.2	38.7
R (Dashen)	44	44	37	—
R (Dashen-violation)	36	37	32	—
$Q(\eta)$	15.6	20.1	23.2	22.2
Q (Dashen)	24	24	22	—
Q (Dashen-violation)	22	22	20	—

Table 3.6: The isospin breaking quantities R are evaluated at p^2 , p^4 and p^6 . The Q values are given with $Q^2 \approx 12.7 R$. See text for details.

Since the process is $\eta \rightarrow 3\pi$ is strongly protected from the electromagnetic interactions due to the chiral symmetry, we expect to obtain the value $m_d - m_u$ rather well from this process. So let us see what our results imply. Using the experimental value[13]

$$\Gamma(\eta \rightarrow \pi^+ \pi^- \pi^0) = 295 \pm 17 \text{ eV} \quad (3.64)$$

and (3.56) and (3.63) we obtain the values for R quoted in Tab. 3.6) in the line labeled $R(\eta)$. For comparison we also quote the values obtained at LO using

$$R_{LO} = \frac{m_{K^0}^2 + m_{K^+}^2 - 2m_{\pi^0}^2}{2(m_{K^0}^2 - m_{K^+}^2)} \quad (3.65)$$

where the QCD part of the masses should be included only. The electromagnetic part of the K^0 and π^0 mass is taken to be negligible and we use

$$m_{K^+ \text{em}}^2 = x_D (m_{\pi^+}^2 - m_{\pi^0}^2). \quad (3.66)$$

We take $x_D = 1$ in the line labeled Dashen[12] and use the estimate $x_D = 1.84$ [64] for the line labeled Dashen-violation. The columns labeled NLO and NNLO quote the results from [34] using the same input. These used $m_s/\hat{m} = 24$ as input but changing it to 26 changes¹¹ the value of R by about half a unit. Note that the limit $R < 44$ [39] is satisfied by all the estimates in Tab. 3.6.

It is harder to draw conclusions on the value of Q . Its value can be obtained from

$$Q^2 = \frac{m_K^2}{m_\pi^2} R_{LO} (1 + \text{NNLO}), \quad (3.67)$$

where again only the QCD part of the masses should be included and m_K^2, m_π^2 are the masses in the isospin limit. The NNLO corrections are known [34] and not negligible. However, they do depend at present on the input value of m_s/\hat{m}

¹¹This can be seen from using the number for m_u/m_d and m_s/\hat{m} from Fig. 3(b) in [34].

used in the chiral fits, this can be seen in Fig. 3(a) of [34]. Varying m_s/\hat{m} from 24 to 26 changes Q by about one unit. The analysis of [39] relied on the NNLO correction being small.

The relation between Q^2 and R can be written as

$$Q^2 = \frac{1}{2} \left(1 + \frac{m_s}{\hat{m}} \right) R. \quad (3.68)$$

The analysis of [39] leads to a factor of about 12.7 using $m_s/\hat{m} = 24.4$, the input value for $m_s/\hat{m} = 24$ to about 12.5 and for $m_s/\hat{m} = 26$ to 13.5. After taking the square root, this range corresponds to an uncertainty on Q of about unit. For completeness we have listed in Tab. 3.6 the values of Q derived from R with the factor equal to 12.7.

3.7 Conclusions

In this paper we have performed a NNLO calculation in standard ChPT of the amplitude for $\eta \rightarrow 3\pi$. This calculation was performed to first order in isospin breaking and we have pulled out the overall factor in the form of $\sin(\epsilon)$, the lowest order π^0 - η mixing angle. The remainder of the amplitude is then dealt with in the isospin limit. How we have dealt with the pion mass is described in Sect. 3.6.1 and with the Dalitz plot distributions and decay rates in Sects. 3.6.3 and 3.6.4.

We find a reasonable enhancement over the NLO result of [10] which is somewhat larger than the estimates from the dispersive analyses [19, 20]. The shape of the amplitude is in better agreement with [20] from comparing the published plots along the line $s = u$. We have also commented on the position of the Adler zero which was used in [20] to determine their subtraction constants. The NNLO result for the Dalitz plot distributions moves somewhat in the direction of the experimental results compared to the NLO result but is not in good agreement. The same is also true for the slope parameter α in the neutral decay. We always obtain a positive value while experiment is consistently negative. The amplitude for this decay has large cancellations and that makes α a difficult parameter to predict, however all methods which include unitarity resummations and have published values [11, 19, 21] get a negative value. This we find puzzling, since the main effect is $\pi\pi$ S -wave rescattering and our input values give a good value for the scattering length a_0^0 [62]. We obtain very good agreement with the ratio r .

Since we find a somewhat larger enhancement of the decay rate then [20] we also find a somewhat larger value for the isospin breaking quantities R and Q , which means that $m_d - m_u$ is somewhat smaller than obtained in [39]. We also find values that are not in agreement with the NNLO order fit to the meson masses [34].

The influence of changes in the input values is under study, a first impression can be had from looking at the results for the $C_i^r = 0$ and the different choices of μ . A more detailed analysis is planned.

Acknowledgments

This work is supported in part by the European Commission RTN network, Contract MRTN-CT-2006-035482 (FLAVIANet), the European Community-Research Infrastructure Activity Contract RII3-CT-2004-506078 (HadronPhysics) and the Swedish Research Council.

3.A A discussion on Dalitz plot parameters and the sign of α

The goal of this appendix is to point a few simple observations about relations between the Dalitzplot parameters. We start by parameterizing the amplitude for the charged decay rate as

$$\begin{aligned} M(s, t, u) &= A \left(1 + \tilde{a}(s - s_0) + \tilde{b}(s - s_0)^2 + \tilde{d}(u - t)^2 + \dots \right) \\ &= A \left(1 + \bar{a}y + \bar{b}y^2 + \bar{d}x^2 + \dots \right) \end{aligned} \quad (3.69)$$

By computing $|M(s, t, u)|^2$ and using (3.53) this leads to the relations

$$\begin{aligned} a &= 2 \operatorname{Re}(\bar{a}) = -2R_\eta \operatorname{Re}(\tilde{a}), \\ b &= |\bar{a}|^2 + 2\operatorname{Re}(\bar{b}) = R_\eta^2 \left(|\tilde{a}|^2 + 2\operatorname{Re}(\tilde{b}) \right), \\ d &= 2\operatorname{Re}(\bar{d}) = 6R_\eta^2 \operatorname{Re}(\tilde{d}). \end{aligned} \quad (3.70)$$

Here we defined $R_\eta = (2m_\eta Q_\eta)/3$. We can now use relation (3.29) and $s + t + u = 3s_0$. We obtain

$$\begin{aligned} \bar{M}(s, t, u) &\equiv \bar{A} (1 + \bar{\alpha}z + \dots) \\ &= A \left(3 + (\tilde{b} + 3\tilde{d}) \left((s - s_0)^2 + (t - s_0)^2 + (u - s_0)^2 \right) + \dots \right) \end{aligned} \quad (3.71)$$

Using the definition of z these two can be related and give

$$\bar{A} = 3A, \quad (3.72)$$

as well

$$\alpha = \operatorname{Re}(\bar{\alpha}) = \frac{1}{2} R_\eta^2 \operatorname{Re}(\tilde{b} + 3\tilde{d}) = \frac{1}{4} (d + b - R_\eta^2 |\tilde{a}|^2). \quad (3.73)$$

We thus obtain the relation

$$\alpha \leq \frac{1}{4} \left(d + b - \frac{1}{4} a^2 \right). \quad (3.74)$$

Under the *assumption* that $\text{Im}(\tilde{a}) = 0$, this turns into an equality. If one looks at the numbers in Tabs. 3.2 and 3.4 we see that there is a very strong cancellation on the r.h.s. of (3.74). Note that the KLOE results satisfy the relation with equality quite well and the theory results satisfy it within 30% or so. The inequality is satisfied in all cases. The underlying reason why it is difficult to get a negative α seems to be that the value obtained for b is too large compared to experiment.

For our NNLO result we can perform the fit also to the amplitude directly and we obtain

$$\begin{aligned} A &= -22.7 - i 4.38, \\ \bar{a} &= -0.631 - i 0.183, \\ \bar{b} &= -0.017 + i 0.025, \\ \bar{d} &= 0.040 - i 0.023. \end{aligned} \quad (3.75)$$

We see that the relation (3.70) is satisfied. In general, \bar{a} is sizable but \bar{b} , \bar{c} , and the higher order in x, y generalizations are small.

3.B The order p^4 expression

In this appendix we quote the precise way in which we have defined the order p^4 contribution. It agrees with the result of [10]. We use the notation

$$P_{\eta\pi} = m_\eta^2 - m_{\pi^0}^2. \quad (3.76)$$

This appears after Δm_1^2 and Δm_2^2 of (3.20) have been rewritten in the physical masses.

The functions are defined in (3.34).

$$\begin{aligned}
M_0^{(4)}(s) = & L_8^r \left(32 m_{K^0}^2 s - 32 m_{\pi^0}^2 s - 256/3 m_{\pi^0}^2 m_{K^0}^2 + 256/3 m_{\pi^0}^4 \right) \\
& + L_7^r \left(96 m_{K^0}^2 s - 96 m_{\pi^0}^2 s - 640/3 m_{\pi^0}^2 m_{K^0}^2 + 640/3 m_{\pi^0}^4 \right) \\
& + L_5^r \left(-8 m_{\pi^0}^2 s + 64/9 m_{\pi^0}^2 m_{K^0}^2 + 32/9 m_{\pi^0}^4 \right) \\
& + L_3^r \left(-16/9 s^2 + 16/3 m_{K^0}^2 s - 64/27 m_{K^0}^4 + 32/3 m_{\pi^0}^2 s \right. \\
& \left. - 256/27 m_{\pi^0}^2 m_{K^0}^2 - 256/27 m_{\pi^0}^4 \right) + \frac{1}{16\pi^2} \left(1/9 s^2 + 1/6 m_{K^0}^2 s - 2/27 m_{K^0}^4 \right. \\
& \left. + 1/3 m_{\pi^0}^2 s - 8/27 m_{\pi^0}^2 m_{K^0}^2 - 8/27 m_{\pi^0}^4 \right) + \bar{A}(m_{\pi^0}^2) P_{\eta\pi}^{-1} \left(4/3 m_{\pi^0}^2 s \right. \\
& \left. - 16/9 m_{\pi^0}^4 \right) + \bar{A}(m_{\pi^0}^2) \left(-3/2 s + 4/9 m_{K^0}^2 + 20/9 m_{\pi^0}^2 \right) \\
& + \bar{A}(m_{K^0}^2) P_{\eta\pi}^{-1} \left(-4/3 m_{\pi^0}^2 s + 16/9 m_{\pi^0}^4 \right) + \bar{A}(m_{K^0}^2) \left(-1/2 s + 2/9 m_{K^0}^2 \right. \\
& \left. - 2/9 m_{\pi^0}^2 \right) + \bar{A}(m_{\eta}^2) \left(1/2 s - 2/3 m_{\pi^0}^2 \right) + \bar{B}(m_{\pi^0}^2, m_{\pi^0}^2, s) \left(-2/3 s^2 \right. \\
& \left. - 4/9 m_{K^0}^2 s + 5/3 m_{\pi^0}^2 s + 2/9 m_{\pi^0}^2 m_{K^0}^2 - 2/3 m_{\pi^0}^4 \right) \\
& + \bar{B}(m_{\pi^0}^2, m_{\eta}^2, s) \left(-2/9 m_{\pi^0}^2 s - 4/27 m_{\pi^0}^2 m_{K^0}^2 + 4/9 m_{\pi^0}^4 \right) \\
& + \bar{B}(m_{K^0}^2, m_{K^0}^2, s) \left(1/2 s^2 - 2/3 m_{K^0}^2 s + 4/9 m_{K^0}^4 - 1/3 m_{\pi^0}^2 s \right) \\
& + \bar{B}(m_{K^0}^2, m_{K^0}^2, 0) \left(3/2 m_{K^0}^2 s - 2/3 m_{K^0}^4 - 1/2 m_{\pi^0}^2 s - 2/3 m_{\pi^0}^2 m_{K^0}^2 \right) \\
& + \bar{B}(m_{\eta}^2, m_{\eta}^2, s) \left(2/9 m_{\pi^0}^2 m_{K^0}^2 - 2/9 m_{\pi^0}^4 \right) + \bar{C}(m_{K^0}^2, m_{K^0}^2, m_{K^0}^2, s) \\
& \left(-1/2 m_{K^0}^2 s^2 + 2/3 m_{K^0}^4 s + 1/2 m_{\pi^0}^2 s^2 - 2/3 m_{\pi^0}^2 m_{K^0}^2 s \right)
\end{aligned} \tag{3.77}$$

$$\begin{aligned}
M_1^{(4)}(t) = & \bar{B}(m_{\pi^0}^2, m_{\pi^0}^2, t) \left(-1/12 t + 1/3 m_{\pi^0}^2 \right) \\
& + \bar{B}(m_{K^0}^2, m_{K^0}^2, t) \left(-1/24 t + 1/6 m_{K^0}^2 \right).
\end{aligned} \tag{3.78}$$

$$\begin{aligned}
M_2^{(4)}(t) = & L_3^r \left(4/3 t^2 \right) + \frac{1}{16\pi^2} \left(-1/12 t^2 \right) + \bar{B}(m_{\pi^0}^2, m_{\pi^0}^2, t) \left(-1/4 t^2 \right. \\
& \left. + 1/3 m_{K^0}^2 t + 1/2 m_{\pi^0}^2 t - 2/3 m_{\pi^0}^2 m_{K^0}^2 \right) + \bar{B}(m_{\pi^0}^2, m_{\eta}^2, t) \left(1/6 m_{\pi^0}^2 t \right. \\
& \left. - 2/9 m_{\pi^0}^2 m_{K^0}^2 \right) + \bar{B}(m_{K^0}^2, m_{K^0}^2, t) \left(3/8 t^2 - m_{K^0}^2 t + 2/3 m_{K^0}^4 \right).
\end{aligned} \tag{3.79}$$

3.C The order p^6 LECs dependent part

In this appendix we give the amplitude dependence on the order p^6 LECs C_i^r in the form of $M_I^C(t)$ as defined (3.36).

$$\begin{aligned}
M_0^C(s) = & +C_{33}^r \left(256 m_{K^0}^4 s - 512/9 m_{K^0}^6 - 128 m_{\pi^0}^2 m_{K^0}^2 s - 1280/9 m_{\pi^0}^2 m_{K^0}^4 \right. \\
& - 128 m_{\pi^0}^4 s - 5120/9 m_{\pi^0}^4 m_{K^0}^2 + 768 m_{\pi^0}^6 \left. \right) + C_{32}^r \left(128 m_{K^0}^4 s - 512/9 m_{K^0}^6 \right. \\
& - 64 m_{\pi^0}^2 m_{K^0}^2 s - 1280/9 m_{\pi^0}^2 m_{K^0}^4 \\
& - 64 m_{\pi^0}^4 s - 1280/9 m_{\pi^0}^4 m_{K^0}^2 + 1024/3 m_{\pi^0}^6 \left. \right) \\
& + C_{31}^r \left(128 m_{K^0}^4 s - 512/9 m_{K^0}^6 - 64 m_{\pi^0}^2 m_{K^0}^2 s - 256/3 m_{\pi^0}^2 m_{K^0}^4 \right. \\
& - 64 m_{\pi^0}^4 s - 1024/3 m_{\pi^0}^4 m_{K^0}^2 + 4352/9 m_{\pi^0}^6 \left. \right) \\
& + C_{29}^r \left(128/3 m_{\pi^0}^2 m_{K^0}^2 s + 64/3 m_{\pi^0}^4 s - 256/9 m_{\pi^0}^2 m_{K^0}^2 - 512/9 m_{\pi^0}^6 \right) \\
& + C_{28}^r \left(256/3 m_{K^0}^4 s - 512/3 m_{\pi^0}^2 m_{K^0}^2 s - 512/3 m_{\pi^0}^2 m_{K^0}^4 + 256/3 m_{\pi^0}^4 s \right. \\
& + 1024/3 m_{\pi^0}^4 m_{K^0}^2 - 512/3 m_{\pi^0}^6 \left. \right) \\
& + C_{27}^r \left(128/3 m_{K^0}^4 s - 256/3 m_{\pi^0}^2 m_{K^0}^2 s - 512/9 m_{\pi^0}^2 m_{K^0}^4 + 128/3 m_{\pi^0}^4 s \right. \\
& + 1792/9 m_{\pi^0}^4 m_{K^0}^2 - 1280/9 m_{\pi^0}^6 \left. \right) \\
& + C_{26}^r \left(- 64/3 m_{\pi^0}^2 m_{K^0}^2 s + 256/9 m_{\pi^0}^2 m_{K^0}^4 - 32/3 m_{\pi^0}^4 s + 128/3 m_{\pi^0}^4 m_{K^0}^2 \right. \\
& - 256/9 m_{\pi^0}^6 \left. \right) + C_{25}^r \left(- 32/3 m_{K^0}^2 s^2 + 64/9 m_{K^0}^4 s - 32/9 m_{\pi^0}^2 s^2 \right. \\
& + 256/9 m_{\pi^0}^2 m_{K^0}^2 s - 256/27 m_{\pi^0}^2 m_{K^0}^4 + 256/9 m_{\pi^0}^4 s - 1024/27 m_{\pi^0}^4 \\
& m_{K^0}^2 - 1024/27 m_{\pi^0}^6 \left. \right) + C_{24}^r \left(- 160/9 m_{K^0}^2 s^2 - 64/3 m_{K^0}^4 s + 512/27 m_{K^0}^6 \right. \\
& + 160/9 m_{\pi^0}^2 s^2 + 128/3 m_{\pi^0}^2 m_{K^0}^2 s + 256/9 m_{\pi^0}^2 m_{K^0}^4 - 64/3 m_{\pi^0}^4 s \\
& - 256/9 m_{\pi^0}^4 m_{K^0}^2 - 512/27 m_{\pi^0}^6 \left. \right) + C_{22}^r \left(- 64/9 m_{K^0}^2 s^2 - 256/9 m_{K^0}^4 s \right. \\
& + 512/27 m_{K^0}^6 + 64/3 m_{\pi^0}^2 s^2 + 128/9 m_{\pi^0}^2 m_{K^0}^2 s + 1024/27 m_{\pi^0}^2 m_{K^0}^4 \\
& - 448/9 m_{\pi^0}^4 s + 256/27 m_{\pi^0}^4 m_{K^0}^2 + 512/27 m_{\pi^0}^6 \left. \right) + C_{21}^r \left(- 256/3 m_{K^0}^6 \right. \\
& + 64 m_{\pi^0}^4 m_{K^0}^2 + 64/3 m_{\pi^0}^6 \left. \right) + C_{20}^r \left(128 m_{K^0}^4 s - 256/3 m_{K^0}^6 - 64 m_{\pi^0}^2 m_{K^0}^2 s \right. \\
& - 256/3 m_{\pi^0}^2 m_{K^0}^4 - 64 m_{\pi^0}^4 s - 192 m_{\pi^0}^4 m_{K^0}^2 + 1088/3 m_{\pi^0}^6 \left. \right)
\end{aligned} \tag{3.80}$$

$$\begin{aligned}
& +C_{19}^r \left(192 m_{K^0}^4 s - 256/3 m_{K^0}^6 - 96 m_{\pi^0}^2 m_{K^0}^2 s - 128 m_{\pi^0}^2 m_{K^0}^4 - 96 m_{\pi^0}^4 s \right. \\
& \left. - 320 m_{\pi^0}^4 m_{K^0}^2 + 1600/3 m_{\pi^0}^6 \right) \\
& +C_{18}^r \left(- 320/3 m_{K^0}^4 s + 512/27 m_{K^0}^6 + 352/3 m_{\pi^0}^2 m_{K^0}^2 s + 256/3 m_{\pi^0}^2 m_{K^0}^4 \right. \\
& \left. - 32/3 m_{\pi^0}^4 s - 128/9 m_{\pi^0}^4 m_{K^0}^2 - 2432/27 m_{\pi^0}^6 \right) + C_{17}^r \left(- 64/3 m_{K^0}^4 s \right. \\
& \left. + 512/27 m_{K^0}^6 + 32 m_{\pi^0}^2 m_{K^0}^2 s - 256/27 m_{\pi^0}^2 m_{K^0}^4 - 80/3 m_{\pi^0}^4 s \right. \\
& \left. + 1472/27 m_{\pi^0}^4 m_{K^0}^2 - 128/3 m_{\pi^0}^6 \right) + C_{16}^r \left(448/3 m_{K^0}^4 s + 256/9 m_{K^0}^6 \right. \\
& \left. - 704/3 m_{\pi^0}^2 m_{K^0}^2 s - 2816/9 m_{\pi^0}^2 m_{K^0}^4 + 400/3 m_{\pi^0}^4 s + 4288/9 m_{\pi^0}^4 m_{K^0}^2 \right. \\
& \left. - 256 m_{\pi^0}^6 \right) + C_{15}^r \left(512/27 m_{K^0}^6 + 256/9 m_{\pi^0}^2 m_{K^0}^4 - 256/9 m_{\pi^0}^4 m_{K^0}^2 \right. \\
& \left. - 512/27 m_{\pi^0}^6 \right) + C_{14}^r \left(- 64/3 m_{K^0}^4 s + 512/27 m_{K^0}^6 - 32 m_{\pi^0}^2 m_{K^0}^2 s \right. \\
& \left. + 512/27 m_{\pi^0}^2 m_{K^0}^4 + 112/3 m_{\pi^0}^4 s + 2240/27 m_{\pi^0}^4 m_{K^0}^2 - 896/9 m_{\pi^0}^6 \right) \\
& +C_{13}^r \left(- 128/3 m_{K^0}^2 s^2 + 128 m_{K^0}^4 s - 512/27 m_{K^0}^6 - 64/3 m_{\pi^0}^2 s^2 \right. \\
& \left. + 320 m_{\pi^0}^2 m_{K^0}^2 s - 1792/9 m_{\pi^0}^2 m_{K^0}^4 + 128 m_{\pi^0}^4 s - 3584/9 m_{\pi^0}^4 m_{K^0}^2 \right. \\
& \left. - 4096/27 m_{\pi^0}^6 \right) + C_{12}^r \left(64/9 m_{K^0}^2 s^2 + 512/9 m_{K^0}^4 s + 512/81 m_{K^0}^6 \right. \\
& \left. - 64/3 m_{\pi^0}^2 s^2 - 256/9 m_{\pi^0}^2 m_{K^0}^2 s - 1024/9 m_{\pi^0}^2 m_{K^0}^4 + 896/9 m_{\pi^0}^4 s + 1792/ \right. \\
& \left. 27 m_{\pi^0}^4 m_{K^0}^2 - 10496/81 m_{\pi^0}^6 \right) + C_{11}^r \left(128/9 m_{K^0}^2 s^2 - 128/3 m_{K^0}^4 s \right. \\
& \left. + 512/27 m_{K^0}^6 + 64/9 m_{\pi^0}^2 s^2 - 320/3 m_{\pi^0}^2 m_{K^0}^2 s + 256/3 m_{\pi^0}^2 m_{K^0}^4 \right. \\
& \left. - 128/3 m_{\pi^0}^4 s + 1024/9 m_{\pi^0}^4 m_{K^0}^2 + 1024/27 m_{\pi^0}^6 \right) + C_{10}^r \left(- 32/9 m_{K^0}^2 s^2 \right. \\
& \left. - 64/9 m_{K^0}^4 s + 256/27 m_{K^0}^6 + 32/3 m_{\pi^0}^2 s^2 - 256/9 m_{\pi^0}^2 m_{K^0}^2 s \right. \\
& \left. + 256/27 m_{\pi^0}^2 m_{K^0}^4 - 256/9 m_{\pi^0}^4 s + 1408/27 m_{\pi^0}^4 m_{K^0}^2 + 128/9 m_{\pi^0}^6 \right) \\
& +C_9^r \left(- 160/9 m_{K^0}^2 s^2 + 512/27 m_{K^0}^6 + 160/9 m_{\pi^0}^2 s^2 - 256/9 m_{\pi^0}^2 m_{K^0}^4 \right. \\
& \left. + 128/3 m_{\pi^0}^4 m_{K^0}^2 - 896/27 m_{\pi^0}^6 \right) + C_8^r \left(- 32/9 m_{K^0}^2 s^2 - 64/9 m_{K^0}^4 s \right. \\
& \left. + 256/27 m_{K^0}^6 + 32/9 m_{\pi^0}^2 m_{K^0}^2 s - 128/27 m_{\pi^0}^2 m_{K^0}^4 + 320/9 m_{\pi^0}^4 s \right. \\
& \left. - 128/27 m_{\pi^0}^4 m_{K^0}^2 - 128/3 m_{\pi^0}^6 \right) + C_6^r \left(- 64/9 m_{K^0}^2 s^2 + 64/3 m_{K^0}^4 s \right. \\
& \left. - 256/27 m_{K^0}^6 - 32/9 m_{\pi^0}^2 s^2 + 160/3 m_{\pi^0}^2 m_{K^0}^2 s - 128/3 m_{\pi^0}^2 m_{K^0}^4 \right. \\
& \left. + 64/3 m_{\pi^0}^4 s - 512/9 m_{\pi^0}^4 m_{K^0}^2 - 512/27 m_{\pi^0}^6 \right) + C_5^r \left(- 32/3 m_{K^0}^2 s^2 \right.
\end{aligned}
\tag{3.81}$$

$$\begin{aligned}
& +128/9 m_{K^0}^4 s + 64/9 m_{\pi^0}^2 s^2 + 224/9 m_{\pi^0}^2 m_{K^0}^2 s - 896/27 m_{\pi^0}^2 m_{K^0}^4 \\
& - 64/9 m_{\pi^0}^4 s - 128/27 m_{\pi^0}^4 m_{K^0}^2 - 128/27 m_{\pi^0}^6 \Big) + C_4^r \Big(- 64/9 s^3 \\
& + 128/27 m_{K^0}^2 s^2 + 128/9 m_{K^0}^4 s - 512/81 m_{K^0}^6 + 256/27 m_{\pi^0}^2 s^2 \\
& - 256/9 m_{\pi^0}^2 m_{K^0}^2 s + 128/9 m_{\pi^0}^4 s + 512/27 m_{\pi^0}^4 m_{K^0}^2 - 1024/81 m_{\pi^0}^6 \Big) \\
& + C_3^r \Big(- 64/9 s^3 + 128/9 m_{K^0}^2 s^2 - 128/9 m_{K^0}^4 s + 512/81 m_{K^0}^6 + 256/9 m_{\pi^0}^2 s^2 \\
& - 896/9 m_{\pi^0}^2 m_{K^0}^2 s + 512/9 m_{\pi^0}^2 m_{K^0}^4 - 704/9 m_{\pi^0}^4 s + 3328/27 m_{\pi^0}^4 m_{K^0}^2 \\
& + 5632/81 m_{\pi^0}^6 \Big) + C_1^r \Big(32/9 s^3 - 64/9 m_{K^0}^2 s^2 + 64/9 m_{K^0}^4 s - 256/81 m_{K^0}^6 - \\
& 128/9 m_{\pi^0}^2 s^2 + 448/9 m_{\pi^0}^2 m_{K^0}^2 s - 256/9 m_{\pi^0}^2 m_{K^0}^4 + 352/9 m_{\pi^0}^4 \\
& s - 1664/27 m_{\pi^0}^4 m_{K^0}^2 - 2816/81 m_{\pi^0}^6 \Big)
\end{aligned} \tag{3.82}$$

$$M_1^C(t) = 0. \tag{3.83}$$

$$\begin{aligned}
M_2^C(t) = & C_{25}^r \Big(32/3 m_{\pi^0}^2 t^2 \Big) + C_{24}^r \Big(- 32/3 m_{K^0}^2 t^2 + 32/3 m_{\pi^0}^2 t^2 \Big) \\
& + C_{22}^r \Big(- 32/3 m_{K^0}^2 t^2 \Big) + C_{13}^r \Big(32 m_{K^0}^2 t^2 + 16 m_{\pi^0}^2 t^2 \Big) + C_{12}^r \Big(32/3 m_{K^0}^2 t^2 \Big) \\
& + C_{11}^r \Big(- 32/3 m_{K^0}^2 t^2 - 16/3 m_{\pi^0}^2 t^2 \Big) + C_{10}^r \Big(- 16/3 m_{K^0}^2 t^2 \Big) \\
& + C_9^r \Big(- 32/3 m_{K^0}^2 t^2 + 32/3 m_{\pi^0}^2 t^2 \Big) + C_8^r \Big(- 16/3 m_{K^0}^2 t^2 + 8 m_{\pi^0}^2 t^2 \Big) \\
& + C_6^r \Big(16/3 m_{K^0}^2 t^2 + 8/3 m_{\pi^0}^2 t^2 \Big) + C_5^r \Big(8/3 m_{\pi^0}^2 t^2 \Big) \\
& + C_4^r \Big(16/3 t^3 - 32/9 m_{K^0}^2 t^2 - 64/9 m_{\pi^0}^2 t^2 \Big) + C_3^r \Big(16/3 t^3 - 32/3 m_{K^0}^2 t^2 \\
& - 64/3 m_{\pi^0}^2 t^2 \Big) + C_1^r \Big(- 8/3 t^3 + 16/3 m_{K^0}^2 t^2 + 32/3 m_{\pi^0}^2 t^2 \Big)
\end{aligned} \tag{3.84}$$

References

- [1] J. Bijnens, G. Faldt and B.M.K. Nefkens (eds.) Phys. Scripta **T99** (2002) 1-282
- [2] B. Höistad and P. Moskal (eds.), Acta Phys. Slov. **56** (2005) 193-409.
- [3] D. G. Sutherland Phys. Lett. **23** (1966) 384
- [4] J. S. Bell and D. G. Sutherland, Nucl. Phys. B **4** (1968) 315.
- [5] J. A. Cronin, Phys. Rev. **161** (1967) 1483.

- [6] H. Osborn and D. J. Wallace, Nucl. Phys. B **20** (1970) 23.
- [7] S. Weinberg, Physica A **96** (1979) 327.
- [8] J. Gasser and H. Leutwyler, Annals Phys. **158** (1984) 142.
- [9] J. Gasser and H. Leutwyler, Nucl. Phys. B **250** (1985) 465.
- [10] J. Gasser and H. Leutwyler, Nucl. Phys. B **250** (1985) 539.
- [11] J. Bijnens and J. Gasser, Phys. Scripta **T99** (2002) 34 [arXiv:hep-ph/0202242].
- [12] R. F. Dashen, Phys. Rev. **183** (1969) 1245.
- [13] W. M. Yao *et al.* [Particle Data Group], J. Phys. G **33** (2006) 1.
- [14] J. F. Donoghue, B. R. Holstein and D. Wyler, Phys. Rev. D **47** (1993) 2089.
- [15] J. Bijnens, Phys. Lett. B **306** (1993) 343 [arXiv:hep-ph/9302217].
- [16] R. Baur, J. Kambor and D. Wyler, Nucl. Phys. B **460** (1996) 127 [arXiv:hep-ph/9510396].
- [17] A. Neveu and J. Scherk, Annals Phys. **57** (1970) 39.
- [18] C. Roiesnel and T. N. Truong, Nucl. Phys. B **187** (1981) 293;
T. N. Truong, Nucl. Phys. Proc. Suppl. **24A** (1991) 93.
- [19] J. Kambor, C. Wiesendanger and D. Wyler, Nucl. Phys. B **465** (1996) 215 [arXiv:hep-ph/9509374].
- [20] A. V. Anisovich and H. Leutwyler, Phys. Lett. B **375** (1996) 335 [arXiv:hep-ph/9601237].
- [21] B. Borasoy and R. Nissler, Eur. Phys. J. A **26** (2005) 383 [arXiv:hep-ph/0510384].
- [22] S. Descotes-Genon, N. H. Fuchs, L. Girlanda and J. Stern, Eur. Phys. J. C **34** (2004) 201 [arXiv:hep-ph/0311120].
- [23] J. Bijnens, Prog. Part. Nucl. Phys. **58** (2007) 521 [arXiv:hep-ph/0604043].
- [24] J. Bijnens, G. Colangelo and J. Gasser, Nucl. Phys. B **427** (1994) 427 [arXiv:hep-ph/9403390].
- [25] G. Amorós, J. Bijnens and P. Talavera, Nucl. Phys. B **585** (2000) 293 [Erratum-ibid. B **598** (2001) 665] [arXiv:hep-ph/0003258].
- [26] A. V. Manohar, arXiv:hep-ph/9606222.
- [27] V. Bernard, N. Kaiser and U. G. Meissner, Int. J. Mod. Phys. E **4** (1995) 193 [arXiv:hep-ph/9501384].
- [28] G. Ecker, Prog. Part. Nucl. Phys. **35** (1995) 1 [arXiv:hep-ph/9501357].
- [29] V. Bernard and U. G. Meissner, arXiv:hep-ph/0611231, to be published in Ann. Rev. Nucl. Part. Sci.
- [30] J. Bijnens, G. Colangelo and G. Ecker, JHEP **9902** (1999) 020 [arXiv:hep-ph/9902437].

-
- [31] J. Bijnens, G. Colangelo, G. Ecker, J. Gasser and M. E. Sainio, Nucl. Phys. B **508** (1997) 263 [Erratum-ibid. B **517** (1998) 639] [arXiv:hep-ph/9707291].
- [32] J. Bijnens, G. Colangelo and G. Ecker, Annals Phys. **280** (2000) 100 [arXiv:hep-ph/9907333].
- [33] C. Aubin *et al.* [MILC Collaboration], Phys. Rev. D **70** (2004) 114501 [arXiv:hep-lat/0407028].
- [34] G. Amorós, J. Bijnens and P. Talavera, Nucl. Phys. B **602** (2001) 87 [arXiv:hep-ph/0101127].
- [35] G. Ecker, J. Gasser, A. Pich and E. de Rafael, Nucl. Phys. B **321** (1989) 311.
- [36] V. Cirigliano, G. Ecker, M. Eidemuller, R. Kaiser, A. Pich and J. Portoles, Nucl. Phys. B **753** (2006) 139 [arXiv:hep-ph/0603205].
- [37] G. Ecker, J. Gasser, H. Leutwyler, A. Pich and E. de Rafael, Phys. Lett. B **223** (1989) 425.
- [38] J. Bijnens, E. Gamiz, E. Lipartia and J. Prades, JHEP **0304** (2003) 055 [arXiv:hep-ph/0304222].
- [39] H. Leutwyler, Phys. Lett. B **378** (1996) 313 [arXiv:hep-ph/9602366].
- [40] M. Knecht, B. Moussallam, J. Stern and N. H. Fuchs, Nucl. Phys. B **457** (1995) 513 [arXiv:hep-ph/9507319].
- [41] J. Bijnens, P. Dhonte and F. Persson, Nucl. Phys. B **648** (2003) 317 [arXiv:hep-ph/0205341].
- [42] G. Amorós, J. Bijnens and P. Talavera, Nucl. Phys. B **568** (2000) 319 [arXiv:hep-ph/9907264].
- [43] J. Bijnens and P. Talavera, JHEP **0203**, 046 (2002) [arXiv:hep-ph/0203049].
- [44] S. Necco, talk at Lattice 2007
- [45] H. Leutwyler, Phys. Lett. B **374** (1996) 181 [arXiv:hep-ph/9601236].
- [46] R. Kaiser and H. Leutwyler, Eur. Phys. J. C **17** (2000) 623 [arXiv:hep-ph/0007101].
- [47] R. Kaiser, talk presented at EuroFlavour06, 2-4 November 2006, Barcelona, Spain.
- [48] K. Kampf, J. Novotny and J. Trnka, Eur. Phys. J. C **50** (2007) 385 [arXiv:hep-ph/0608051].
- [49] J. Bijnens, Acta Phys. Slov. **56** (2005) 305 [arXiv:hep-ph/0511076].
- [50] F. Ambrosino *et al.* [KLOE Collaboration], arXiv:0707.2355 [hep-ex].
- [51] A. Abele *et al.* [Crystal Barrel Collaboration], Phys. Lett. B **417** (1998) 197.
- [52] J. G. Layter, J. A. Appel, A. Kotlewski, W. Y. Lee, S. Stein and J. J. Thaler, Phys. Rev. D **7** (1973) 2565.

- [53] M. Gormley, E. Hyman, W. Y. Lee, T. Nash, J. Peoples, C. Schultz and S. Stein, Phys. Rev. D **2** (1970) 501.
- [54] F. Ambrosino *et al.* [KLOE collaboration], arXiv:0707.4137 [hep-ex].
- [55] T. Capussela [KLOE Collaboration], Acta Phys. Slov. **56** (2005) 341; S. Giovannella *et al.* [KLOE Collaboration], 40th Rencontres de Moriond on QCD and High Energy Hadronic Interactions, La Thuile, Aosta Valley, Italy, 12-19 Mar 2005 arXiv:hep-ex/0505074.
- [56] W. B. Tippens *et al.* [Crystal Ball Collaboration], Phys. Rev. Lett. **87** (2001) 192001.
- [57] M. Bashkanov *et al.*, arXiv:0708.2014 [nucl-ex].
- [58] A. Abele *et al.* [Crystal Barrel Collaboration], Phys. Lett. B **417** (1998) 193.
- [59] D. Alde *et al.* [Serpukhov-Brussels-Annecey(LAPP) Collaboration], Z. Phys. C **25** (1984) 225 [Yad. Fiz. **40** (1984) 1447].
- [60] M. N. Achasov *et al.*, JETP Lett. **73** (2001) 451 [Pisma Zh. Eksp. Teor. Fiz. **73** (2001) 511].
- [61] B. V. Martemyanov and V. S. Sopov, Phys. Rev. D **71** (2005) 017501 [arXiv:hep-ph/0502023].
- [62] J. Bijnens, P. Dhonte and P. Talavera, JHEP **0401** (2004) 050 [arXiv:hep-ph/0401039].
- [63] D. B. Kaplan and A. V. Manohar, Phys. Rev. Lett. **56** (1986) 2004.
- [64] J. Bijnens and J. Prades, Nucl. Phys. B **490** (1997) 239 [arXiv:hep-ph/9610360].

Isospin breaking in $K\pi$ vector
form-factors for the weak and
rare decays K_{l3} , $K \rightarrow \pi\nu\bar{\nu}$ and
 $K \rightarrow \pi l^+\bar{l}^+$

Paper III

**Isospin breaking in $K\pi$ vector form-factors for
the weak and rare decays $K_{\ell 3}$, $K \rightarrow \pi\nu\bar{\nu}$ and
 $K \rightarrow \pi\ell^+\ell^-$**

Johan Bijnens¹ and Karim Ghorbani²

Department of Theoretical Physics, Lund University,
Sölvegatan 14A, S 223-62 Lund, Sweden

abstract

We calculate the two form-factors for the four Kaon to pion transitions via a vector current to order p^6 in Chiral Perturbation Theory to first order in isospin breaking via the quark masses. In addition we derive relations between these form-factors valid to first order in the up-down quark-mass difference but to all orders in Chiral Perturbation Theory.

We present numerical results for all eight form-factors at $t = 0$ and for varying t and for the scalar form-factors at the Callan-Treiman point.

PACS:11.30.Rd, 12.39.Fe, 12.15.Hh, 14.40.Aq.

¹Electronic Address: bijnens@thep.lu.se

²Electronic Address: karim.ghorbani@thep.lu.se

4.1 Introduction

The semileptonic decays of a Kaon to a pion and two leptons play a significant role in flavour physics. On the one hand, the weak decays $K_{\ell 3}$ are a main source of our knowledge of the CKM matrix element V_{us} and on the other hand, the rare decays to a lepton-anti-lepton or neutrino-antineutrino pair provide a good testing bed for loop effects in flavour physics. The form-factors themselves quantize the hadronic uncertainties as can be exemplified by the so-called master formulae. This is e.g. for $K_{\ell 3}$, see [1] and references therein,

$$\Gamma(K^i \rightarrow \pi^j \ell^+ \nu_\ell) = C_{ij}^2 \frac{G_F^2 S_{EW} m_K^5}{192\pi^3} |V_{us} f_+^{K^i \pi^j}|^2 \mathcal{I}_\ell^{ij} (1 + 2\Delta_{EM}^{ij}). \quad (4.1)$$

A similar formula exists for the rare decays, see [2] and references therein. We will refer to the $K_{\ell 3}$ decays as weak decays and the ones with a lepton-antilepton pair as rare decays.

Theoretical work on these form-factors goes back a long way. In Chiral Perturbation Theory (ChPT), the lowest-order (LO) result dates back to [3] while the next-to-leading-order (NLO) was evaluated by Gasser and Leutwyler [4]. They calculated the vector form-factor f_+ for the weak decays including the isospin breaking due to $m_u - m_d$ and the scalar form-factor f_0 in the isospin limit. The form-factors are known in the isospin limit to next-to-next-to-leading order (NNLO) in Chiral Perturbation Theory (ChPT) [5, 6]. In [5] a comparison with experimental results was done and a useful relation for the order p^6 constants needed for $f_+(0)$ obtained. The isospin breaking to NLO for the vector form-factors $f_+(t)$ for the rare decays was done in [2] to NLO. The electromagnetic corrections to NLO, i.e. order $e^2 p^2$, are also known, for the weak decays [7] and for the rare decays [2]. In this paper we calculate the isospin breaking corrections due to the quark-mass difference $m_u - m_d$ to the vector and scalar form-factors to NNLO order in ChPT for all eight form-factors. The NNLO results are new for all form-factors while the NLO results are new for the scalar form-factors. Some preliminary results were reported in [8]. In addition we discuss the results on ratios of form-factors to NNLO. Some of these ratios were observed to have special features at NLO in [4] and [2]. We prove that the relations (4.11) and (4.12) are valid to all orders in ChPT to first order in $m_u - m_d$. The double ratio (4.12) was also discussed in [2] but not proven there. There exists also work using dispersion relation for the form-factors in the isospin limit, see [9, 10] and references therein.

This paper is organized as follows. We define the form-factors and derive the relations that the form-factors should satisfy to all orders in ChPT and first order in $m_u - m_d$ in Sect. 4.2. Next we give a short discussion of ChPT in Sect. 4.3 and derive how π^0 - η mixing can be taken into account to NNLO in ChPT in Sect. 4.4. Sect. 4.5 defines the various ratios of form-factors we

use and discusses how they are obeyed at NLO and NNLO. We also discuss there some general aspects of our calculation and give the LO results. Explicit formulas are not provided at NNLO, they are simply too long but we present the NLO formulas in App. 4.A and the dependence on the order p^6 low-energy constants (LECs) in App. 4.B. The estimate of these order p^6 LECs we use is presented in Sect. 4.6. Our main results are presented numerically in Sect. 4.7. These include, numerical results on the values of $f_+(0)$, its t -dependence, ratios as a function of t and the deviation from F_K/F_π at the Callan-Treiman point. A short summary is given in Sect. 4.8.

4.2 Form-factors and isospin relations

In this paper we deal with the four matrix-elements

$$\langle \pi^0(p') | \bar{s} \gamma_\mu u(0) | K^+(p) \rangle = \frac{1}{\sqrt{2}} \left[(p' + p)_\mu f_+^{K^+ \pi^0}(t) + (p - p')_\mu f_-^{K^+ \pi^0}(t) \right], \quad (4.2)$$

$$\langle \pi^-(p') | \bar{s} \gamma_\mu u(0) | K^0(p) \rangle = \left[(p' + p)_\mu f_+^{K^0 \pi^-}(t) + (p - p')_\mu f_-^{K^0 \pi^-}(t) \right], \quad (4.3)$$

$$\langle \pi^+(p') | \bar{s} \gamma_\mu d(0) | K^+(p) \rangle = \left[(p' + p)_\mu f_+^{K^+ \pi^+}(t) + (p - p')_\mu f_-^{K^+ \pi^+}(t) \right]. \quad (4.4)$$

$$\langle \pi^0(p') | \bar{s} \gamma_\mu d(0) | K^0(p) \rangle = \frac{-1}{\sqrt{2}} \left[(p' + p)_\mu f_+^{K^0 \pi^0}(t) + (p - p')_\mu f_-^{K^0 \pi^0}(t) \right]. \quad (4.5)$$

We have thus in total a set of 8 form-factors. They depend on

$$t = (p' - p)^2, \quad (4.6)$$

the square of the four momentum transfer to the leptons. The form-factors are normalized such that

$$f_+^{K^i \pi^j}(0) = 1 \quad (4.7)$$

in the $SU(3)$ limit of $m_u = m_d = m_s$. In the isospin limit

$$f_\pm = f_\pm^{K\pi} = f_\pm^{K^+ \pi^0} = f_\pm^{K^0 \pi^-} = f_\pm^{K^+ \pi^+} = f_\pm^{K^0 \pi^0}. \quad (4.8)$$

$f_+^{K\pi}$ is referred to as the vector form-factor, because it specifies the P -wave projection of the crossed channel matrix-elements $\langle \bar{s} \gamma_\mu q(0) | | K^i, \pi^j \text{ in } \rangle$. The S -wave projection is described by the scalar form-factor

$$f_0^{K^i \pi^j}(t) = f_+^{K^i \pi^j}(t) + \frac{t}{m_{K^i}^2 - m_{\pi^j}^2} f_-^{K^i \pi^j}(t). \quad (4.9)$$

We will refer to the decays as the charged weak for (4.2), neutral weak for (4.3), charged rare for (4.4) and neutral rare for (4.5).

In this paper we derive the isospin breaking due to the quark-mass difference $m_u - m_d$ to NNLO for the eight form-factors defined above. We do this to first order in isospin breaking. Let us now derive first some general properties. The isospin-breaking operator $(1/2)(m_u - m_d)(\bar{u}u - \bar{d}d)$ has isospin one. The pions have isospin one and the Kaons as well as the vector operator are in an isospin 1/2 multiplet. To first order in isospin breaking from $\delta = m_u - m_d$ the form-factors described above can be rewritten in the form

$$\begin{aligned} f_\ell^{K^+\pi^0}(t) &= f_\ell^A(t) + \delta f_\ell^B(t) + \mathcal{O}(\delta^2), \\ f_\ell^{K^0\pi^-}(t) &= f_\ell^A(t) - \delta f_\ell^D(t) + \mathcal{O}(\delta^2), \\ f_\ell^{K^+\pi^+}(t) &= f_\ell^A(t) + \delta f_\ell^D(t) + \mathcal{O}(\delta^2), \\ f_\ell^{K^0\pi^0}(t) &= f_\ell^A(t) - \delta f_\ell^B(t) + \mathcal{O}(\delta^2), \end{aligned} \quad (4.10)$$

for $\ell = +, -, 0$. The form (4.10) is a direct consequence of the Wigner-Eckart theorem. This can be interpreted as that the size of isospin breaking depends on the final pion and the sign also depends on which kaon is in the initial state.

As a consequence of (4.10) we obtain the relations

$$f_\ell^{K^+\pi^0}(t) - f_\ell^{K^0\pi^-}(t) - f_\ell^{K^+\pi^+}(t) + f_\ell^{K^0\pi^0}(t) = 0 + \mathcal{O}(\delta^2), \quad (4.11)$$

and

$$r(t) \equiv \frac{f_\ell^{K^+\pi^0}(t)f_\ell^{K^0\pi^0}(t)}{f_\ell^{K^0\pi^-}(t)f_\ell^{K^+\pi^+}(t)} = 1 + \mathcal{O}(\delta^2) \quad (4.12)$$

These relations do not have to be satisfied when electromagnetic corrections are included. Photon exchange contains isospin 0, 1 and 2 parts allowing different corrections to all four amplitudes. The isospin 0 and 1 parts do satisfy the same relations, but not the isospin 2 part.

The relations are valid for all three form-factors $f_\ell^{K^i\pi^j}$ with $\ell = +, -, 0$. They are also valid if the currents in (4.2-4.5) are replaced by the scalar densities $\bar{s}u(0)$ and $\bar{s}d(0)$.

4.3 Chiral Perturbation Theory

Chiral Perturbation Theory (ChPT) is an effective field theory to describe the strong interactions at very low energy. The effective Lagrangian is constructed based on two important properties of the physical hadron spectrum. Pseudo-scalar mesons, the lowest-lying states in the spectrum are separated from the rest of the hadrons, i.e. there exists a mass gap. This allows the heavier particles to decouple from the dynamics of the pseudo-scalar mesons. Their

influence can be described by point-like couplings. The other important fact is that the spectrum does not show the chiral symmetry of the underlying theory (QCD). The pseudo-scalars are assumed to be the pseudo-Goldstone particles emerging from the spontaneous breaking of this chiral symmetry. The nonzero but small mass of the pseudo-scalar mesons are because quarks have a finite mass in, reality which breaks the chiral symmetry explicitly.

According to the Goldstone's theorem, the Goldstone particles do not interact at zero momentum. This immediately offers a weakly interacting theory as a basis for perturbation theory. The first systematic consideration on the applicability of the effective Lagrangians was made by Weinberg [11] and Gasser and Leutwyler [12]. The effective chiral Lagrangian is an expansion in momentum and quark masses. In the chiral power-counting, quark masses are of order p^2 . Taking into account the Lorentz invariance and chiral symmetry, the lowest order chiral Lagrangian which also complies with the discrete symmetries can be written down as

$$\mathcal{L}_2 = \frac{F_0^2}{4} (\langle D_\mu U D^\mu U^\dagger \rangle + \langle \chi U^\dagger + U \chi^\dagger \rangle) \quad (4.13)$$

and the next-to-leading Lagrangian with the introduction of the external field technique was written down by Gasser and Leutwyler [13] and reads

$$\begin{aligned} \mathcal{L}_4 = & L_1 \langle D_\mu U^\dagger D^\mu U \rangle^2 + L_2 \langle D_\mu U^\dagger D_\nu U \rangle \langle D^\mu U^\dagger D^\nu U \rangle \\ & + L_3 \langle D^\mu U^\dagger D_\mu U D^\nu U^\dagger D_\nu U \rangle + L_4 \langle D^\mu U^\dagger D_\mu U \rangle \langle \chi^\dagger U + \chi U^\dagger \rangle \\ & + L_5 \langle D^\mu U^\dagger D_\mu U (\chi^\dagger U + U^\dagger \chi) \rangle + L_6 \langle \chi^\dagger U + \chi U^\dagger \rangle^2 \\ & + L_7 \langle \chi^\dagger U - \chi U^\dagger \rangle^2 + L_8 \langle \chi^\dagger U \chi^\dagger U + \chi U^\dagger \chi U^\dagger \rangle \\ & - i L_9 \langle F_{\mu\nu}^R D^\mu U D^\nu U^\dagger + F_{\mu\nu}^L D^\mu U^\dagger D^\nu U \rangle \\ & + L_{10} \langle U^\dagger F_{\mu\nu}^R U F^{L\mu\nu} \rangle + H_1 \langle F_{\mu\nu}^R F^{R\mu\nu} + F_{\mu\nu}^L F^{L\mu\nu} \rangle + H_2 \langle \chi^\dagger \chi \rangle. \end{aligned} \quad (4.14)$$

The matrix $U \in SU(3)$ contains the pseudo-scalars and its exponential representation is

$$U(\phi) = \exp(i\sqrt{2}\phi/F_0), \quad (4.15)$$

where

$$\phi(x) = \begin{pmatrix} \frac{\pi_3}{\sqrt{2}} + \frac{\eta_8}{\sqrt{6}} & \pi^+ & K^+ \\ \pi^- & -\frac{\pi_3}{\sqrt{2}} + \frac{\eta_8}{\sqrt{6}} & K^0 \\ K^- & \bar{K}^0 & -\frac{2\eta_8}{\sqrt{6}} \end{pmatrix}. \quad (4.16)$$

The external fields are defined through the covariant derivatives and field strength tensor as

$$D_\mu U = \partial_\mu U - i r_\mu U + i U l_\mu, \quad F_{\mu\nu}^L = \partial_\mu l_\nu - \partial_\nu l_\mu - i [l_\mu, l_\nu], \quad (4.17)$$

The right-handed and left-handed external fields are denoted by r_μ and l_μ respectively. The Hermitian 3×3 matrix χ contains the scalar (s) and pseudo-scalar (p) external densities and is given as $\chi = 2B_0 (s + ip)$. The constants F_0 and B_0 are related to the pion decay constant and quark condensate respectively. There are however, 10+2 unknown free parameters in the Lagrangian \mathcal{L}_4 where these effective constants contains the effects of heavy degrees of freedom and can be determined by invoking the experimental data as well as by Lattice QCD technique. One of the theoretical approach, on the other hand, is the application of the resonance chiral perturbation which provides an approximate estimation of the low energy constants (LECs). The extension of the chiral Lagrangian to the next-to-next-to-leading order is also accomplished [14]. At this order there are a large number of LECs, 90+4.

The external scalar field s contains the quark masses and the mass terms in the lowest order Lagrangian \mathcal{L}_2 can be diagonalized exactly. In the presence of $m_u \neq m_d$ the physical π^0 and η differ from the triplet and octet states via a lowest-order mixing angle ϵ as

$$\begin{aligned}\pi_3 &= \pi^0 \cos(\epsilon) - \eta \sin(\epsilon) \\ \eta_8 &= \pi^0 \sin(\epsilon) + \eta \cos(\epsilon)\end{aligned}\tag{4.18}$$

The lowest order mixing angle is

$$\begin{aligned}\tan(2\epsilon) &= \frac{\sqrt{3} m_d - m_u}{2 m_s - \hat{m}}, \\ \hat{m} &= (m_u + m_d)/2.\end{aligned}\tag{4.19}$$

A review on ChPT to order p^6 is [15]. References to other recent reviews and lectures can be found there.

4.4 Matrix-elements in the presence of mixing

For this work we need to work out the matrix elements defined earlier in the presence of mixing. These matrix elements can be determined from three-point Green functions. Two of the external legs are the meson propagators and the third one is the external field. The matrix element is obtained from the Green function using the Lehmann-Symanzik-Zimmermann (LSZ) reduction formula. The matrix element is related to the residue of the Green function in momentum space where all the propagators are continued to the on-shell mass. The case of two point-function with one leg undergoing mixing is worked out in [16] and we generalized this to a four point-function with mixing on two external legs in [17]. In this article we study the form-factors in $K^i \rightarrow \pi^j$ transitions where, in case of the neutral pion in the decay product, mixing should also taken into account. Fig. 4.1 depicts the three-point Green function relevant for this work

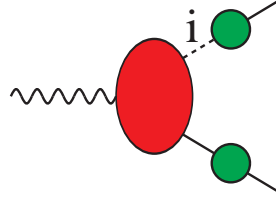


Figure 4.1: The full three-point Green function is represented. The oval stands for the amputated three-point Green function and circles indicate the full two-point functions. The solid lines are external mesons and the dashed line labeled by i , indicates the sum over states implied in the external leg where mixing occurs. The wiggly line indicates the external vector current.

where we have only considered mixing in one external propagator. Amplitudes are obtained via

$$\mathcal{A}_{i_1 \dots i_n} = \left(\frac{(-i)^n}{\sqrt{Z_{i_1} \dots Z_{i_n}}} \right) \prod_{i=1}^n \lim_{k_i^2 \rightarrow m_i^2} (k_i^2 - m_i^2) G_{i_1 \dots i_n}(k_1, \dots, k_n). \quad (4.20)$$

This formula shows the general case with n -outgoing particles. The function $G_{i_1 \dots i_n}$ is the full n -point Green function where we now express it in terms of the amputated Green functions and only two meson propagators to suite for the current article as follows

$$G_{43,extv} = G_{44}(p^2 \approx m_{4\text{phys}}^2) G_{3i}(p^2 \approx m_{3\text{phys}}^2) \mathcal{G}_{4i,extv}. \quad (4.21)$$

Summation over index i runs over two possibilities of being a neutral pion or eta. \mathcal{G}_{4i} is the amputated Green function that contains both on-shell and off-shell Feynman diagrams. The two-point functions are expanded near the physical poles as

$$G_{ii}(p^2 \approx m_{i\text{phys}}^2) = \frac{iZ_i}{p^2 - m_{i\text{phys}}^2}. \quad (4.22)$$

The function Z_i is called the wavefunction renormalization factor. The expansion of the off-diagonal two-point functions around the physical poles is somewhat more involved but can be done in terms of the one-particle irreducible two-point functions $\Pi_{ij}(m^2)$ and the mass differences needed in the propagator of the i -leg in Fig. 4.1 as explained in [16]. We now expand all quantities to the required chiral order and use the fact that we have exactly diagonalized the lowest Lagrangian to obtain for the full amplitudes to order p^6 :

$$\mathcal{A}_{43,extv} = \mathcal{A}_{43,extv}^{(2)} + \mathcal{A}_{43,extv}^{(4)} + \mathcal{A}_{43,extv}^{(6)} + \dots, \quad (4.23)$$

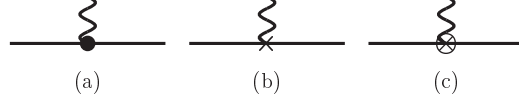


Figure 4.2: The tree level Feynman diagrams for the Kaon transition form-factors. The wiggly line indicates the insertion of the vector current, a dot an order p^2 vertex, a cross an order p^4 vertex and a crossed circle an order p^6 vertex.

$$\mathcal{A}_{43,extv}^{(2)} = \mathcal{G}_{43,extv}^{(2)}, \quad (4.24)$$

$$\begin{aligned} \mathcal{A}_{43,extv}^{(4)} &= \mathcal{G}_{43,extv}^{(4)} - \left(\frac{1}{2} Z_{44}^{(4)} + \frac{1}{2} Z_{33}^{(4)} \right) \mathcal{G}_{43,extv}^{(2)} \\ &\quad - \frac{\Pi_{38}^{(4)}(3)}{\Delta m_2^2} \mathcal{G}_{48,extv}^{(2)}, \end{aligned} \quad (4.25)$$

$$\begin{aligned} \mathcal{A}_{43,extv}^{(6)} &= \mathcal{G}_{43,extv}^{(6)} - \frac{1}{2} \left(Z_{33}^{(6)} + Z_{44}^{(6)} \right) \mathcal{G}_{43,ext}^{(2)} - \frac{1}{2} \left(Z_{33}^{(4)} + Z_{44}^{(4)} \right) \mathcal{G}_{43,extv}^{(4)} \\ &\quad + \frac{3}{8} \left(\left(Z_{33}^{(4)} \right)^2 + \left(Z_{44}^{(4)} \right)^2 \right) \mathcal{G}_{43,ext}^{(2)} + \frac{1}{4} \left(Z_{33}^{(4)} Z_{44}^{(4)} \right) \mathcal{G}_{43,extv}^{(2)} \\ &\quad + \frac{\Pi_{38}(3)^{(4)}}{\Delta m_2^2} \mathcal{G}_{48,extv}^{(4)} + \frac{\Pi_{38}(3)^{(6)}}{\Delta m_2^2} \mathcal{G}_{48,extv}^{(2)} - \frac{1}{2} \left(Z_{38}^{(4)} \frac{\Pi_{38}(3)^{(4)}}{\Delta m_2^2} \right) \\ &\quad \mathcal{G}_{43,extv}^{(2)} + \frac{\Pi_{38}(3)^{(4)} \Pi_{88}(3)^{(4)}}{\Delta m_2^2} \mathcal{G}_{48,extv}^{(2)} \\ &\quad - \frac{1}{2} \left(Z_{33}^{(4)} \frac{\Pi_{38}(3)^{(4)}}{\Delta m_2^2} + Z_{44}^{(4)} \frac{\Pi_{38}(3)^{(4)}}{\Delta m_2^2} \right) \mathcal{G}_{48,extv}^{(2)}. \end{aligned} \quad (4.26)$$

The Z and Π factors have been valuated earlier [16, 17] and we thus need to evaluate the various \mathcal{G} amputated amplitudes.

4.5 Analytical results and ratios of form-factors

To do the calculation, we need to calculate the tree level diagrams of Fig.4.2, the one- and two-loop diagrams of Fig. 4.3 and the two-loop diagrams with overlapping divergences of Fig. 4.4 with isospin breaking kept in the masses and vertices. These amplitudes should then be put together with the wave-function renormalization and mixing effects given in (4.23). The lowest order

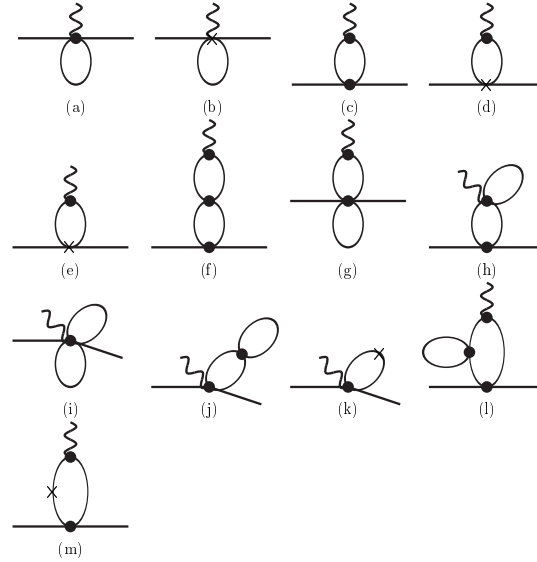


Figure 4.3: The one- and two-loop Feynman diagrams for the Kaon transition form-factors without overlapping divergences. Notation as in Fig. 4.2.

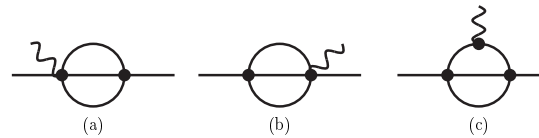


Figure 4.4: The two-loop Feynman diagrams for the Kaon transition form-factors with overlapping divergences. Notation as in Fig. 4.2.

expressions are quite simple. The form-factors $f_-^{K^i \pi^j}$ all vanish and the others are

$$\begin{aligned}
 f_+^{K^+ \pi^0}(t) &= \cos \epsilon + \sqrt{3} \sin \epsilon, \\
 f_+^{K^0 \pi^-}(t) &= 1, \\
 f_+^{K^+ \pi^+}(t) &= 1, \\
 f_+^{K^0 \pi^0}(t) &= \cos \epsilon - \sqrt{3} \sin \epsilon.
 \end{aligned}
 \tag{4.27}$$

The NLO expressions agree with the isospin breaking ones calculated in [4, 2] for the f_+ form-factors. The isospin breaking in the f_- and f_0 form-factors is new. The NLO results are given in App. 4.A. The full NNLO results are very lengthy but we have performed two independent calculations that are in agreement. All eight form-factors are also finite using the general subtractions calculated in [18]. The nonlocal divergences and the other quantities that can be removed using \overline{MS} subtraction also cancel as they should. These consistency checks are described in detail in [19]. The loop integrals are computed using the methods described in [20, 21].

The main existing previous work is for $K_{\ell 3}$ decays. Isospin breaking to order p^4 for f_+ was done in [4] and the electromagnetic parts worked out in [7] to order $e^2 p^2$.

While this work was in progress, an analysis of the isospin breaking in the rare decay form-factors $f_+^{K^+\pi^+}$ and $f_+^{K^0\pi^0}$ to NLO and order $e^2 p^2$ appeared [2]. They also noted that the relation (4.12) was satisfied but do not seem to have realized it is an immediate consequence of isospin.

Isospin breaking in $f_-^{K^i\pi^j}$ has not been discussed earlier within the context of ChPT.

In [4] another relation valid to NLO and first order in isospin breaking was found. The ratio of form-factors

$$\frac{f_+^{K^0\pi^-}(t)}{f_+^{K^+\pi^0}(t)} = \frac{f_+^{K^0\pi^0}(t)}{f_+^{K^+\pi^+}(t)} \quad (4.28)$$

is independent of momenta and can be cleanly predicted in terms of pseudo-scalar meson masses. The equality follows from the use of (4.12).

Our results satisfy the relations (4.11) and (4.12), we had to use a large number of relations between the various integrals to check this and obtained in this way another nontrivial check on our results. The NLO relation found by [4] is no longer true at NNLO. There are t -dependent corrections at order NNLO of all³ types, pure two-loop, L_i^r -dependent and C_i^r -dependent ones. The relation (4.28) is also not true for the scalar form-factors $f_0^{K^i\pi^j}(t)$ nor for $f_-^{K^i\pi^j}(t)$ already at NLO.

We define here also two more ratios for later use, first the ratio of the two weak decay form-factors

$$r_{0-}(t) = \frac{f_+^{K^+\pi^0}(t)}{f_+^{K^0\pi^-}(t)} \quad (4.29)$$

and second the ratio of the rare to the weak decay with charged pions in the final state

$$r_K(t) = \frac{f_+^{K^+\pi^+}(t)}{f_+^{K^0\pi^-}(t)}. \quad (4.30)$$

³That it was not valid for the C_i^r contributions at order p^6 was also noticed in [2].

We define similarly definitions of $r^0(t)$, $r_{0-}^0(t)$ and $r_K^0(t)$ for ratios of the scalar form-factors $f_0^{K^i\pi^j}(t)$.

4.6 Resonance estimate of the contribution from the C_i^r

This contribution is the most difficult to estimate. In the isospin limit, $f_+^{K\pi}(0)$ only depends on the combination $(C_{12}^r + C_{34}^r)(m_K^2 - m_\pi^2)^2$ [5] and its estimate is the main uncertainty in the chiral prediction for $f_+^{K\pi}(0)$. A review can be found in [1]. The underlying reason for the factor $(m_K^2 - m_\pi^2)^2$ is the Ademollo-Gatto theorem[22]. The reasoning used there remains valid also in the case with isospin breaking for the form-factors that do not involve π^0 - η mixing. The isospin conserving case is proportional to $(m_s - \hat{m})^2$, but including isospin breaking, the form-factor for the neutral weak decay is proportional to $(m_s - m_u)^2$ and for the charged rare decay it is proportional to $(m_s - m_d)^2$. The full order p^6 tree level contribution in these cases is again proportional to $C_{12}^r + C_{34}^r - (L_5^r)^2$ just as was found for the isospin conserved case in [5, 23].

The general method we use to estimate the C_i^r is of saturation by a finite number of resonances introduced by [24, 25]. We use the vector Lagrangian in the Proca formulation with parameters as determined in [19, 5]. The scalar effect was studied in detail in [23] and more generally in [26]. Some problems with this procedure are discussed in [27].

The vector exchange contribution does not contribute to the values at $t = 0$ for $f_+^{K^i\pi^j}(t)$. It does however contribute strongly away from zero. The estimate we use here for the C_i^r from vector exchange is described in [5]. In particular, the same estimate is in good agreement with the estimate of the curvature in the pion electromagnetic form-factor which leads to an experimental determination of[21]

$$-4(C_{88}^r - C_{90}^r) = (0.22 \pm 0.02) 10^{-3} \quad (4.31)$$

compared with a prediction of $0.26 10^{-3}$. This is the part that estimates the contribution from the C_i^r in Fig. 4.6. The way we have implemented it here is via the effect on the C_i^r directly as given in [28].

Second, we take into account the contribution from the singlet pseudo-scalar degree of freedom P_1 . We use the simple Lagrangian

$$\mathcal{L}_{\eta'} = \frac{1}{2}\partial_\mu P_1 \partial^\mu P_1 - \frac{1}{2}M_{\eta'}^2 P_1^2 + i\tilde{d}_m P_1 \langle \chi_- \rangle. \quad (4.32)$$

Integrating out P_1 leads to the order p^4 term with L_7 and the order p^6 Lagrangian

$$\mathcal{L}_{\eta'} = -\frac{\tilde{d}_m^2}{2M_{\eta'}^4} \partial_\mu \langle \chi_- \rangle \partial^\mu \langle \chi_- \rangle \text{ with } \tilde{d}_m = 20 \text{ MeV}. \quad (4.33)$$

The latter was rewritten in general in terms of the basis of operators of [14] in [17]. The result is⁴

$$\begin{aligned} \partial_\mu \langle \chi_- \rangle \partial_\mu \langle \chi_- \rangle &= O_{18} + \frac{2}{9} O_{19} - \frac{1}{3} O_{20} + \frac{1}{3} O_{21} + 2O_{27} + \frac{2}{3} O_{31} - \frac{1}{3} O_{32} \\ &\quad + \frac{1}{3} O_{33} - 2O_{35} + O_{37} - \frac{8}{3} O_{94}. \end{aligned} \quad (4.34)$$

The result is that the singlet P_1 contributes via the order p^6 constants C_i^r also to the isospin breaking in the values for $f_+^{K^i \pi^j}(0)$ but it does so only via π^0 - η mixing. The numerical result is

$$\begin{aligned} f_+^{K^+ \pi^0}(0) \Big|_{P_1} &= 0.00065, \\ f_+^{K^0 \pi^0}(0) \Big|_{P_1} &= -0.00065. \end{aligned} \quad (4.35)$$

4.7 Numerical results

4.7.1 Input parameters

For the masses we use the particle data book masses except for the eta where we use for consistency the value 547.3 MeV. The input values for the order p^4 constants L_i^r we use are fit 10 of [16]. This fit used the K_{e4} data from E865, and input values $m_s/\hat{m} = 24$ and $F_K/F_\pi = 1.22$. For the masses it used the physical masses. Electromagnetic corrections to the Kaon mass were included with the estimate of the violation of Dashen's theorem of [31] included. An extensive discussion of this fit can be found in [29] using the older K_{e4} data and working fully in the isospin limit.

We will always quote results for the isospin conserving formulas of [21] where the kaon mass is taken to be the mass of the kaon involved and similarly, we use for the pion mass the mass of the particle involved in the matrix element. For the results with the formulas including isospin breaking, we have used for the Kaons their physical masses but for both charged and neutral pion the same mass, since to first order in $m_u - m_d$ these have the same mass. We have always taken the mass of the final state pion involved in the matrix element. The reason for this choice is to always have the kinematics right in the matrix elements. The effect of changing the pion mass can be judged by looking at the results for the isospin symmetric formulae which we quote for different input Kaon and pion masses in Tab. 4.1.. The order p^6 constants C_i^r have been put to zero at the scale $\mu = 770$ MeV unless otherwise noted in Sect. 4.7.2. In Sects.

⁴This was derived by the authors of [29] but not included in the final manuscript. It also agrees with the expression shown by Kaiser[30].

	$f_+^{K^+\pi^0}$	$f_+^{K^0\pi^-}$	$f_+^{K^+\pi^+}$	$f_+^{K^0\pi^0}$
order p^2	1.00000	1.00000	1.00000	1.00000
order p^4	-0.02276	-0.02266	-0.02226	-0.02316
order p^6	0.01423	0.01462	0.01406	0.01480
p^6 2-loop	0.01104	0.01130	0.01090	0.01145
p^6 L_i^r -dependent	0.00320	0.00332	0.00316	0.00336
sum of p^2 , p^4 and p^6	0.99156	0.99196	0.99180	0.99164

Table 4.1: The different contributions to $f_+^{K^i\pi^j}(0)$ using the isospin *conserving* amplitudes of [5]. We have also shown the break-up of the order p^6 expressions in the pure two-loop part and the L_i^r -dependent part. The part depending on the C_i^r is *not* included.

4.7.3, 4.7.4 and 4.7.5 we have put the C_i^r at the value estimated by vector and singlet pseudo-scalar exchange at $\mu = 700$ MeV.

The main fit 10 with Dashen's violation gave $m_u/m_d = 0.45$ while removing the violation of Dashen's theorem gave $m_u/m_d = 0.52$. The standard values without order p^6 and without violation of Dashen's theorem gave $m_u/m_d = 0.585$ [16]. These values, together with the input value for m_s/\hat{m} correspond to $\sin \epsilon = 0.0143$, 0.0119 and 0.00986 respectively. This can be compared with the value of 0.0106 ± 0.0008 used in [2] which used the input neglecting order p^6 effects. Note however that the recent evaluation from $\eta \rightarrow 3\pi$ [17] leads to somewhat different values.

4.7.2 $f_+^{K^i\pi^j}(0)$

Here we give the results for the form-factor values at zero. In Tab. 4.1 we first show the results for the isospin conserving formula of [5]. Here the only isospin breaking effect is the different kaon and pion mass used as described in Sect. 4.7.1. The results for the charged and neutral weak decay are in agreement with [5]. We have in fact checked that the formulas including isospin breaking numerically agree with the isospin conserving formula if the masses are set to the same isospin conserving masses and $\sin \epsilon = 0$. As is clear from the numbers in Tab. 4.1, the isospin breaking effects from varying the masses in the loops is quite small.

In contrast, we have shown the equivalent set of values for our amplitudes including isospin violation. It can be seen that effect is much larger for the amplitudes with a neutral pion in the final state. That is, as can already be seen at lowest order, pion-eta mixing is important for this decay. The values in Tab. 4.2 are with $m_u/m_d = 0.45$ or $\sin \epsilon = 0.01429$.

To show the variation with the input for m_u/m_d , we show in Tab. 4.3 using

	$f_+^{K^+\pi^0}$	$f_+^{K^0\pi^-}$	$f_+^{K^+\pi^+}$	$f_+^{K^0\pi^0}$
order p^2	1.02465	1.00000	1.00000	0.97514
order p^4	-0.01775	-0.02292	-0.02197	-0.02838
order p^6	0.00809	0.01470	0.01391	0.02095
p^6 2-loop	0.00159	0.01145	0.01081	0.02092
p^6 L_i^r -dependent	0.00650	0.00325	0.00309	0.00004
sum of p^2 , p^4 and p^6	1.01499	0.99177	0.99194	0.96772

Table 4.2: The different contributions to $f_+^{K^i\pi^j}(0)$ using the amplitudes *including isospin breaking*. We have also shown the break-up of the order p^6 expressions in the pure two-loop part and the L_i^r -dependent part. The part depending on the C_i^r is *not* included. We used here $m_u/m_d = 0.45$ corresponding to the two-loop fit of [16] including Dashen's theorem violations.

	$f_+^{K^+\pi^0}$	$f_+^{K^0\pi^-}$	$f_+^{K^+\pi^+}$	$f_+^{K^0\pi^0}$
order p^2	1.01702	1.00000	1.00000	0.98288
order p^4	-0.01931	-0.02282	-0.02202	-0.02675
order p^6	0.00986	0.01467	0.01395	0.01919
p^6 2-loop	0.00435	0.01142	0.01084	0.01815
p^6 L_i^r -dependent	0.00551	0.00325	0.00311	0.00104
sum of p^2 , p^4 and p^6	1.00757	0.99186	0.99193	0.97532

Table 4.3: The different contributions to $f_+^{K^i\pi^j}(0)$ using the amplitudes *including isospin breaking*. We have also shown the break-up of the order p^6 expressions in the pure two-loop part and the L_i^r -dependent part. The part depending on the C_i^r is *not* included. We used here $m_u/m_d = 0.585$ corresponding to the one-loop fit of [16] without violations of Dashen's theorem.

the same inputs as for Tab. 4.2 but with $m_u/m_d = 0.585$ or $\sin \epsilon = 0.009857$. This corresponds to the fit for m_u/m_d without violations of Dashen's theorem and using order p^4 expressions. Our results, except for the lowest order in (4.27), are explicitly linear in $\sin \epsilon$. The numbers are slightly different from the preliminary results quoted in [8]. This due to a slightly different way of treating the pion masses.

Using the results of Tab. 4.2 we can also quote numerical results for the various ratios defined earlier at the point $t = 0$. First the ratio of charged to neutral weak decay. This is

$$r_{0-}(0) = 1.02465 + 0.00587 - 0.00711 = 1.02341, \quad (4.36)$$

where we see that the order p^6 contributions lower the result and essentially

cancel the enhancement from the ratio at order p^4 . If we add the contribution from singlet P_1 exchange we obtain $r_{0-} = 1.024068$. However, compared to the standard value, we get again an enhancement due to the larger value of $\sin \epsilon$ obtained from the order p^6 fit. We showed the contributions to the ratio at order p^2 , p^4 and p^6 . This should be compared to the experimental ratio as determined from the global FLAVIANet fit [32]

$$r_{0-exp} = 1 + \Delta_{SU(2)} = 1.0284 \pm 0.0040. \quad (4.37)$$

As we see, we obtain a reasonable agreement.

We can also look at the double ratio r from (4.12). Our formulas satisfy it exactly. The main numerical source of the difference at higher orders results from the fact that we used a different pion mass in the denominator and the numerator. The result is

$$r = 0.99918 - 0.00161 + 0.00085 = 0.99842, \quad (4.38)$$

where a fairly sizable cancellation happens between the order p^4 and order p^6 contributions. We again showed the contributions to the ratio at order p^2 , p^4 and p^6 .

The final ratio, of weak to rare decays with a charged pion in the final state is

$$r_K = 1.00000 + 0.00097 - 0.00080 = 1.00017. \quad (4.39)$$

The three numbers in the middle part are once more the contributions to the ratio at order p^2 , p^4 and p^6 . Once more, we see a significant cancellation between the order p^4 and p^6 contributions.

4.7.3 $f_+^{K^i\pi^j}(t)$

In this subsection we show the results as a function of t for the the $f_+^{K^i\pi^j}$ form-factors. We first show the case for the neutral weak decay in Figs. 4.5 and 4.6. Fig. 4.5 shows the result to lowest order, NLO and NNLO. It can be seen that there is a nice convergence in the entire region shown.

We show the various subparts of the order p^6 contribution in Fig. 4.6. The contributions shown are the two-loop contribution, the part dependent on the order p^4 LECs L_i^r as well as the part that depends on the order p^6 LECs C_i^r .

The results shown so far for $f_+^{K^0\pi^-}$ are essentially the same as those in the isospin limit of [5]. We have included isospin breaking but it is a rather small effect for this form-factor. Rather than showing similar plots for the other three form-factors we show here the ratios as a function of t . First we show the variation of the full ratio r as a function of t . The ratio r is somewhat more different from one than naively expected since we included different pion masses. The ratio r_{0-} defined in (4.29) is shown as a function of t in Fig. 4.8. It

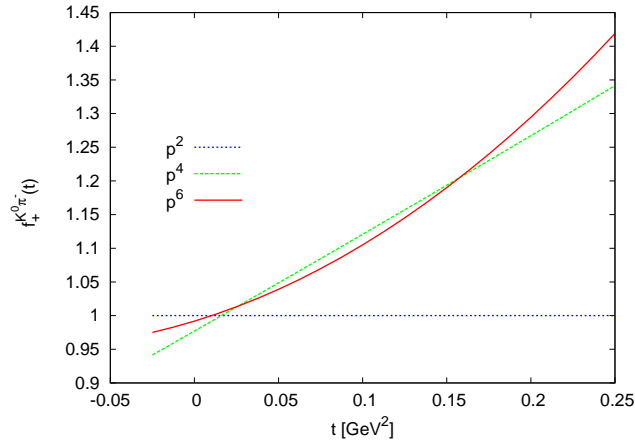


Figure 4.5: The form-factor $f_+^{K^0\pi^-}(t)$ as a function of t . Shown are the lowest order (p^2), NLO (p^4) and NNLO result (p^6). Isospin breaking is included.

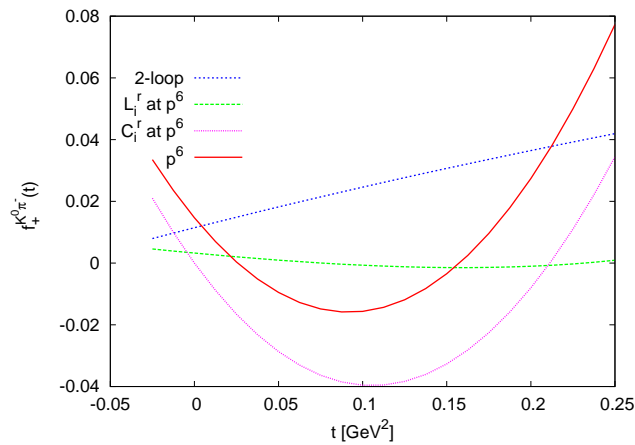


Figure 4.6: The form-factor $f_+^{K^0\pi^-}(t)$ as a function of t . Shown are the full order p^6 contribution and its three constituent parts, the pure two-loop contribution, the L_i^r -dependent part and the C_i^r -dependent part. The contribution to the quadratic slope comes mainly from the C_i^r dependent part but that is fixed from the pion electromagnetic form-factor [21]. Isospin breaking is included.

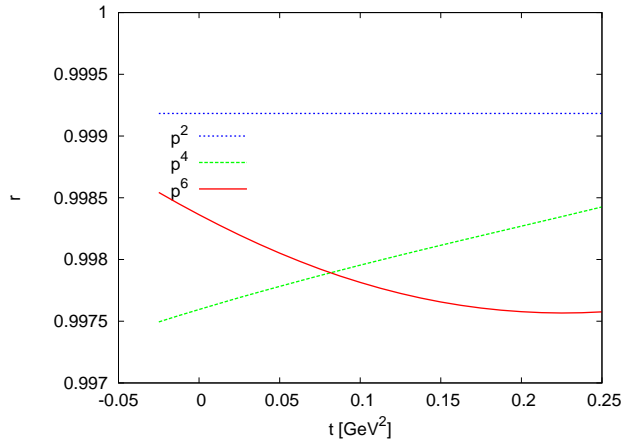


Figure 4.7: The ratio r as defined in (4.12) as a function of t . Both the deviation from 1 and the t dependence are effects of higher order in isospin breaking.

was shown in [4] that at NLO this ratio is independent of t . We have checked that this is no longer true at NNLO as is clearly visible in the figure. However, there is clearly no sign of an anomalously large isospin breaking effect in this ratio. We also show the similar ratio for the charged rare to neutral weak decay, r_K as defined in (4.30) in Fig. 4.9.

4.7.4 $f_0^{K^i\pi^j}(t)$

In this subsection we show the results as a function of t for the the $f_0^{K^i\pi^j}$ form-factors. We first show the case for the neutral weak decay in Figs. 4.10 and 4.11. Fig. 4.10 shows the result to lowest order, NLO and NNLO. It can be seen that there is a nice convergence in the entire region shown.

We show the various subparts of the order p^6 contribution in Fig. 4.11. The contributions shown are the two-loop contribution, the part dependent on the order p^4 LECs L_i^r as well as the part that depends on the order p^6 LECs C_i^r . The latter is essentially zero here since the vector exchange contribution to the scalar form-factor vanishes to the order considered here and the singlet pseudo-scalar doesn't contribute either. A scalar exchange would contribute but we have not included such an estimate here. The curvature visible is here mainly coming from the loops.

The results shown so far for $f_0^{K^0\pi^-}$ are essentially the same as those in the isospin limit of [5]. We have included isospin breaking but it is a rather small effect for this form-factor. Rather than showing similar plots for the other

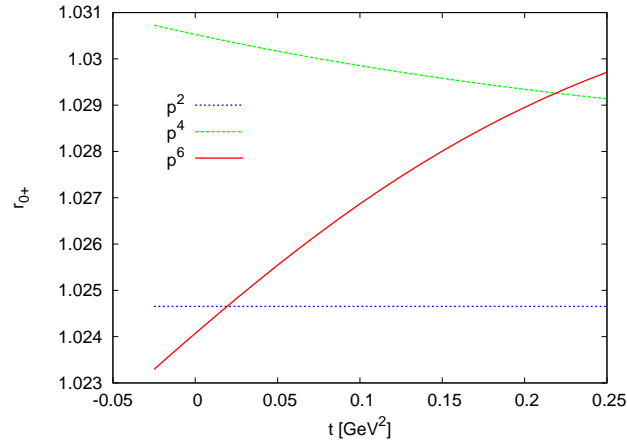


Figure 4.8: The ratio r_{0+} as defined in (4.29) as a function of t . This is the ratio of the charged to neutral weak decay. The t dependence for the NLO result is higher order in isospin breaking but is first order at NNLO.

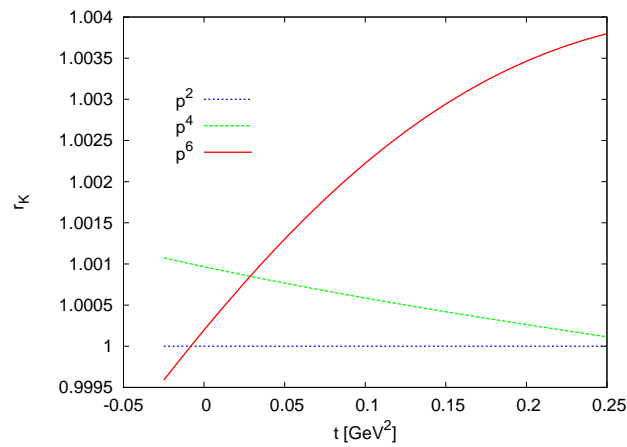


Figure 4.9: The ratio r_K as defined in (4.30) as a function of t . This is the ratio of the charged rare to neutral weak decay.

three form-factors we show here the ratios as a function of t . First we show the variation of the full ratio r^0 as a function of t . The ratio r^0 is somewhat larger than naively expected since we included different pion masses. The ratio r_{0+}^0

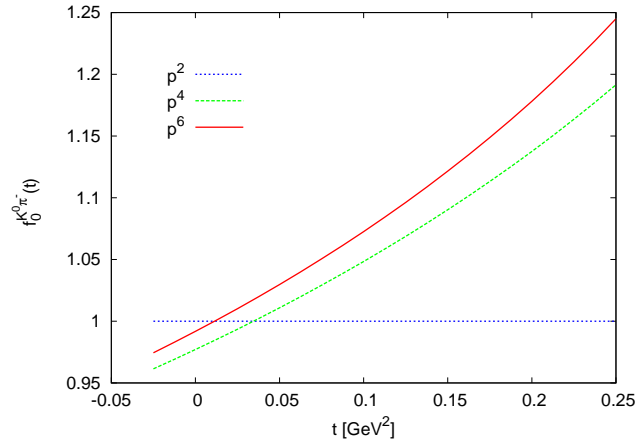


Figure 4.10: The form-factor $f_0^{K^0\pi^-}(t)$ as a function of t . Shown are the lowest order (p^2), NLO (p^4) and NNLO result (p^6). Isospin breaking is included.

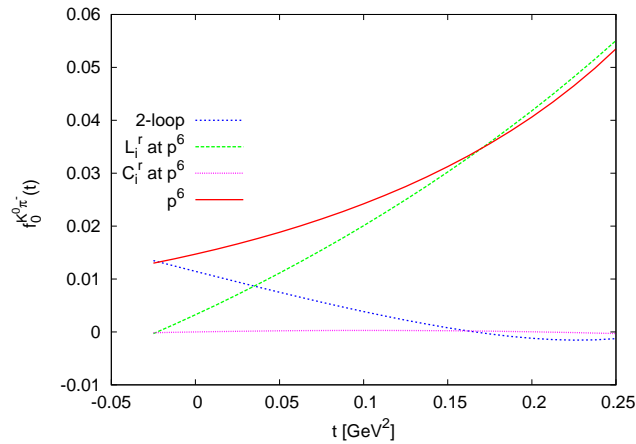


Figure 4.11: The form-factor $f_0^{K^0\pi^-}(t)$ as a function of t . Shown are the full order p^6 contribution and its three constituent parts, the pure two-loop contribution, the L_i^r -dependent part and the C_i^r -dependent part. Isospin breaking is included.

defined in (4.29) but for the scalar form-factor is shown as a function of t in Fig. 4.13. This ratio can be t -dependent already at NLO which is clearly visible.

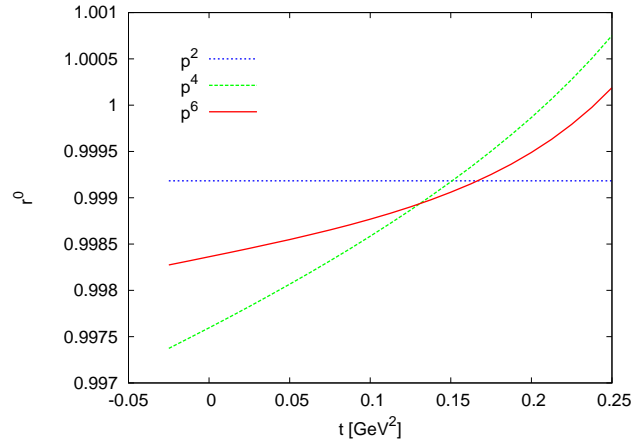


Figure 4.12: The ratio r^0 as defined in (4.12) but for the scalar form-factor as a function of t . Both the deviation from 1 and the t dependence are effects of higher order in isospin breaking.

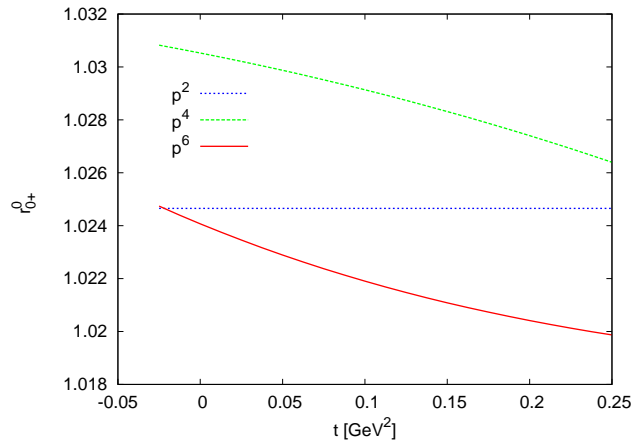


Figure 4.13: The ratio r_{0-}^0 as defined in (4.29) but for the scalar form-factor as a function of t . This is the ratio of the charged to neutral weak decay. The t dependence is first order in isospin breaking both at NLO and NNLO.

However, there is no sign of an anomalously large isospin breaking effect in this ratio. We also show the similar ratio for the charged rare to neutral weak decay,

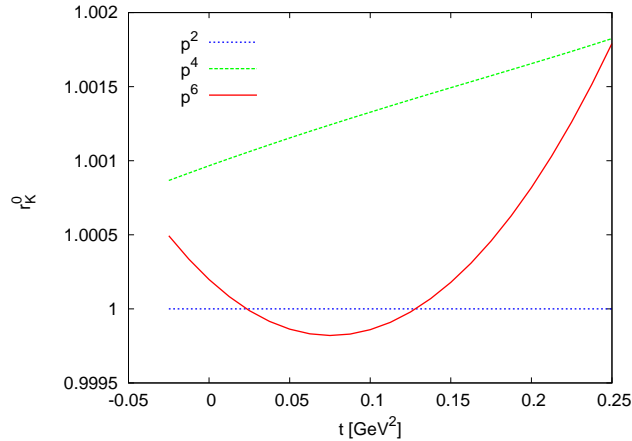


Figure 4.14: The ratio r_K^0 as defined in (4.30) but for the scalar form-factor as a function of t . This is the ratio of the charged rare to neutral weak decay.

r_K^0 as defined in (4.30) in Fig. 4.14. The scalar form-factors are not needed for the weak decays to an electron or the rare decays to a neutrino-antineutrino pair. They do contribute to the weak decays to a muon and the rare decays with a muon-anti-muon pair via the axial current couplings to the latter from the short-distance contributions.

4.7.5 Callan-Treiman point

The Callan-Treiman relation [33] states that the scalar form-factor at $t = m_K^2 - m_\pi^2$ satisfies

$$f_0(m_K^2 - m_\pi^2) = \frac{F_K}{F_\pi} + \mathcal{O}(m_u, m_d). \quad (4.40)$$

This relation is derived using current algebra in the up-down-sector and should thus have rather small corrections of order m_π^2 . The relation is exact when the up and down quark masses are zero. The correction at NLO was worked out in [4] and found to be

$$\Delta_{CT} \equiv f_0(m_K^2 - m_\pi^2) - \frac{F_K}{F_\pi} = -3.5 \cdot 10^{-3} [4]. \quad (4.41)$$

The correction in the isospin limit at NNLO was never presented in [5]. We have calculated this and also for the four different amplitudes at order p^4 but for the

C_i^r estimates we have used the vector and pseudo-scalar singlet contributions as described in Sect. 4.6.

The inputs we used produce $F_K/F_\pi = 1.22$, which is what we have subtracted from the $f_0^{K^i\pi^j} (m_{K^i}^2 - m_{\pi^j}^2)$ in the numbers quoted below. The isospin symmetric expression with $m_K^2 = m_{K^0}^2$ and $m_\pi^2 = m_{\pi^+}^2$ gives

$$\Delta_{CT} = -6.2 \cdot 10^{-3}. \quad (4.42)$$

As we see there is a substantial NNLO correction. Note that we did not include the contributions from nonzero C_{12}^r, C_{34}^r in this expression. These read

$$\Delta_{CT}|_{C_i^r} = \frac{16}{F_\pi^4} (2C_{12}^r + C_{34}^r) m_\pi^2 (m_K^2 - m_\pi^2). \quad (4.43)$$

It is clear that this satisfies the Callan-Treiman theorem. Notice that the same combination of order p^6 LECs shows up in the scalar slope when the part via F_K/F_π is subtracted as in Eq. (5.2) of [5].

For the expression including isospin breaking we simply present the numerical results directly

$$\begin{aligned} \Delta_{CT}^{K^+\pi^0} &= 15.1 \cdot 10^{-3}, \\ \Delta_{CT}^{K^0\pi^-} &= -5.6 \cdot 10^{-3}, \\ \Delta_{CT}^{K^+\pi^+} &= -9.4 \cdot 10^{-3}, \\ \Delta_{CT}^{K^0\pi^0} &= -26.4 \cdot 10^{-3}. \end{aligned} \quad (4.44)$$

Recently, Leutwyler discussed the experimental measurements and the extrapolation to the Callan-Treiman point [34]. The results we obtained are clearly not sufficient to explain the large value of $\Delta_{CT} = -0.071 \pm 0.014_{NA48} \pm 0.002_{theo} \pm 0.005_{ext}$ observed by NA48 in the charged weak decay [35] but are in reasonable agreement with the one observed by KLOE for the neutral weak decay [36].

4.8 Conclusions

In this paper we have calculated all the vector form-factors of Kaon to Pion transitions to first order in the quark mass difference $m_u - m_d$ and to NNLO in ChPT. We have thus calculated the eight different form-factors defined in Eqs. (4.2-4.5) to order $p^6(m_u - m_d)$. This complements the earlier calculations to order $p^4(m_u - m_d)$ done for the f_+ form-factors in [4] and [2] and to order p^6 in the isospin limit for the vector and scalar form-factor.

What we find in all cases is that the NNLO results diminish the effects of isospin breaking but due to the change in m_u/m_d from a NLO to a NNLO

fit the total effect is to increase the isospin breaking in the form-factors. This goes some way towards reconciling the determinations of V_{us} from the charged and neutral weak $K_{\ell 3}$ decays but does not explain the full difference. We have also calculated isospin breaking in all the scalar form-factors. Here again, the effects are sizable but not unexpectedly large. In particular, they are not large enough to explain the discrepancy with the Callan-Treiman point observed by NA48[35].

We have presented numerical results for the values at $t = 0$ and for the t -dependence as well as for various ratios of the form-factors. In particular, we have shown that the relations (4.11) and (4.12) are valid to all orders in ChPT and to first order in $m_u - m_d$. We presented numerical results for the ratios r , r_{0-} and r_K as well as for their equivalents for the scalar form-factors.

Acknowledgments

This work is supported in part by the European Commission RTN network, Contract MRTN-CT-2006-035482 (FLAVIANet), the European Community-Research Infrastructure Activity Contract RII3-CT-2004-506078 (HadronPhysics) and the Swedish Research Council.

4.A The order p^4 expression

In this appendix we explicitly write out our order p^4 results. We have checked that they agree with the published results for the f_+ form-factors of [4] and [2]. They also satisfy the relation (4.12) when the integrals are expanded to obtain a common Kaon mass, but we have quoted all eight formfactors here since by rewriting one can move things between the order p^4 and p^6 . The expressions quoted here are the ones we used to define the order p^4 part. The integrals used below are the standard one-loop integrals defined in many places, see e.g.

[20].

$$\begin{aligned}
f_+^{K^+\pi^0(4)}(t) &= \frac{1}{F_\pi^2 (m_{\pi^0}^2 - m_\eta^2)} \left(-2/3 \bar{A}(m_{K^+}^2) m_{K^+}^2 - 1/3 \bar{A}(m_{K^+}^2) m_{\pi^0}^2 \right. \\
&\quad \left. + 2/3 \bar{A}(m_{K^0}^2) m_{K^+}^2 + 1/3 \bar{A}(m_{K^0}^2) m_{\pi^0}^2 \right) \\
&\quad + \frac{\sin \epsilon}{\sqrt{3} F_\pi^2 (m_{\pi^0}^2 - m_\eta^2)} \left(+128 m_{K^+}^4 L_8^r + 384 m_{K^+}^4 L_7^r \right. \\
&\quad - 256 m_{\pi^0}^2 m_{K^+}^2 L_8^r - 768 m_{\pi^0}^2 m_{K^+}^2 L_7^r + 128 m_{\pi^0}^4 L_8^r \\
&\quad + 384 m_{\pi^0}^4 L_7^r - 4/3 \bar{A}(m_{\pi^+}^2) m_{K^+}^2 + 16/3 \bar{A}(m_{\pi^+}^2) m_{\pi^0}^2 \\
&\quad - 2 \bar{A}(m_{\pi^0}^2) m_{K^+}^2 + 2 \bar{A}(m_{\pi^0}^2) m_{\pi^0}^2 - \bar{A}(m_{K^+}^2) m_{\pi^0}^2 \\
&\quad + 4/3 \bar{A}(m_{K^0}^2) m_{K^+}^2 - 13/3 \bar{A}(m_{K^0}^2) m_{\pi^0}^2 + 2 \bar{A}(m_\eta^2) m_{K^+}^2 \\
&\quad \left. - 2 \bar{A}(m_\eta^2) m_{\pi^0}^2 \right) + \frac{\sin \epsilon}{\sqrt{3} F_\pi^2} \left(+6 L_9^r t - 1/4 \bar{A}(m_{\pi^+}^2) \right. \\
&\quad + 9/8 \bar{A}(m_{\pi^0}^2) + 7/4 \bar{A}(m_{K^+}^2) + 3/2 \bar{A}(m_{K^0}^2) + 3/8 \bar{A}(m_\eta^2) \\
&\quad - 3 \bar{B}_{22}(m_{\pi^+}^2, m_{K^0}^2, t) - 9/2 \bar{B}_{22}(m_{\pi^0}^2, m_{K^+}^2, t) \\
&\quad \left. - 3/2 \bar{B}_{22}(m_{K^+}^2, m_\eta^2, t) \right) + \frac{1}{F_\pi^2} \left(+2 L_9^r t + 1/4 \bar{A}(m_{\pi^+}^2) \right. \\
&\quad + 1/8 \bar{A}(m_{\pi^0}^2) + 3/4 \bar{A}(m_{K^+}^2) + 3/8 \bar{A}(m_\eta^2) - \bar{B}_{22}(m_{\pi^+}^2, m_{K^0}^2, t) \\
&\quad \left. - 1/2 \bar{B}_{22}(m_{\pi^0}^2, m_{K^+}^2, t) - 3/2 \bar{B}_{22}(m_{K^+}^2, m_\eta^2, t) \right), \\
f_+^{K^0\pi^-(4)}(t) &= \frac{\sin \epsilon}{\sqrt{3} F_\pi^2} \left(+3/4 \bar{A}(m_{\pi^0}^2) - 3/4 \bar{A}(m_\eta^2) - 3 \bar{B}_{22}(m_{\pi^0}^2, m_{K^+}^2, t) \right. \\
&\quad \left. + 3 \bar{B}_{22}(m_{K^+}^2, m_\eta^2, t) \right) \\
&\quad + \frac{1}{F_\pi^2} \left(2 L_9^r t + 1/4 \bar{A}(m_{\pi^+}^2) + 1/8 \bar{A}(m_{\pi^0}^2) + 1/2 \bar{A}(m_{K^+}^2) \right. \\
&\quad + 1/4 \bar{A}(m_{K^0}^2) + 3/8 \bar{A}(m_\eta^2) - \bar{B}_{22}(m_{\pi^+}^2, m_{K^0}^2, t) \\
&\quad \left. - 1/2 \bar{B}_{22}(m_{\pi^0}^2, m_{K^+}^2, t) - 3/2 \bar{B}_{22}(m_{K^+}^2, m_\eta^2, t) \right), \\
f_+^{K^+\pi^+(4)}(t) &= + \frac{\sin \epsilon}{\sqrt{3} F_\pi^2} \left(-3/4 \bar{A}(m_{\pi^0}^2) + 3/4 \bar{A}(m_\eta^2) + 3 \bar{B}_{22}(m_{\pi^0}^2, m_{K^0}^2, t) \right. \\
&\quad \left. - 3 \bar{B}_{22}(m_{K^0}^2, m_\eta^2, t) \right) \\
&\quad + \frac{1}{F_\pi^2} \left(2 L_9^r t + 1/4 \bar{A}(m_{\pi^+}^2) + 1/8 \bar{A}(m_{\pi^0}^2) + 1/4 \bar{A}(m_{K^+}^2) \right. \\
&\quad + 1/2 \bar{A}(m_{K^0}^2) + 3/8 \bar{A}(m_\eta^2) - \bar{B}_{22}(m_{\pi^+}^2, m_{K^+}^2, t) \\
&\quad \left. - 1/2 \bar{B}_{22}(m_{\pi^0}^2, m_{K^0}^2, t) - 3/2 \bar{B}_{22}(m_{K^0}^2, m_\eta^2, t) \right),
\end{aligned}$$

$$\begin{aligned}
f_+^{K^0\pi^0(4)}(t) &= \frac{1}{F_\pi^2 (m_{\pi^0}^2 - m_\eta^2)} \left(+ 2/3 \bar{A}(m_{K^+}^2) m_{K^0}^2 + 1/3 \bar{A}(m_{K^+}^2) m_{\pi^0}^2 \right. \\
&\quad \left. - 2/3 \bar{A}(m_{K^0}^2) m_{K^0}^2 - 1/3 \bar{A}(m_{K^0}^2) m_{\pi^0}^2 \right) \\
&\quad + \frac{\sin \epsilon}{F_\pi^2 \sqrt{3} (m_{\pi^0}^2 - m_\eta^2)} \left(- 128 m_{K^0}^4 L_8^r - 384 m_{K^0}^4 L_7^r \right. \\
&\quad + 256 m_{\pi^0}^2 m_{K^0}^2 L_8^r + 768 m_{\pi^0}^2 m_{K^0}^2 L_7^r - 128 m_{\pi^0}^4 L_8^r \\
&\quad - 384 m_{\pi^0}^4 L_7^r + 4/3 \bar{A}(m_{\pi^+}^2) m_{K^0}^2 - 16/3 \bar{A}(m_{\pi^+}^2) m_{\pi^0}^2 \\
&\quad + 2 \bar{A}(m_{\pi^0}^2) m_{K^0}^2 - 2 \bar{A}(m_{\pi^0}^2) m_{\pi^0}^2 - 4/3 \bar{A}(m_{K^+}^2) m_{K^0}^2 \\
&\quad + 13/3 \bar{A}(m_{K^+}^2) m_{\pi^0}^2 + \bar{A}(m_{K^0}^2) m_{\pi^0}^2 - 2 \bar{A}(m_\eta^2) m_{K^0}^2 \\
&\quad \left. + 2 \bar{A}(m_\eta^2) m_{\pi^0}^2 \right) + \frac{\sin \epsilon}{F_\pi^2 \sqrt{3}} \left(\right. \\
&\quad - 6 L_9^r t + 1/4 \bar{A}(m_{\pi^+}^2) - 9/8 \bar{A}(m_{\pi^0}^2) \\
&\quad - 3/2 \bar{A}(m_{K^+}^2) - 7/4 \bar{A}(m_{K^0}^2) - 3/8 \bar{A}(m_\eta^2) \\
&\quad + 3 \bar{B}_{22}(m_{\pi^+}^2, m_{K^+}^2, t) + 9/2 \bar{B}_{22}(m_{\pi^0}^2, m_{K^0}^2, t) \\
&\quad \left. + 3/2 \bar{B}_{22}(m_{K^0}^2, m_\eta^2, t) \right) + \frac{1}{F_\pi^2} \left(2 L_9^r t + 1/4 \bar{A}(m_{\pi^+}^2) \right. \\
&\quad + 1/8 \bar{A}(m_{\pi^0}^2) + 3/4 \bar{A}(m_{K^0}^2) + 3/8 \bar{A}(m_\eta^2) \\
&\quad - \bar{B}_{22}(m_{\pi^+}^2, m_{K^+}^2, t) - 1/2 \bar{B}_{22}(m_{\pi^0}^2, m_{K^0}^2, t) \\
&\quad \left. - 3/2 \bar{B}_{22}(m_{K^0}^2, m_\eta^2, t) \right), ; \\
f_-^{K^+\pi^0(4)}(t) &= \frac{\sin \epsilon}{F_\pi^2 \sqrt{3}} \left(- 6 m_{K^+}^2 L_9^r + 12 m_{K^+}^2 L_5^r + 6 m_{\pi^0}^2 L_9^r - 12 m_{\pi^0}^2 L_5^r \right. \\
&\quad + 1/2 \bar{A}(m_{\pi^+}^2) + 3/4 \bar{A}(m_{\pi^0}^2) - 7/4 \bar{A}(m_{K^+}^2) - \bar{A}(m_{K^0}^2) \\
&\quad + 1/2 \bar{A}(m_\eta^2) + \bar{B}(m_{\pi^+}^2, m_{K^0}^2, t) (-1/2 t - 3/2 m_{K^+}^2 + 5/2 m_{\pi^0}^2) \\
&\quad + \bar{B}(m_{\pi^0}^2, m_{K^+}^2, t) - 3/4 t - 5/4 m_{K^+}^2 + 15/4 m_{\pi^0}^2 \\
&\quad + \bar{B}(m_{K^+}^2, m_\eta^2, t) (+1/4 t - 5/4 m_{K^+}^2 + 3/4 m_{\pi^0}^2) \\
&\quad + \bar{B}_1(m_{\pi^+}^2, m_{K^0}^2, t) + 1/2 t + 9/2 m_{K^+}^2 - 13/2 m_{\pi^0}^2 \\
&\quad + \bar{B}_1(m_{\pi^0}^2, m_{K^+}^2, t) (+3/4 t + 19/4 m_{K^+}^2 - 39/4 m_{\pi^0}^2) \\
&\quad + \bar{B}_1(m_{K^+}^2, m_\eta^2, t) (-1/4 t + 13/4 m_{K^+}^2 - 9/4 m_{\pi^0}^2) \\
&\quad + \bar{B}_{21}(m_{\pi^+}^2, m_{K^0}^2, t) (+t - 3 m_{K^+}^2 + 3 m_{\pi^0}^2) \\
&\quad + \bar{B}_{21}(m_{\pi^0}^2, m_{K^+}^2, t) (+3/2 t - 9/2 m_{K^+}^2 + 9/2 m_{\pi^0}^2) \\
&\quad + \bar{B}_{21}(m_{K^+}^2, m_\eta^2, t) (-1/2 t - 3/2 m_{K^+}^2 + 3/2 m_{\pi^0}^2) \\
&\quad + \bar{B}_{22}(m_{\pi^+}^2, m_{K^0}^2, t) + 3/2 \bar{B}_{22}(m_{\pi^0}^2, m_{K^+}^2, t) \\
&\quad \left. - 1/2 \bar{B}_{22}(m_{K^+}^2, m_\eta^2, t) \right)
\end{aligned}$$

$$\begin{aligned}
& + \frac{1}{F_\pi^2} \left(-2m_{K^+}^2 L_9^r + 4m_{K^+}^2 L_5^r + 2m_{\pi^0}^2 L_9^r - 4m_{\pi^0}^2 L_5^r \right. \\
& - 1/2 \bar{A}(m_{\pi^+}^2) + 1/12 \bar{A}(m_{\pi^0}^2) - 5/12 \bar{A}(m_{K^+}^2) + \bar{A}(m_{K^0}^2) \\
& + 1/2 \bar{A}(m_\eta^2) + \bar{B}(m_{\pi^+}^2, m_{K^0}^2, t) (+1/2t - 1/2m_{K^+}^2 \\
& - 1/2m_{\pi^0}^2) + \bar{B}(m_{\pi^0}^2, m_{K^+}^2, t) (-1/12t + 1/12m_{K^+}^2 \\
& + 5/12m_{\pi^0}^2) + \bar{B}(m_{K^+}^2, m_\eta^2, t) (+1/4t - 7/12m_{K^+}^2 \\
& + 1/12m_{\pi^0}^2) + \bar{B}_1(m_{\pi^+}^2, m_{K^0}^2, t) (-1/2t + 3/2m_{K^+}^2 \\
& + 1/2m_{\pi^0}^2) + \bar{B}_1(m_{\pi^0}^2, m_{K^+}^2, t) (+1/12t + 1/12m_{K^+}^2 \\
& - 13/12m_{\pi^0}^2) + \bar{B}_1(m_{K^+}^2, m_\eta^2, t) (-1/4t + 23/12m_{K^+}^2 \\
& - 11/12m_{\pi^0}^2) + \bar{B}_{21}(m_{\pi^+}^2, m_{K^0}^2, t) (-t - m_{K^+}^2 \\
& + m_{\pi^0}^2) + \bar{B}_{21}(m_{\pi^0}^2, m_{K^+}^2, t) (+1/6t - 1/2m_{K^+}^2 \\
& + 1/2m_{\pi^0}^2) + \bar{B}_{21}(m_{K^+}^2, m_\eta^2, t) (-1/2t - 3/2m_{K^+}^2 \\
& + 3/2m_{\pi^0}^2) - \bar{B}_{22}(m_{\pi^+}^2, m_{K^0}^2, t) + 1/6 \bar{B}_{22}(m_{\pi^0}^2, m_{K^+}^2, t) \\
& \left. - 1/2 \bar{B}_{22}(m_{K^+}^2, m_\eta^2, t) \right), \\
f_-^{K^0 \pi^- (4)}(t) & = \frac{\sin \epsilon}{F_\pi^2 \sqrt{3}} \left(-1/2 \bar{A}(m_{\pi^0}^2) \right. \\
& + 1/2 \bar{A}(m_{K^+}^2) + \bar{A}(m_\eta^2) + \bar{B}(m_{\pi^0}^2, m_{K^+}^2, t) (+1/2t - 3/2m_{K^0}^2 \\
& + 1/2m_{\pi^+}^2) + \bar{B}(m_{K^+}^2, m_\eta^2, t) (+1/2t + 1/2m_{K^0}^2 - 1/2m_{\pi^0}^2 \\
& - m_{\pi^+}^2) + \bar{B}_1(m_{\pi^0}^2, m_{K^+}^2, t) (-1/2t + 9/2m_{K^0}^2 \\
& - 5/2m_{\pi^+}^2) + \bar{B}_1(m_{K^+}^2, m_\eta^2, t) (-1/2t - 5/2m_{K^0}^2 + m_{\pi^0}^2 \\
& + 7/2m_{\pi^+}^2) + \bar{B}_{21}(m_{\pi^0}^2, m_{K^+}^2, t) (-t - 3m_{K^0}^2 + 3m_{\pi^+}^2 \\
& + \bar{B}_{21}(m_{K^+}^2, m_\eta^2, t) (-t + 3m_{K^0}^2 - 3m_{\pi^+}^2) \\
& \left. - \bar{B}_{22}(m_{\pi^0}^2, m_{K^+}^2, t) - \bar{B}_{22}(m_{K^+}^2, m_\eta^2, t) \right) \\
& + \frac{1}{F_\pi^2} \left(-2m_{K^0}^2 L_9^r + 4m_{K^0}^2 L_5^r - 4m_{\pi^0}^2 L_5^r + 2m_{\pi^+}^2 L_9^r \right. \\
& - 1/6 \bar{A}(m_{\pi^+}^2) - 1/4 \bar{A}(m_{\pi^0}^2) + 1/4 \bar{A}(m_{K^+}^2) + 1/3 \bar{A}(m_{K^0}^2) \\
& + 1/2 \bar{A}(m_\eta^2) + \bar{B}(m_{\pi^+}^2, m_{K^0}^2, t) (+1/6t - 1/6m_{K^0}^2 \\
& + 1/6m_{\pi^+}^2) + \bar{B}(m_{\pi^0}^2, m_{K^+}^2, t) (+1/4t - 1/4m_{K^0}^2 \\
& - 1/4m_{\pi^0}^2) + \bar{B}(m_{K^+}^2, m_\eta^2, t) (+1/4t - 7/12m_{K^0}^2 \\
& - 1/6m_{\pi^0}^2 + 1/4m_{\pi^+}^2) + \bar{B}_1(m_{\pi^+}^2, m_{K^0}^2, t) (-1/6t + 5/6m_{K^0}^2 \\
& - 5/6m_{\pi^+}^2) + \bar{B}_1(m_{\pi^0}^2, m_{K^+}^2, t) (-1/4t + 3/4m_{K^0}^2 + 1/2m_{\pi^0}^2 \\
& - 1/4m_{\pi^+}^2) + \bar{B}_1(m_{K^+}^2, m_\eta^2, t) (-1/4t + 23/12m_{K^0}^2 + 1/3m_{\pi^0}^2
\end{aligned}$$

$$\begin{aligned}
& -5/4 m_{\pi^+}^2 + \overline{B}_{21}(m_{\pi^+}^2, m_{K^0}^2, t) (-1/3 t - m_{K^0}^2 + m_{\pi^+}^2 \\
& + \overline{B}_{21}(m_{\pi^0}^2, m_{K^+}^2, t) (-1/2 t - 1/2 m_{K^0}^2 + 1/2 m_{\pi^+}^2) \\
& + \overline{B}_{21}(m_{K^+}^2, m_{\eta}^2, t) (-1/2 t - 3/2 m_{K^0}^2 + 3/2 m_{\pi^+}^2) \\
& -1/3 \overline{B}_{22}(m_{\pi^+}^2, m_{K^0}^2, t) - 1/2 \overline{B}_{22}(m_{\pi^0}^2, m_{K^+}^2, t) \\
& -1/2 \overline{B}_{22}(m_{K^+}^2, m_{\eta}^2, t) \Big), \\
f_-^{K^+\pi^+(4)}(t) = & \frac{\sin \epsilon}{F_\pi^2 \sqrt{3}} \Big(+1/2 \overline{A}(m_{\pi^0}^2) - 1/2 \overline{A}(m_{K^0}^2) - \overline{A}(m_{\eta}^2) \\
& + \overline{B}(m_{\pi^0}^2, m_{K^0}^2, t) (-1/2 t + 3/2 m_{K^+}^2 - 1/2 m_{\pi^+}^2) \\
& + \overline{B}(m_{K^0}^2, m_{\eta}^2, t) (-1/2 t - 1/2 m_{K^+}^2 + 1/2 m_{\pi^0}^2 + m_{\pi^+}^2) \\
& + \overline{B}_1(m_{\pi^0}^2, m_{K^0}^2, t) (+1/2 t - 9/2 m_{K^+}^2 + 5/2 m_{\pi^+}^2) \\
& +, \overline{B}_1(m_{K^0}^2, m_{\eta}^2, t) (+1/2 t + 5/2 m_{K^+}^2 - m_{\pi^0}^2 - m_{\pi^+}^2) \\
& + \overline{B}_{21}(m_{\pi^0}^2, m_{K^0}^2, t) (+t + 3 m_{K^+}^2 - 3 m_{\pi^+}^2) \\
& + \overline{B}_{21}(m_{K^0}^2, m_{\eta}^2, t) (+t - 3 m_{K^+}^2 + 3 m_{\pi^+}^2) \\
& + \overline{B}_{22}(m_{\pi^0}^2, m_{K^0}^2, t) + \overline{B}_{22}(m_{K^0}^2, m_{\eta}^2, t) \Big) \\
& + \frac{1}{F_\pi^2} \Big(-2 m_{K^+}^2 L_9^r + 4 m_{K^+}^2 L_5^r - 4 m_{\pi^0}^2 L_5^r + 2 m_{\pi^+}^2 L_9^r \\
& -1/6 \overline{A}(m_{\pi^+}^2) - 1/4 \overline{A}(m_{\pi^0}^2) + 1/3 \overline{A}(m_{K^+}^2) + 1/4 \overline{A}(m_{K^0}^2) \\
& +1/2 \overline{A}(m_{\eta}^2) + 1/6 \overline{B}(m_{\pi^+}^2, m_{K^+}^2, t) (+1/6 t - 1/6 m_{K^+}^2 \\
& +1/6 m_{\pi^+}^2) + 1/4 \overline{B}(m_{\pi^0}^2, m_{K^0}^2, t) (+1/4 t - 1/4 m_{K^+}^2 - 1/4 m_{\pi^0}^2) \\
& + \overline{B}(m_{K^0}^2, m_{\eta}^2, t) (+1/4 t - 7/12 m_{K^+}^2 - 1/6 m_{\pi^0}^2 + 1/4 m_{\pi^+}^2) \\
& + \overline{B}_1(m_{\pi^+}^2, m_{K^+}^2, t) (-1/6 t + 5/6 m_{K^+}^2 - 5/6 m_{\pi^+}^2) \\
& + \overline{B}_1(m_{\pi^0}^2, m_{K^0}^2, t) (-1/4 t + 3/4 m_{K^+}^2 + 1/2 m_{\pi^0}^2 - 1/4 m_{\pi^+}^2) \\
& + \overline{B}_1(m_{K^0}^2, m_{\eta}^2, t) (-1/4 t + 23/12 m_{K^+}^2 + 1/3 m_{\pi^0}^2 - 5/4 m_{\pi^+}^2 \\
& + \overline{B}_{21}(m_{\pi^+}^2, m_{K^+}^2, t) (-1/3 t - m_{K^+}^2 + m_{\pi^+}^2) \\
& + \overline{B}_{21}(m_{\pi^0}^2, m_{K^0}^2, t) (-1/2 t - 1/2 m_{K^+}^2 + 1/2 m_{\pi^+}^2) \\
& + \overline{B}_{21}(m_{K^0}^2, m_{\eta}^2, t) (-1/2 t - 3/2 m_{K^+}^2 + 3/2 m_{\pi^+}^2) \\
& -1/3 \overline{B}_{22}(m_{\pi^+}^2, m_{K^+}^2, t) - 1/2 \overline{B}_{22}(m_{\pi^0}^2, m_{K^0}^2, t) \\
& -1/2 \overline{B}_{22}(m_{K^0}^2, m_{\eta}^2, t) \Big) \\
f_-^{K^0\pi^0(4)}(t) = & \frac{\sin \epsilon}{F_\pi^2 \sqrt{3}} \Big(+6 m_{K^0}^2 L_9^r - 12 m_{K^0}^2 L_5^r - 6 m_{\pi^0}^2 L_9^r + 12 m_{\pi^0}^2 L_5^r \\
& -1/2 \overline{A}(m_{\pi^+}^2) - 3/4 \overline{A}(m_{\pi^0}^2) + \overline{A}(m_{K^+}^2) + 7/4 \overline{A}(m_{K^0}^2) \\
& -1/2 \overline{A}(m_{\eta}^2) + \overline{B}(m_{\pi^+}^2, m_{K^+}^2, t) (+1/2 t + 3/2 m_{K^0}^2 - 5/2 m_{\pi^0}^2)
\end{aligned}$$

$$\begin{aligned}
& + \bar{B}(m_{\pi^0}^2, m_{K^0}^2, t) (+3/4 t + 5/4 m_{K^0}^2 - 15/4 m_{\pi^0}^2) \\
& + \bar{B}(m_{K^0}^2, m_{\eta}^2, t) (-1/4 t + 5/4 m_{K^0}^2 - 3/4 m_{\pi^0}^2) \\
& + \bar{B}_1(m_{\pi^+}^2, m_{K^+}^2, t) (-1/2 t - 9/2 m_{K^0}^2 + 13/2 m_{\pi^0}^2) \\
& + \bar{B}_1(m_{\pi^0}^2, m_{K^0}^2, t) (-3/4 t - 19/4 m_{K^0}^2 + 39/4 m_{\pi^0}^2) \\
& + \bar{B}_1(m_{K^0}^2, m_{\eta}^2, t) (+1/4 t - 13/4 m_{K^0}^2 + 9/4 m_{\pi^0}^2) \\
& + \bar{B}_{21}(m_{\pi^+}^2, m_{K^+}^2, t) (-t + 3 m_{K^0}^2 - 3 m_{\pi^0}^2) \\
& + \bar{B}_{21}(m_{\pi^0}^2, m_{K^0}^2, t) (-3/2 t + 9/2 m_{K^0}^2 - 9/2 m_{\pi^0}^2) \\
& + \bar{B}_{21}(m_{K^0}^2, m_{\eta}^2, t) (+1/2 t + 3/2 m_{K^0}^2 - 3/2 m_{\pi^0}^2) \\
& - \bar{B}_{22}(m_{\pi^+}^2, m_{K^+}^2, t) - 3/2 \bar{B}_{22}(m_{\pi^0}^2, m_{K^0}^2, t) \\
& + 1/2 \bar{B}_{22}(m_{K^0}^2, m_{\eta}^2, t) + \frac{1}{F_\pi^2} \left(-2 m_{K^0}^2 L_9^r + 4 m_{K^0}^2 L_5^r \right. \\
& + 2 m_{\pi^0}^2 L_9^r - 4 m_{\pi^0}^2 L_5^r - 1/2 \bar{A}(m_{\pi^+}^2) + 1/12 \bar{A}(m_{\pi^0}^2) + \bar{A}(m_{K^+}^2) \\
& - 5/12 \bar{A}(m_{K^0}^2) + 1/2 \bar{A}(m_{\eta}^2) + \bar{B}(m_{\pi^+}^2, m_{K^+}^2, t) (+1/2 t \\
& - 1/2 m_{K^0}^2 - 1/2 m_{\pi^0}^2) + \bar{B}(m_{\pi^0}^2, m_{K^0}^2, t) (-1/12 t \\
& + 1/12 m_{K^0}^2 + 5/12 m_{\pi^0}^2) + \bar{B}(m_{K^0}^2, m_{\eta}^2, t) (+1/4 t - 7/12 m_{K^0}^2 \\
& + 1/12 m_{\pi^0}^2) + \bar{B}_1(m_{\pi^+}^2, m_{K^+}^2, t) (-1/2 t \\
& + 3/2 m_{K^0}^2 + 1/2 m_{\pi^0}^2) + \bar{B}_1(m_{\pi^0}^2, m_{K^0}^2, t) (+1/12 t \\
& + 1/12 m_{K^0}^2 - 13/12 m_{\pi^0}^2) + \bar{B}_1(m_{K^0}^2, m_{\eta}^2, t) (-1/4 t \\
& + 23/12 m_{K^0}^2 - 11/12 m_{\pi^0}^2) + \bar{B}_{21}(m_{\pi^+}^2, m_{K^+}^2, t) (-t - m_{K^0}^2 \\
& + m_{\pi^0}^2) + \bar{B}_{21}(m_{\pi^0}^2, m_{K^0}^2, t) (+1/6 t - 1/2 m_{K^0}^2 + 1/2 m_{\pi^0}^2) \\
& + \bar{B}_{21}(m_{K^0}^2, m_{\eta}^2, t) (-1/2 t - 3/2 m_{K^0}^2 + 3/2 m_{\pi^0}^2 \\
& \left. - \bar{B}_{22}(m_{\pi^+}^2, m_{K^+}^2, t) + 1/6 \bar{B}_{22}(m_{\pi^0}^2, m_{K^0}^2, t) - 1/2 \bar{B}_{22}(m_{K^0}^2, m_{\eta}^2, t) \right).
\end{aligned} \tag{4.45}$$

4.B The order p^6 LECs dependent part

In this appendix we write out explicitly the part dependent on the order p^6 LECs C_i^r . We use here a notation which uses the property (4.10).

$$\begin{aligned}
f_\ell^{K^+\pi^0}(t)\Big|_{C_i^r} &= \frac{1}{F_\pi^4} \left(f_\ell^A(t) + \frac{\sin \epsilon}{\sqrt{3}} f_\ell^B(t) + \frac{\sin \epsilon}{\sqrt{3}(m_{\pi^0}^2 - m_\eta^2)} f_\ell^E(t) \right), \\
f_\ell^{K^0\pi^-}(t)\Big|_{C_i^r} &= \frac{1}{F_\pi^4} \left(f_\ell^A(t) - \frac{\sin \epsilon}{\sqrt{3}} f_\ell^D(t) \right), \\
f_\ell^{K^+\pi^+}(t)\Big|_{C_i^r} &= \frac{1}{F_\pi^4} \left(f_\ell^A(t) + \frac{\sin \epsilon}{\sqrt{3}} f_\ell^D(t) \right), \\
f_\ell^{K^0\pi^0}(t)\Big|_{C_i^r} &= \frac{1}{F_\pi^4} \left(f_\ell^A(t) - \frac{\sin \epsilon}{\sqrt{3}} f_\ell^B(t) - \frac{\sin \epsilon}{\sqrt{3}(m_{\pi^0}^2 - m_\eta^2)} f_\ell^E(t) \right).
\end{aligned} \tag{4.46}$$

We also use the notation

$$m_\sigma^2 = m_{K^+}^2 + m_{K^0}^2 - m_\pi^2. \tag{4.47}$$

The pion mass we have used generically since they are the same to the order of our calculation.

The C_i^r dependence is now given by

$$\begin{aligned}
f_+^A(t) &= +t^2(-4C_{88}^r + 4C_{90}^r) + m_\sigma^2 t(-4C_{12}^r - 16C_{13}^r - 4C_{63}^r - 4C_{64}^r \\
&\quad - 2C_{90}^r) + m_\pi^2 t(-12C_{12}^r - 32C_{13}^r - 4C_{63}^r - 8C_{64}^r - 4C_{65}^r - 6C_{90}^r) \\
&\quad + m_\sigma^4(-2C_{12}^r - 2C_{34}^r) + m_\pi^2 m_\sigma^2(4C_{12}^r + 4C_{34}^r) \\
&\quad + m_\pi^4(-2C_{12}^r - 2C_{34}^r), \\
f_+^B(t) &= +t^2(-12C_{88}^r + 12C_{90}^r) + m_\sigma^2 t(-4C_{12}^r - 48C_{13}^r - 4C_{63}^r - 12C_{64}^r \\
&\quad - 2C_{90}^r) + m_\pi^2 t(-44C_{12}^r - 96C_{13}^r - 20C_{63}^r - 24C_{64}^r - 12C_{65}^r \\
&\quad - 22C_{90}^r) + m_\sigma^4(2C_{12}^r + 16C_{14}^r + 16C_{17}^r + 48C_{18}^r - 14C_{34}^r - 24C_{35}^r) \\
&\quad + m_\pi^2 m_\sigma^2(-4C_{12}^r - 32C_{14}^r - 32C_{17}^r - 96C_{18}^r + 28C_{34}^r + 48C_{35}^r) \\
&\quad + m_\pi^4(2C_{12}^r + 16C_{14}^r + 16C_{17}^r + 48C_{18}^r - 14C_{34}^r - 24C_{35}^r), \\
f_+^E(t) &= +m_\sigma^6(96C_{19}^r + 64C_{20}^r + 64C_{31}^r + 64C_{32}^r + 128C_{33}^r) \\
&\quad + m_\pi^2 m_\sigma^4(-32C_{14}^r - 32C_{17}^r - 96C_{18}^r) + m_\pi^4 m_\sigma^2(64C_{14}^r + 64C_{17}^r \\
&\quad + 192C_{18}^r - 288C_{19}^r - 192C_{20}^r - 192C_{31}^r - 192C_{32}^r - 384C_{33}^r) \\
&\quad + m_\pi^6(-32C_{14}^r - 32C_{17}^r - 96C_{18}^r + 192C_{19}^r + 128C_{20}^r \\
&\quad + 128C_{31}^r + 128C_{32}^r \\
&\quad + 256C_{33}^r), \\
f_+^D(t) &= +m_\sigma^2 t(8C_{12}^r - 8C_{63}^r + 8C_{65}^r + 4C_{90}^r) + m_\pi^2 t(-8C_{12}^r + 8C_{63}^r \\
&\quad - 8C_{65}^r - 4C_{90}^r) + m_\sigma^4(8C_{12}^r + 8C_{34}^r) + m_\pi^2 m_\sigma^2(-16C_{12}^r - 16C_{34}^r) \\
&\quad + m_\pi^4(8C_{12}^r + 8C_{34}^r), \\
f_-^A(t) &= +m_\sigma^2 t(-4C_{12}^r + 2C_{88}^r - 2C_{90}^r) + m_\pi^2 t(4C_{12}^r - 2C_{88}^r + 2C_{90}^r) \\
&\quad + m_\sigma^4(6C_{12}^r + 8C_{13}^r + 4C_{14}^r + 4C_{15}^r + 2C_{34}^r + 2C_{63}^r + 2C_{64}^r + C_{90}^r) \\
&\quad + m_\pi^2 m_\sigma^2(12C_{12}^r + 8C_{13}^r + 4C_{15}^r + 8C_{17}^r + 4C_{34}^r + 2C_{64}^r + 2C_{65}^r \\
&\quad + 2C_{90}^r) + m_\pi^4(-18C_{12}^r - 16C_{13}^r - 4C_{14}^r - 8C_{15}^r - 8C_{17}^r - 6C_{34}^r \\
&\quad - 2C_{63}^r - 4C_{64}^r - 2C_{65}^r - 3C_{90}^r), \\
f_-^B(t) &= +m_\sigma^2 t(-4C_{12}^r + 2C_{88}^r - 2C_{90}^r) + m_\pi^2 t(4C_{12}^r - 2C_{88}^r + 2C_{90}^r) \\
&\quad + m_\sigma^4(-6C_{12}^r + 8C_{13}^r - 4C_{14}^r + 4C_{15}^r - 32C_{17}^r - 48C_{18}^r - 18C_{34}^r \\
&\quad - 24C_{35}^r - 2C_{63}^r + 2C_{64}^r - C_{90}^r) \\
&\quad + m_\pi^2 m_\sigma^2(36C_{12}^r + 8C_{13}^r + 16C_{14}^r + 4C_{15}^r + 72C_{17}^r + 96C_{18}^r + 44C_{34}^r \\
&\quad + 48C_{35}^r + 8C_{63}^r + 2C_{64}^r + 2C_{65}^r + 6C_{90}^r) \\
&\quad + m_\pi^4(-30C_{12}^r - 16C_{13}^r - 12C_{14}^r - 8C_{15}^r - 40C_{17}^r - 48C_{18}^r - 26C_{34}^r \\
&\quad - 24C_{35}^r - 6C_{63}^r - 4C_{64}^r - 2C_{65}^r - 5C_{90}^r), \\
f_-^E(t) &= 0, \\
f_-^D(t) &= +m_\sigma^2 t(8C_{12}^r - 4C_{88}^r + 4C_{90}^r) + m_\pi^2 t(-8C_{12}^r + 4C_{88}^r - 4C_{90}^r) + m_\sigma^4 \\
&\quad (-24C_{12}^r - 16C_{13}^r - 8C_{15}^r - 16C_{17}^r - 8C_{34}^r - 4C_{64}^r - 4C_{65}^r - 4C_{90}^r)
\end{aligned}$$

$$\begin{aligned}
& +m_\pi^2 m_\sigma^2 (-16 C_{13}^r - 16 C_{14}^r - 8 C_{15}^r + 16 C_{17}^r - 8 C_{63}^r - 4 C_{64}^r + 4 C_{65}^r) + m_\pi^4 \\
& (24 C_{12}^r + 32 C_{13}^r + 16 C_{14}^r + 16 C_{15}^r + 8 C_{34}^r + 8 C_{63}^r + 8 C_{64}^r + 4 C_{90}^r).
\end{aligned}
\tag{4.48}$$

References

- [1] V. Cirigliano, PoS KAON (2007) 007.
- [2] F. Mescia and C. Smith, arXiv:0705.2025 [hep-ph].
- [3] J. A. Cronin, Phys. Rev. **161** (1967) 1483.
- [4] J. Gasser and H. Leutwyler, Nucl. Phys. B **250** (1985) 517.
- [5] J. Bijnens and P. Talavera, Nucl. Phys. B **669** (2003) 341 [arXiv:hep-ph/0303103].
- [6] P. Post and K. Schilcher, Eur. Phys. J. C **25** (2002) 427 [arXiv:hep-ph/0112352].
- [7] V. Cirigliano, M. Knecht, H. Neufeld, H. Rupertsberger and P. Talavera, Eur. Phys. J. C **23** (2002) 121 [arXiv:hep-ph/0110153].
- [8] J. Bijnens, PoS KAON (2007) 027 [arXiv:0707.0419 [hep-ph]].
- [9] V. Bernard, M. Oertel, E. Passemar and J. Stern, arXiv:0707.4194 [hep-ph]; Phys. Lett. B **638** (2006) 480 [arXiv:hep-ph/0603202].
- [10] M. Jamin, J. A. Oller and A. Pich, JHEP **0402** (2004) 047 [arXiv:hep-ph/0401080].
- [11] S. Weinberg, Physica A **96** (1979) 327.
- [12] J. Gasser and H. Leutwyler, Annals Phys. **158** (1984) 142.
- [13] J. Gasser and H. Leutwyler, Nucl. Phys. B **250** (1985) 465.
- [14] J. Bijnens, G. Colangelo and G. Ecker, JHEP **9902** (1999) 020 [arXiv:hep-ph/9902437].
- [15] J. Bijnens, Prog. Part. Nucl. Phys. **58** (2007) 521 [arXiv:hep-ph/0604043].
- [16] G. Amoros, J. Bijnens and P. Talavera, Nucl. Phys. B **602** (2001) 87 [arXiv:hep-ph/0101127].

-
- [17] J. Bijnens and K. Ghorbani, arXiv:0709.0230 [hep-ph].
- [18] J. Bijnens, G. Colangelo and G. Ecker, *Annals Phys.* **280** (2000) 100 [arXiv:hep-ph/9907333].
- [19] J. Bijnens, G. Colangelo, G. Ecker, J. Gasser and M. E. Sainio, *Nucl. Phys. B* **508** (1997) 263 [Erratum-ibid. B **517** (1998) 639] [arXiv:hep-ph/9707291].
- [20] G. Amorós, J. Bijnens and P. Talavera, *Nucl. Phys. B* **568** (2000) 319 [arXiv:hep-ph/9907264].
- [21] J. Bijnens and P. Talavera, *JHEP* **0203**, 046 (2002) [arXiv:hep-ph/0203049].
- [22] M. Ademollo and R. Gatto, *Phys. Rev. Lett.* **13** (1964) 264;
R. E. Behrends and A. Sirlin, *Phys. Rev. Lett.* **4**, 186 (1960).
- [23] V. Cirigliano, G. Ecker, M. Eidemuller, R. Kaiser, A. Pich and J. Portoles, *JHEP* **0504**, 006 (2005) [arXiv:hep-ph/0503108].
- [24] G. Ecker, J. Gasser, A. Pich and E. de Rafael, *Nucl. Phys. B* **321** (1989) 311.
- [25] G. Ecker, J. Gasser, H. Leutwyler, A. Pich and E. de Rafael, *Phys. Lett. B* **223** (1989) 425.
- [26] V. Cirigliano, G. Ecker, M. Eidemuller, R. Kaiser, A. Pich and J. Portoles, *Nucl. Phys. B* **753** (2006) 139 [arXiv:hep-ph/0603205].
- [27] J. Bijnens, E. Gamiz, E. Lipartia and J. Prades, *JHEP* **0304** (2003) 055 [arXiv:hep-ph/0304222].
- [28] K. Kampf, J. Novotny and J. Trnka, *Eur. Phys. J. C* **50** (2007) 385 [arXiv:hep-ph/0608051].
- [29] G. Amorós, J. Bijnens and P. Talavera, *Nucl. Phys. B* **585** (2000) 293 [Erratum-ibid. B **598** (2001) 665] [arXiv:hep-ph/0003258].
- [30] R. Kaiser, talk presented at EuroFlavour06, 2-4 November 2006, Barcelona, Spain.
- [31] J. Bijnens and J. Prades, *Nucl. Phys. B* **490** (1997) 239 [arXiv:hep-ph/9610360].
- [32] M. Palutan, PoS KAON (2007) 020
- [33] C. G. Callan and S. B. Treiman, *Phys. Rev. Lett.* **16** (1966) 153.

- [34] H. Leutwyler, arXiv:0706.3138 [hep-ph].
- [35] A. Lai *et al.* [NA48 Collaboration], arXiv:hep-ex/0703002.
- [36] F. Ambrosino *et al.* [KLOE Collaboration], arXiv:0707.4631 [hep-ex].